Development of a UV-tolerant strain of the South African isolate of Cryptophlebia leucotreta granulovirus for use as an enhanced biopesticide for Thaumatotibia leucotreta control on citrus

Patrick Mwanza

2020

Development of a UV-tolerant strain of the South African isolate of Cryptophlebia leucotreta granulovirus for use as an enhanced biopesticide for Thaumatotibia leucotreta control on citrus

By

Patrick Mwanza

Submitted in fulfilment of the requirements for the degree of *Philosophiae Doctor* in the Faculty of Science at the Nelson Mandela University

April 2020

Promoter: Prof G.B. Dealtry

Co-Promoters: Dr S. D. Moore

Prof M. Lee

Table of Contents

NELSON MANDELA UNIVERSITY

Declaration by Candidate

NAME: Patrick Mwanza

STUDENT NUMBER: 209201009

QUALIFICATION: PhD Biochemistry

TITLE OF PROJECT: Development of a UV-tolerant strain of the South African isolate of Cryptophlebia leucotreta granulovirus for use as an enhanced biopesticide for Thaumatotibia leucotreta control on citrus

DECLARATION:

In accordance with Rule G5.6.3, I hereby declare that the above-mentioned thesis is my own work and that it has not previously been submitted for assessment to another University or for another qualification.

SIGNATURE: 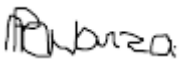

DATE: **04/12/2019**

Acknowledgements

I would like to thank the following individuals and organisations:

- My Promoter, Prof G. Dealtry; for her supervision, guidance and care throughout the duration of this study,
- My co- promoter, Dr S. Moore; for his unwavering support and expert advice,
- My co-promoter, Prof M. Lee; for his assistance with the electron microscopy aspect of the study
- Candice Blom and Arno van Vuuren for their technical assistance with TEM sample preparation and imaging
- William Goosen and Ettienne Minnaar; for their assistance with the operation of the SEM and FTIR respectively.
- Dr Michael Jukes; for his assistance with genome sequence analysis.
- River Bioscience for the timeous and consistent supply of FCM eggs and larvae
- CRI Port Elizabeth staff, for collection of eggs and use of laboratories for bioassays
- CSIR Port Elizabeth for granting me access to the Q-sun Test Chamber
- Sappi South Africa for their generation donation lignin sulphate used in this study
- Citrus Research International, NRF-THRIP and Nelson Mandela University for funding and support of this project.
- The staff and students in the Department of Microbiology, Biochemistry and Physiology; for all their support.
- My friends and family who have inspired and encouraged me to reach greater heights.
- My Pastor David du Preez and the congregation at Port Elizabeth Christian Assembly, for encouragement and prayers
- My mother, who sacrificed her entire life so I could achieve the best education.

- My beautiful wife Dawn, for her love, support, encouragement and patience throughout the course of this study.

- My daughter Atarah Ruvarashe, the bright spark in my life, I hope this thesis will always remind you that you can achieve anything, if you put your mind to it.

- Last but not least, I give all the honour and thanks to the the Almighty God who has guided me with His tender hand throughout the duration of this study.

List of Figures

Chapter 1: Introduction and Literature Review

Chapter 3: Genome sequencing and analysis of CrleGV-SA after cycle 1 and cycle 5 UV exposure

List of Tables

Chapter 1. Introduction and Literature Review

Chapter 2. Selection of UV-tolerant CrleGV-SA

Chapter 3. Genome sequencing and analysis of CrleGV-SA after cycle 1 and cycle 5 UV exposure

Chapter 4. The effect of ultraviolet radiation on the morphology of Cryptophlebia leucotreta granulovirus

Chapter 5. The effect of selected UV-Protectants on CrleGV-SA and UV-tolerant CrleGV-SA in the laboratory

Appendices I-IIV.

Abbreviations

AaIT	-	*Androctonus australis* insect toxin
Ac32		Homolog of the fibroblast growth factor
AcMNPV	-	Autographa californica multiple nucleopolyhedrovirus
AdorGV	-	Adoxophyes orana granulovirus
AdorGV-E	-	English isolate of Adoxophyes orana granulovirus
AgMNPV	-	Anticarsia gemmatalis multiple nucleopolyhedrovirus
ATR	-	Attenuated total reflection
ATR-FTIR	-	Attenuated total reflection Fourier transform infrared spectroscopy
BASF	-	Badische Anilin und Soda Fabrik
BmNPV	-	Bombyx mori nucleopolyhedrovirus
bp	-	Base pair
BV	-	Budded virion
C1	-	CrleGV-SA sample isolated from UV exposure cycle 1
C5	-	CrleGV-SA sample isolated from UV exposure cycle 5
CDS	-	Coding sequence
CE	-	Columnar epithelium
CGA	-	Citrus Growers' Association
cm	-	Centimetres
CPC		Crop Protection Compendium
CpGV	-	Cydia pomonella granulovirus
CpGV-M	-	Mexican isolate of Cydia pomonella granulovirus
CpGV-ZY	-	Chinese isolate (from Zhangye region) of Cydia pomonella granulovirus

CrleGV	-	Cryptophlebia leucotreta granulovirus
CrleGV-CV3	-	Cape Verde Isolate of Cryptophlebia leucotreta granulovirus
CrleGV-SA	-	South African Isolate of Cryptophlebia leucotreta granulovirus
CRI	-	Citrus Reseach International
CSIR	-	Council for Scientific and Industrial Research
CTAB	-	Hexadecyl trimethyl ammonium bromide
DBP	-	DNA binding protein
DF	-	Degrees of freedom
DNA	-	Deoxyribonucleic acid
egt	-	*Ecdysteroid uridine 5´-diphosphate – glucosyltransferase*
EPA	-	Environmental Protection Agency
et al.	-	*Et alia* (and others)
FCM	-	False codlling moth
FFT	-	Fast-Fourier Transform
fgf	-	Fibroblast growth factor
FFDCA	-	Federal Food, Drug, and Cosmetic Act
FIFRA	-	The Federal Insecticide, Fungicide, and Rodenticide Act
FTIR	-	Fourier transform infrared spectroscopy
GmNPV	-	Galleria mellonella nuclear polyhedrosis virus
g	-	Gram (unit of mass)
g		Relative Centrifugal Force
GV	-	Granulovirus
h	-	Hours
HearNPV	-	Helicoverpa armigera nucleopolyhedrovirus

HearNPV-CBE1	-	Helicoverpa armigera nucleopolyhedrovirus Coimbatore isolate
HzSNPV	-	Helicorvepa zea single-nucleopolyhedrovirus
ICTV	-	International Committee on Taxonomy of Viruses
IPM	-	Integrated Pest Management
IR	-	Infrared
kDa	-	kilodalton
L	-	Litres
LC_{50}	-	median lethal concentration
LC_{90}	-	90 % lethal concentration
LD_{50}	-	median lethal dosage
LT_{50}	-	Median lethal time
LdMNPV	-	Lymantria dispar multiple nucleopolyhedrovirus
LdMNPV-45/0	-	North American strain of Lymantria dispar multiple nucleopolyhedrovirus
LdMNPV-27/0	-	Western Siberia (Asian) strain of Lymantria dispar multiple nucleopolyhedrovirus
Ltd	-	Limited
MAP		Mitogen-activated protein
min	-	Minutes
ml	-	Millilitre
mm^2	-	Square millimeters
NDA	-	National Department of Agriculture
NFkb		nuclear factor kappa-light-chain-enhancer of activated B cells
ng	-	Nanogram
NGS	-	Next generation sequencing
nm	-	Nanometres

NPV	-	Nucleopolyhedrovirus
OAR	-	Original activity remaining
OBs	-	Occlusion bodies
OBs/ha	-	Occlusion bodies per hectare
OB/L	-	Occlusion bodies per litre
ODV	-	Occlusion derived virion
OpMNPV	-	Orgyia pseudotsugata multiple-nucleopolyhedrovirus
OpSNPV	-	Orgyia pseudotsugata single-nulceopolyhedrovirus
ORF	-	Open reading frame
PbGV	-	Pieris brassicae granulovirus
PoGV	-	Pthorimeae opercula (Zeller) granulovirus
PCR	-	Polymerase chain reaction
PE	-	Polyhedron envelope
PhD	-	Philosophiae Doctor
PIB	-	Polyhedral inclusion bodies
PM	-	Peritrophic matrix
Pty	-	Proprietary
REN	-	Restriction enzyme analysis
SA	-	South Africa
SDS	-	Sodium dodecyl sulfate
SE	-	Secondary electron
SeMNPV	-	Spodoptera exigua multiple nucleopolyhedrovirus
SfMNPV	-	Spodoptera frugiperda multiple nucleopolyhedrovirus
Sf9	-	A clonal isolate of *Spodoptera frugiperda* Sf21 cells
SNPs	-	Single nucleotide polymorphisms

spp.	-	Species
TEM	-	Transmission Electron Microscopy
TiO_2	-	Titanium oxide
TnMNPV	-	Trichoplusia ni multiple nucleopolyhedrosis virus
USA	-	United States of America
USDA	-	United States Development Agency
UV	-	Ultraviolet
vfgf	-	Homolog of the fibroblast growth factor
w/v	-	Weight per volume
w/w	-	Weight per weight
ZnO	-	Zinc oxide
°C	-	Degrees celsius
µl	-	Microlitre
µm	-	Micrometre
%	-	Percent

Abstract

Baculoviruses are pathogenic to insects in the orders Diptera, Hymenoptera, and Lepidoptera. As a result of this natural relationship with insects they provide an environmentally friendly method to combat crop and forest pests. As such, a number of baculoviruses have been formulated into biopesticides. The use of baculovirus biopesticides is gaining popularity as the use of chemical pesticides has come under stringent regulatory conditions imposed by governments and continental blocks such as the European Union. Baculoviruses have a narrow host range and therefore do not harm non-pests or humans who consume the crops.

One such baculovirus is Cryptophlebia leucotreta granulovirus (CrleGV), which is pathogenic to the citrus pest *Thaumatotibia leucotreta*, commonly referred to as the false codling moth (FCM). CrleGV has an occlusion body (OB) that encloses a single virion. Several CrleGV biopesticides have been registered in South Africa for use on citrus, avocadoes, macadamias, grapes and other crops by two commercial producers, River Bioscience (SA) and Andermatt (Switzerland). These biopesticides are used as part of the FCM integrated pest management (IPM) programme, a multi-facetted approach to controlling FCM.

However, baculoviruses are susceptible to the ultraviolet (UV) radiation component of sunlight and lose their activity within hours to a few days, after exposure to UV. Several substances have been tested as UV protectants to improve the persistence of baculovirus biopesticides in the field. These include optical brighteners, UV absorbers and anti-oxidants. While very promising in the laboratory, UV-protectants have not been as successful in the field. A few published reports have reported, that UV-tolerant baculoviruses could be isolated from a population by repeatedly exposing and re-

exposing the virus to UV irradiation with a propagation step in insect host fourth or fifth instars between each exposure cycle.

In this study, the South African isolate of Cryptophlebia leucotreta (CrleGV-SA) was exposed to UV irradiation for 5 exposure cycles in a Q-Sun Xe-3 HC test chamber (Q-lab, USA) with parameters set to mimic a typical summer day in the Sundays River Valley, Eastern Cape Province, in South Africa. In between exposures the virus survivors were allowed to multiply in FCM fifth instars. Surface dose bioassays were also conducted to determine the LC_{50} of the virus after each exposure cycle. Samples from exposure cycle 1 and cycle 5 (UV-tolerant) irradiated for 72 h were prepared for Next Generation Sequencing (NGS) of DNA. The resultant sequence data were analysed using the Geneious R11 software (New Zealand) and compared with the unexposed CrleGV-SA sequence. In-silico restriction enzyme analsysis (REN) with several enzymes was also carried on both the cycle 1 and cycle 5 exposed samples and the resulting digestion patterns were compared with the original CrleGV-SA digestion patterns. The same samples were also analysed by transmission electron microscopy (TEM) and Attenuated Reflectance Fourier Transform Infrared Spectroscopy (ATR-FTIR) to evaluate the effect of UV irradiation on the structure of the CrleGV-SA OB. In addition, three UV protectants, lignin sulphate (Sappi, SA), BREAK-THRU®OE446 (OE446) (Evonik Industries, Germany) and Uvinul Easy (BASF, Germany) were prepared with CrleGV-SA to give final protectant concentrations of 0.09 %, 0.9 % and 9 %. The protectant-virus suspensions were exposed to UV for 24 h in the Q-Sun test chamber and bioassays conducted to determine the protective effect of each protectant concentration. The most successful protectants were then combined with the UV-tolerant CrleGV-SA and exposed to UV for 24 h in the Q-Sun test chamber and surface dose bioassays conducted afterwards.

Samples exposed to UV in cycle 5 had lower LC_{50} values compared to samples in the early cycles. With each re-exposure cycle the LC_{50} values moved closer to that of the unexposed control. The LC_{50} of virus samples decreased from 2.89 x 10^8 OBs/ml after 24 h UV-exposure in cycle 1 to 2.16 x 10^5 OBs/ml after the same duration of exposure in cycle 5; and from 2.11 x 10^9 OBs/ml in cycle 1 after 72 h UV-exposure to 1.73 x 10^6 OBs/ml after the same duration of exposure. This represented a 1338-fold difference and a 1220-fold difference, respectively. When the UV-tolerant samples were sequenced seven SNPs were identified in cycle 1, which were thought to help establish UV tolerance, while a further seven SNPs were identified in cycle 5 samples; these were thought to further establish and maintain the UV-tolerance. Additionally, REN analysis with EcoR1 for both test samples yielded digestion patterns that were different from those of the original CrleGV-SA. TEM data showed that UV damages the virion as well as the crystalline structure of the OB. This is the first time visual evidence for UV damage to baculoviruses has been published. Comparison of cycle 1 and cycle 5 UV exposed OBs revealed that the cycle 5 OBs were significantly larger than the cycle 1 OBs ($P \leq 0.05$). In addition, several peaks in the fingerprint region were shown to have either appeared or disapeered from the ATR-FTIR spectra after UV irradiation. However, there was no difference in the spectra of the Cycle 1 and Cycle 5 virus samples. The tests with potential UV-protectants revealed that the 0.9 % lignin, 9 % OE446 and 9 % Uvinul Easy were the most effective in protecting the virus from UV. However, there was no significant difference in their protection of UV tolerant CrleGV-SA and wild type CrleGV-SA. Going forward, it is recommended that the 0.9 % lignin, 9 % OE446 and 9 % Uvinul Easy combinations be explored further in future studies, particulary in the field. This study therefore forms an important foundation for the development of UV-tolerant baculovirus that will last longer in the field.

Chapter 1

Introduction and Literature Review

1.1 Introduction

In recent years, biological control of agricultural pests has gained popularity, due to pressure on the need to reduce agrochemicals in the environment and in food as well as to provide alternatives to combat pest resistance to chemical pesticides (Szewczyk *et al*., 2006). Stricter regulations have been implemented by governments to limit the manufacture and use of agrochemicals. In the United States of America (U.S.A), several legislative acts have been passed to regulate and control the use of pesticides. The Federal Insecticide, Fungicide, and Rodenticide Act (FIFRA) of 1947, was first enacted to control pesticide quality and has been amended several times to ensure that more was known about each chemical before it is registered for use in the field and limitations were placed on how much residual pesticide was acceptable in or on food products where the pesticides where applied (Arthurs & Dara, 2018). A 1972 amendment to FIFRA, gave the US Environmental Protection Agency (EPA) authority over pesticide regulation in that country. The EPA also regulates pesticides under the Federal Food, Drug, and Cosmetic Act (FFDCA). The FFDCA governs issues related to human exposure to pesticides and the setting of allowable limits of pesticides in and on food (Leahy *et al.,* 2014; Arthurs & Dara, 2018). In South Africa several chemical pesticides have been withdrawn through legislative instruments since the 1970s. Examples of banned or restricted chemicals in South Africa include, kepone (1971), 2,4-D (dimethylane salt) whose aerial application was banned in 1991, chlordane

whose use was restricted to citrus stems and structures by pest control operators and eventually withdrawn as agricultural product in 2000 and monocrotophs that were banned in 2005 (NDA, 2019). This has resulted in a higher cost for synthetic pesticides available and in some cases their shortage as well (Haase *et al*., 2015). The development of pest resistance to synthetic pesticides has also accelerated the rise of biological control as an alternative (Szewczyk *et al.,* 2006). Biological control involves the conservation, introduction or augmentation of natural enemies or pathogens in an environment to control a species that has attained pest status (Lacey *et al.,* 2001; Szewczyk *et al.,* 2006). Natural pathogens such as bacteria, fungi and viruses are gaining popularity as biological controls for pests. These are generally specific for their target organisms and so are safe for beneficial insects as well as for human application and consumption (Knox *et al.,* 2015). Biological control methods are part of the integrated pest management (IPM) programme which incorporates cultural, physical, chemical and biological methods to control pests (Orr, 2009).

The Baculoviridae is one virus family that has been studied extensively for its potential in pest control in agriculture and forestry. These viruses have been isolated from a wide range of insect hosts in the orders Lepidoptera, Hymenoptera and Diptera (Herniou *et al.,* 2011). Baculoviruses are regarded as safe to vertebrates and highly specific to their target host (most cases infecting only a single species) (Lacey *et al.,* 2001). A large number of baculovirus biopesticide formulations are registered across the world presently (Moscardi, 1999; Knox *et al.,* 2015; Haase *et al.,* 2015). The main setback for their usage however is the susceptibility of baculoviruses to ultraviolet radiation (UV) (Arthurs *et al.,* 2008). Therefore, there is a need to investigate ways in which baculovirus formulations may be improved to increase their persistence in the field.

This chapter discusses baculoviruses as biopesticides, challenges associated with the use of baculovirus biopesticides particularly UV irradiation, Cryptophlebia leucotreta granulovirus (CrleGV) and the citrus pest *Thaumatotibia leucotreta* the false codling moth (FCM). In addition, the aim and objectives of this study are defined.

1.2 Baculoviruses

1.2.1 History

Research into silkworm diseases led to the initial discovery of baculoviruses. Infected silkworms displayed dense insoluble occlusion bodies (OB). These silkworm diseases were called polyhedrosis due to the polyhedron shape of the OBs (Rohrmann, 2013). Advances in the field of electron microscopy led to the discovery of the presence of rod-shaped virions within these OBs, as well as identifying the crystalline nature of the OB (Bergold, 1947).

1.2.2 Taxonomy

Baculoviruses were initially classified according to their morphology. This resulted in two main groups, the nucleopolyhedrovirus (NPVs) and granuloviruses (GVs) (Murphy *et al.,* 1995). The main difference between these groups being the OB protein composition. NPVs have polyhedrin as the main OB protein, while GVs have granulin (Akermann & Smirnoff, 1983). Advances in molecular techniques have enabled researchers to compare genomes of various baculoviruses. These phylogenetic studies have revealed distinct patterns of relationships among the baculoviruses, in which lineages are associated by the hosts they infect (Jehle *et al.,* 2006a). This has led to a new classification system proposed by Jehle *et al.* (2006b) and ratified in the 9th International Committee on Taxonomy of Viruses (ICTV) report (Herniou *et al*.,

2011). Under the current classification, four genera have been identified and these are: *Alphabaculovirus* and *Betabaculovirus*, which consist of lepidopteran NPVs and GVs respectively, while *Gammabaculovirus* and *Deltabaculovirus* are pathogenic to sawfly (hymenopteran) NPVs and mosquito (dipteran) NPVs respectively (Jehle *et al.,* 2006b, Herniou *et al.,* 2011). The alphabaculoviruses are further divided into group I and group II. Group I alphabaculoviruses use Gp64 as the major envelope fusion protein while Group II alphabaculoviruses and betaculoviruses use the envelope protein F (Pearson and Rohrmann, 2002). It is still considered acceptable to refer to alphabaculoviruses and betabaculoviruses as NPVs and GVs, respectively. The NPVs may have single (S) or multiple nucleocapsids (M) (Fig.1.1).

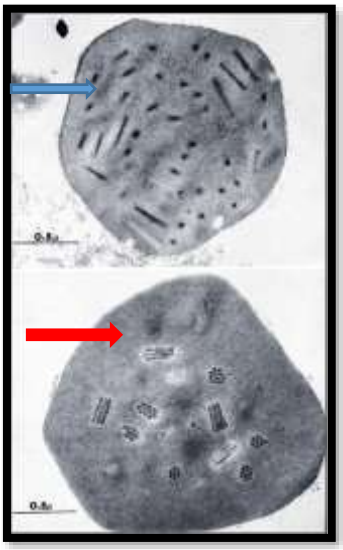

Figure 1.1: Two NPVs pathogenic for *Orgyia pseudotsugata* showing single (OpSNPV) (blue arrow) and multiple (OpMNPV) (red arrow) nucleocapsids (Hughes & Addison, 1970).

1.2.3 Baculovirus Structure

Virus particles (virions) occur in two morphologically distinct forms. These are the budded virions (BV) and the virus occlusion derived virions (ODV) (Fig.1.2). Both have an identical nucleocapsid and carry the same genetic information but serve distinctly different functional roles (Blissard, 1996). ODVs are mainly involved with initiating infection in host epithelial cells of the midgut. BVs on the other hand facilitate the infection into the rest of the tissues within the insect (Blissard, 1996).

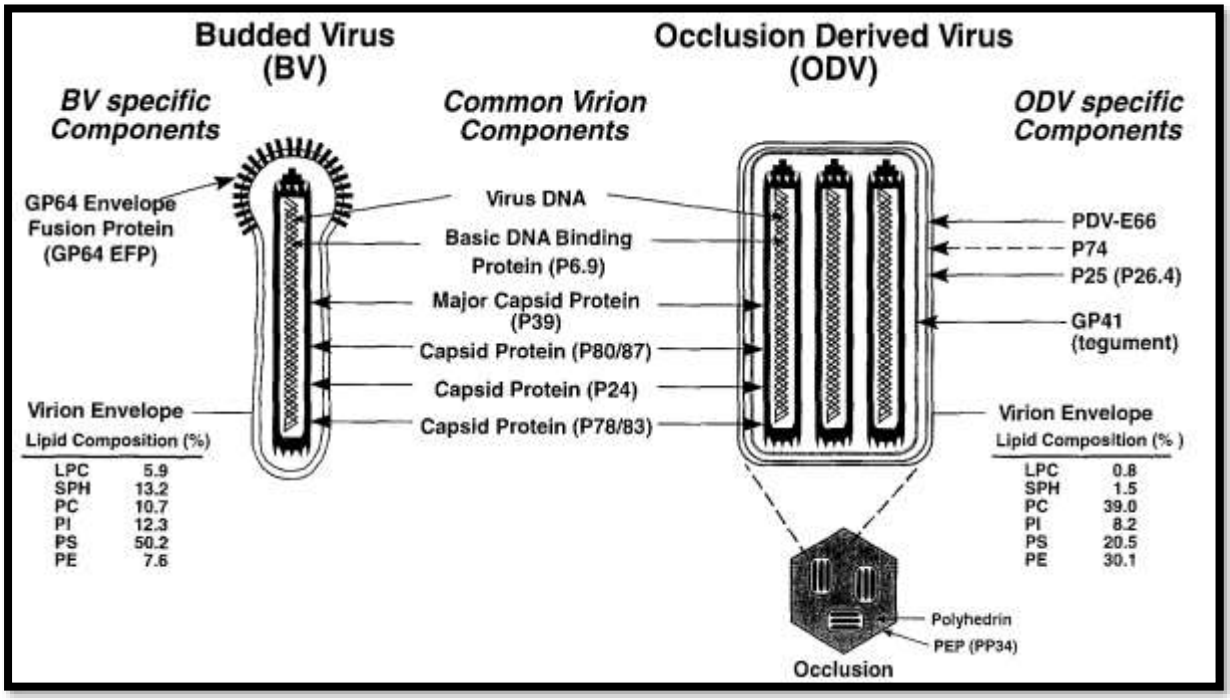

Figure 1.2: Structural composition of the two baculovirus virion phenotypes. Major features associated with the budded virus (BV) and occlusion derived virus (ODV) are indicated in the diagram (Blissard, 1996).

The Baculoviridae are enveloped within a proteinaceous OB. The main OB protein is polyhedrin in NPVs (Fig 1.3a) and granulin in GVs (Fig 1.3b). The polyhedrin/granulin OB is crystalline in nature and surrounds virions. This OB confers environmental stability to the baculoviruses and prevents solubilisation unless when subjected to

harsh alkaline conditions (Russell & Rohrmann, 1990). The OB allows the virion to remain infectious for a very long time (Rohrmann, 2013). The hyperexpressed polyhedrin and granulin proteins, both contain approximately 250 amino acid residues and are the most conserved baculovirus proteins (Rohrmann, 1986). NPV OBs have a diameter of about 0.6-2.0 µm while GVs have diameters in the range 0.2-0.4 µm (Akermann & Smirnoff, 1983).

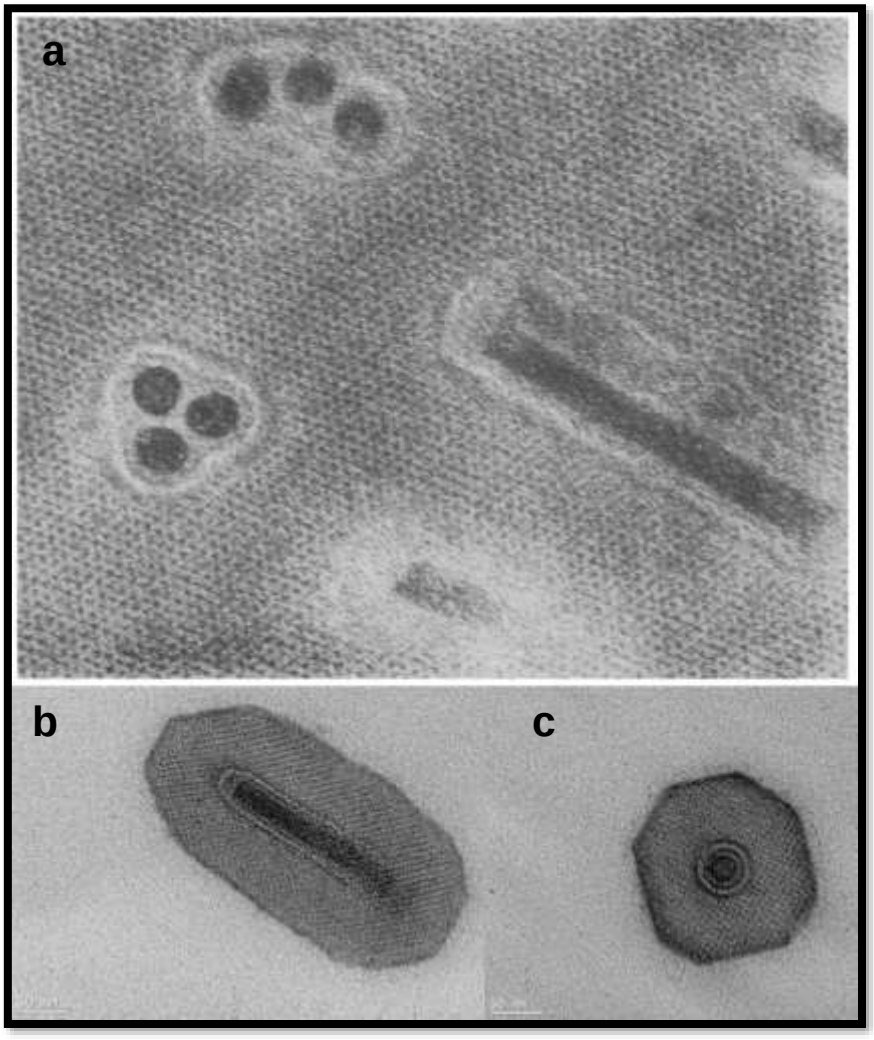

Figure 1.3: The Crystalline structure of polyhedrin (a) (Rohrmann, 1986) and granulin in longitudinal and transverse sections OBs (b & c).

In addition to polyhedrin/granulin, two other proteins, p10 protein and the polyhedron envelope (PE) protein also form part of the OB. The hyper expressed p10 protein

appears to be required for the formation of the polyhedron envelope (Rohrmann 1992). Evidence for this is derived from experiments involving the complete deletion of the p10 gene, which resulted in the formation of incomplete patches of the PE, and hence fragile OBs that disintegrated readily (Williams *et al.,* 1989). When the p10 gene was replaced with the β-galactosidase gene controlled by the p10 promoter, the PE was completely absent (Zuidema *et al.,* 1989).

The third protein making up the OB is the PE protein which is associated with the polyhedron envelope (also known as the calyx). The PE surrounds polyhedra and acts to seal the polyhedra surface, thereby conferring more stability. The 34 kDa PE protein has been observed to associate with the periphery of prominent infected cell-specific fibril-like structures in the cytoplasm and nucleus (Whitt & Manning, 1988; Russell & Rohrmann, 1990). Laboratory experiments showed that after alkaline treatment the PE remains as a bag-like structure in which the virions are enclosed. Furthermore, it was reported that PE protein was sensitive to a protease suggesting the associated PE protein was responsible for the integrity of the PE (Russell & Rohrmann, 1990). Thus, it is possible that the combination of the alkaline mid-gut conditions and action of proteinases aids virion release within the insect mid-gut.

1.2.4 Baculovirus life cycle

Insect larvae ingest OBs as contaminants while feeding on foliage or fruit. The alkaline conditions of the mid- gut dissolve the OB leading to the release of the ODV (Fig.1.4) (Blissard, 1996). It is thought that proteinases in the insect gut or OB-associated proteinases digest the calyx surrounding the OB (Russell & Rohrmann, 1990). Other bacterial proteinases from non-specific contamination in the insect gut, as well as metalloproteins, known as enhacins, encoded by the baculovirus aid in the digestion

of a mucin component of the insect peritrophic matrix (PM), giving the ODV access to the underlying gut epithelial cells (Wang & Granados, 1997; Toprak *et al.,* 2012). ODVs enter the epithelial cells after fusion with microvilli membranes and initiate primary infection of these columnar epithelial cells (Moscardi *et al*., 2011). Upon entry into the cells ODVs are then transported by actin transport to the nuclear membrane (Blissard, 1996; Ohkawa *et al.*, 2010; Rohrmann, 2013). Ohkawa *et al.* (2010) investigated the transport mechanism of nucleocapsids of the baculovirus Autographa californica multiple nucleopolyhedrovirus (AcMNPV) and determined that the virus requires actin transport for motility across the cytoplasm immediately after entering the cell. This is followed by translocation through the nuclear pore complex into the nucleus and subsequent transport across the cytoplasm after nucleocapsid assembly in the nucleus (Fig.1.5). Au and Pante (2012) corroborated these findings when they confirmed that nucleocapsid translocation into the nucleus is facilitated via the nuclear pore complex. In the nucleus, transcription is initiated, viral nucleocapsids are assembled and transported by kinesin to nuclear membrane (Rohrmann, 2013). Virions bud out of the nucleus and are enveloped by the nuclear membrane, which is then lost as the virion (now termed the budded virus (BV)) moves through the cytoplasm (Granados & Lawler, 1981). In preparation to release the BV, virus derived envelope proteins form clusters on the cell membrane (Fig.1.5) (Rohrmann, 2013). In group I alphabaculoviruses the envelope proteins are GP64 and the F protein, while in group II alphabaculoviruses and betabaculoviruses homologs of the F protein are involved in membrane modification (Blissard & Rohrmann, 1989; Pearson *et al*., 2000; Pearson *et al.,* 2001). In AcMNPV infected insect mid-gut cells, Gp64 is mainly distributed towards the basal and lateral aspects of the cell so as to promote systemic infection of susceptible tissues and neighbouring cells and prevent virions from

budding back into the gut lumen (Keddie *et al.,* 1989; Engelhard *et al.,* 1994; Monsma *et al.,* 1996).

Systemic or secondary infection follows the budding of BV (Rohrmann, 2013). In order to achieve this, BV must cross the insect gut basal lamina. The fibroblast growth factor (fgf) homolog vfgf (Ac32) has been cited as essential in facilitating movement of the BV across the basal lamina (Katsuma *et al.,* 2006; Detvisitsakun *et al.,* 2007; Katsuma *et al.,* 2008; Means & Passarelli, 2010). When the vfgf gene was deleted from both AcMNPV and Bombyx mori nucleopolyhedrovirus (BmNPV) in cell culture no differences were observed from the wild types, however when the mutants were fed to larvae, the time of death was delayed (Katsuma *et al.,* 2006; Detvisitsakun *et al.,* 2007). The slower time of death in the mutants suggests that vfgf accelerates the rate of infection and insect death (Means & Passarelli, 2010). It has been suggested that Ac32 (vfgf) plays a role in assisting BVs to transverse the basal lamina by two processes (Rohrmann, 2013). vFGF in virus infected mid-gut cells diffuses through the basal lamina, attracting tracheal cells to the mid-gut cells with the basal lamina being the only barrier between the two types of cells. Activation of vFGF receptors leads to the activation of matrix metalloproteases using either a MAP kinase or NFkB pathway. These in turn activate caspases to move and digest the lamnin content of the basal lamina. This allows the BV to infect the tracheal cells and provides passage to infect other tissues (Means & Passarelli, 2010).

GP64 or F protein are required for secondary infection depending on what type of baculovirus is involved. In Group I alphabaculoviruses, GP64 is involved in initiating infection of other cells (Fig.1.6) (Blissard & Rohrmann, 1989; Ijkel *et al.,* 2000; Pearson *et al*., 2001). AcMNPV studies suggest that micropinocytosis, dynamin- and clathrin-dependent endocytosis and cholesterol in the plasma membrane may be involved in

virus entry into mammalian cells (Means & Passarelli, 2010). It is also suggested that gp64 mediated cell entry may be as a result of specific receptor independent fusion (Tani *et al*., 2001; Long *et al.,* 2006; Kataoka *et al.,* 2012). A clathrin mediated endocytosis making use of non-specific receptors such as phospholipids is therefore suggested (Tani *et al*., 2001). Acidification of resultant endosomes causes the viral envelope to merge with the endosome membrane, leading to the release of the nucleocapsid into the cytoplasm (Rohrmann, 2013). The nucleocapsid then transverses the cytoplasm and into the nucleus through the nuclear pores and secondary replication is initiated (Long *et al.,* 2006). Newly assembled nucleocapsids either exit to further systemic infection, or remain in the nucleus and become occluded. In NPVs, hyper-expression of the very late genes, polyhedrin and p10 takes place and gives rise to a high concentration of the proteins polyhedrin and P10 in the nucleus (Rohrmann, 2013). Subsequent crystallization of polyhedrin into a lattice surrounding the virion gives rise to OBs. Several proteins such as Ac68 and P10 are thought to be involved in this process (Patmanidi *et al*., 2003; Carpentier *et al.,* 2008; Xu *et al.,* 2008a).

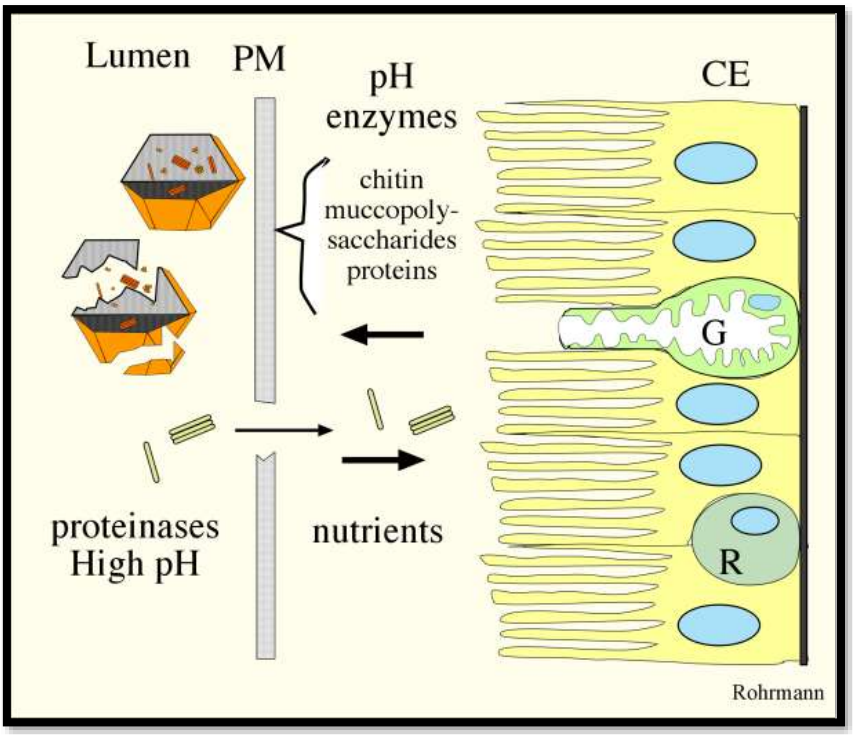

Figure 1.4: Virus infection in the insect midgut. The peritrophic matrix (PM) is established by the secretion of chitin, muccoplysaccharides and proteins by the midgut cells. The cells also secrete digestive enzymes and ions that regulate the midgut pH. Three types of midgut cells are shown: columnar epithelium (CE), goblet cells (G), and regenerative cells (R) (Rohrmann, 2013).

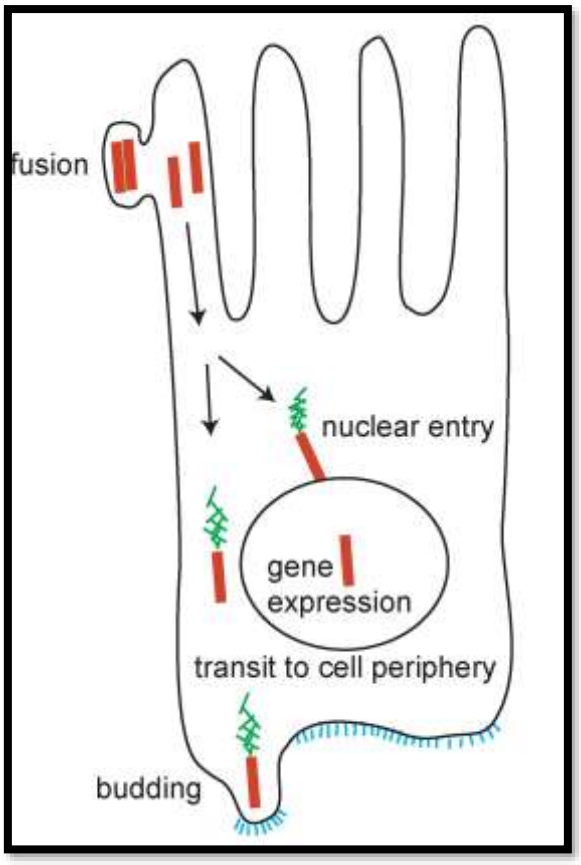

Figure 1.5: The roles of actin-based motility in baculovirus transport during the early phase of infection of a midgut epithelial cell. Nucleocapsids are shown in red, actin in green and GP64 in blue Ohkawa *et al*., (2010).

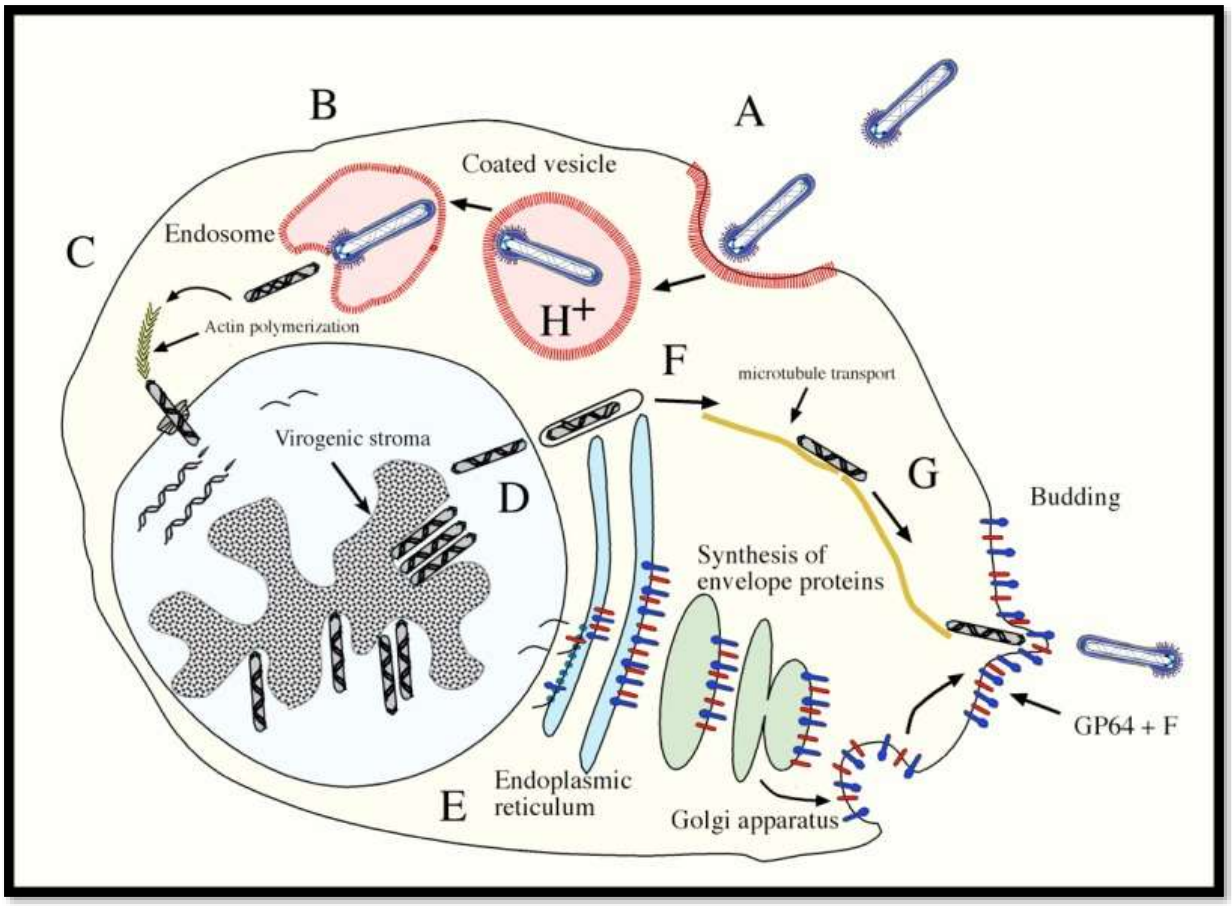

Figure 1.6: Stages in budded virus infection of a Group I virus. (A) BV attachment to receptors and endocytosis. (B) Acidification of endocytotic vesicle and fusion of endosomal membrane with virion envelope to release the nucleocapsid into the cytoplasm. (C) Passage into the nucleus and transcription of genes followed by (D) DNA replication and nucleocapsid assembly in the virogenic stroma. (E) Synthesis of GP64 and F proteins and their subsequent incorporation into the cytoplasmic membrane. (F) Nucleocapsids exit the nucleus and (G) bud through the F- and GP64-modified cytoplasmic membrane (Rohrmann, 2013).

1.3 Baculoviruses as biopesticides

The use of synthetic chemical pesticides has been decreasing over the past few years. This is due to several reasons. Most of the chemical pesticides are broad spectrum pesticides that tend to unintentionally kill non-target insects (Szewczyk *et al*., 2006). These non-target insects may be pollinators such as bees, predators or parasitoids of

other pests, which would now thrive because of the absence or decreased numbers of the natural enemies (Hajek, 2004). Public outcry over human health and environmental effects such as pollution, the contribution to the reduction of the ozone layer and to global warming caused by chemical pesticides has led to various governments drafting legislation aimed at strictly regulating the use of chemical pesticides (Hajek, 2004). In addition, the increase in resistance of target pests to chemical pesticides has culminated in the reduction of their use and an increase in the search for alternatives (Casida and Quistad, 1998; Fitches *et al.*, 2010; Al-Zaidi *et al.*, 2011).

The challenges to the use of synthetic chemical pesticides have necessitated alternative approaches to pest control. One such approach is integrated pest management (IPM) which is a sustainable approach to managing pests by combining biological, cultural, physical, and chemical tools in a way that minimizes economic, health, and environmental risks (Food Quality Protection Act. 1998; Chandler *et al*., 2011; Knox *et al.,* 2015). Baculoviruses play a crucial role in IPM programmes of various crops. Despite the fact that there are many insect viruses, only the baculoviruses have been developed into commercial biopesticides (Erlandson, 2008). In addition to their role in pest control, baculoviruses are also used as gene expression vectors, delivery systems in gene therapy and in the production of new generation vaccines (Moscardi, 1999; Kost *et al.,* 2005; Hu, 2006; Moscardi *et al.,* 2011; Lapointe *et al.,* 2012; Pidre *et al.,* 2013). Baculovirus biopesticides are currently being employed in various IPM programmes around the world. The use of baculoviruses as biopesticides dates back as far as the early 19th century, particularly in forestry and in the production of orchard and field crops (Szewczyk *et al.,* 2006). There are several advantages to the use of baculovirus biopesticides. Individual baculoviruses are highly

specific to their host, with most baculovirus species being pathogenic to a single insect species or closely related insect species (Beas-Catena *et al*., 2014). Another advantage of baculovirus biopesticides is that they are generally safe to vertebrates and other beneficial organisms (Beas-Catena *et al*., 2014). Presently over 50 biopesticide formulations (some include the same baculovirus marketed under a different name) have been produced around the world (Szewczyk *et al*., 2006; Moscardi *et al*., 2011; Knox *et al*., 2015).

1.3.1 Challenges facing the use baculovirus biopesticides

1.3.1.1 High specificity

The use of baculovirus biopesticides faces various challenges. Their high specificity while being an advantage, can be a disadvantage too. The high specificity of baculoviruses is useful if there are other beneficial insect species present (Reardon *et al.*, 2009). However, crops may be more than one pest at a time and therefore highly specific baculovirus biopesticide treatment is ineffective against the other pests (Claus *et al.,* 2012). This could result in other pesticides being required to combat the different pests and increased costs to the farmer. This would encourage farmers to opt for broad-spectrum pesticides instead (Harrison & Hoover, 2012). Consequently, most of the registered baculoviruses biopesticide are against economically significant pests such as *Thaumatotibia leucotreta* (FCM) and *Cydia pomonella*. Where possible the use of broad host-range baculoviruses such as AcMNPV may be a solution to this challenge provided they are susceptible at economically acceptable and feasible concentrations in the field (Black *et al.,* 1997).

1.3.1.2 Slow Action

The slow action of baculoviruses is another disadvantage. It takes time before the effect of the baculovirus is manifested, and this results in increased crop damage. This might be attributed to the presence of the *egt* gene in baculoviruses, which has been shown to prolong the host larval stage to allow for replication of virus (Maeda, 1989). It is possible to overcome this by genetically modifying the baculovirus to achieve a faster speed of kill (O'Reilly & Miller, 1991). A second option which has been suggested is to target hormones of insect larvae. It was with the case with the introduction of a diuretic hormone to BmNPV, which led to a 20 % increase in the speed of kill of *Bombyx mori* larvae compared to the wild type virus (Maeda, 1989). Loss of water was thought to be the reason for the increase in speed of kill (Maeda, 1989). The introduction of the scorpion toxin gene AaIT in an AcMNPV genome led to a 40 % increase in the speed of kill of *Autographa californic*a larvae and 60 % reduction in feeding damage (Maeda *et al.,* 1991; Inceoglu *et al.,* 2001). The peptide AaIT targets sodium channels in insects in a similar way as do synthetic chemicals (Bloomquist, 1996). However, at this stage there has been no reported commercial recombinant baculovirus biopesticide (Szewczyk *et al.*, 2006). The challenges with recombinant virus production is the negative public sentiment towards this technology, restrictive regulations imposed on the use of such biopesticides and the high production cost. As a consequence, it may be years before recombinant baculovirus biopesticides are commercially available (Szewczyk *et al*., 2006). Other alternatives that could be used to improve the speed of kill include selection by repeated passage through a heterologous host or by application of virus combinations (Arrizubieta *et al.,* 2015; Graillot *et al.,* 2017)

1.3.1.3 Baculovirus Mass production

One of the most important fundamental requirements for baculovirus biopesticide production is the need to produce the biopesticide of a suitable quality, in sufficient quantities and at an affordable cost (Grzywacz & Moore, 2017). Commercial baculovirus production is currently carried out *in vivo* in host insects in specialised production facilities or in the field (Shapiro, 1986; Black *et al*., 1997; Grzywacz *et al.,* 2014a). Susceptible insect hosts are infected with the baculovirus under appropriate rearing conditions. This enables the baculovirus to multiply within the host and be extracted from the infected (dead or very sickly) (Grzywacz *et al.,* 2014b). However, this is a labour intensive process and has challenges with scaling up production to ensure profitability (Claus *et al.,* 2012). The cost of production of baculovirus *in vivo* in insect larvae remains generally high, compared to the cost of production of chemical pesticides, and as a consequence, the cost per hectare on the farm is difficult to reduce to below US $20 (Lacey *et al.,* 2015). The majority of *in vivo* baculovirus production takes place in specialised laboratory facilities, however this can also be carried out in the field as is the case with Spodoptera exempta nucleopolyhedrovirus (SpexNPV) used in the control of the African armyworm, a major migrant pest in Africa (Grzywacz *et al.,* 2014b).

Cell-culture based mass production has been identified to have several advantages over using host insects and potentially presents an alternative to overcome the challenges currently limiting production of baculoviruses (Black *et al.,* 1997; Moscardi *et al.,* 2011; Claus *et al.,* 2012; Lacey *et al.,* 2015). Cell-culture based production could potentially allow for a more affordable and flexible system. This could be achieved by having a single bioreactor to support a variety of frozen cell lines and potentially be used to produce as many baculoviruses as needed (Claus *et al.,* 2012; Reid *et al.,*

2014). Cell-culture based mass production could also allow for the production of genetically modified baculoviruses (Black *et al.,* 1997; Inceoglu *et al.,* 2006).

While producing virus *in vitro* in cell culture is an alternative, insect cell lines are generally difficult to maintain in the commercial environment and at this stage only a few cell lines have been found to have the requisite properties to ensure virus production at a profitable rate (Pedrini *et al.,* 2011; Claus *et al.,* 2012). These requisite properties for a prospective cell include, susceptibility of cell line to virus, which should be able to replicate quickly (<24 h) and produce high yields of BVs and OBs (>200 OBs/cell), the nutrition and metabolism of the cell line should be well characterised and be readily adaptable to growth in suspension cultures and in low cost serum, and in industrial bioreactors. Additionally, the cell line should be stable and not lead to virus variation (Claus *et al.,* 2012; Reid *et al.,* 2014). Currently, one of the main challenges with *in vitro* baculovirus production is the low OB/cell yield and the variable OB quality (Nguyen *et al.,* 2011). Furthermore, despite the development of many insect cell lines that can support viral replication, only a few meet the above mentioned prerequisites (Lynn, 2007). Presently, a few cell lines namely Sf9 and BTI-TN-5B1-4 are able to produce high yields of OBs at levels required for commercial production. Several cell lines have various limitations which restricts their use at a commercial level. For example, the cell line BCIRL-HZ-AM1 used in the production of *H. armigera* single nucleopolyhedrovirus (HearSNPV) which can grow in a low cost serum free medium and produce high yield of OBs has limited BV production which are an essential requirement for scaling up (Lua & Reid, 2003; Pedrini *et al.,* 2011). The cell line saUFL-AG-286, used in the production of AgMNPV also grows in a low cost serum free suspension cultures but the production of OBs is inhibited at cell densities higher than 8×10^5 cells/ml, thus reducing the volumetric yield of OBs (Micheloud *et al*., 2009).

While small scale production of functional OBs has been achieved, scaling up to industrial production has not yet been achieved, with reduced yield and virulence being the main drawbacks (Lua & Reid, 2003; Grzywacz & Moore, 2017). To adequately meet the commercial requirements for baculovirus production, bioreactors of size greater than 10 000 L would be required (Black *et al.,* 1997; Reid *et al.,* 2014). Because cell cultures would require oxygen, stirred tank reactors would be the most suitable, however this creates a new challenge of balancing the need for oxygen with physical stress from the stirrers that could damage the cells. As the bioreactors become larger the turbines can create forces enough to damage cells (Claus *et al.,* 2012; Grzywacz & Moore, 2017). Thus, while there is a lot of research being conducted to develop cost effective in vitro systems for the production of baculoviruses, there is more that needs to be done if mass cell culture techniques are to be used to produce OBs at an industrial scale (Reid *et al.,* 2014; Lacey *et al*., 2015).

1.3.1.4 Development of resistance to baculovirus biopesticides

A more serious challenge emerging over the past few years is the development of resistance against baculovirus biopesticides. The development of resistance in Cydia pomonella granulovirus (CpGV) is a case in point. CpGV is used in protection of apple orchards against the codling moth, *Cydia pomonella*. Before resistance to CpGV was detected, CpGV products were made using the Mexican isolate, CpGV-M (Eberle *et al.*, 2008). Fritsch *et al*. (2005) reported on the possible existence of codling moth resistance to CpGV in 2005. Several more cases have been reported across Europe since then (Sauphanor *et al*., 2006, Jehle *et al.,* 2017). Some of the resistant populations were found to be 1000-100000 times less susceptible to CpGV than normal larvae (Asser-Kaiser *et al.*, 2007).

Three types of resistance have been identified. In the CpGV-M strain, systemic resistance was detected in all CpRR1 codling moth instars and an early block in virus replication was found to be inherited in an incompletely dominant monogenic mode linked to the Z chromosome (Asser- Kaiser *et al.*, 2007, 2010a; 2010b; Jehle *et al*., 2017). This type 1 resistance only targeted CPGV-M (Type A), while the rest of the isolates B-E were able to overcome the resistance. Genome sequencing of different CpGV isolates revealed that all resistance-breaking isolates lacked a repeat insertion of 24 bp in the gene pe38 (ORF24) as the only common difference to CpGV-M (Gebhardt *et al.,* 2014). As such, type I resistance could be overcome by using isolates other than the CpGV-M isolate (Eberle *et al.,* 2008; Berling *et al.,* 2009).

A second type of resistance that affects isolates of CpGV-M as well CpGV groups C-E was recently identified in a codling moth population NRW-WE. Sauer *et al*. (2017a) demonstrated that type II resistance followed a dominant, monogenic but autosomal inheritance pattern. CpGV-M and CpGV-S also showed cross resistance. A third type of resistance was identified after a *C. pomonella* field population from north-eastern Germany, called SA-GO, also showed a reduced susceptibility to both CpGV-M and CpGV-S. Statistical data from crossing experiments suggested a polygenic inheritance pattern in the majority of the backcrosses for resistance to both viruses (Sauer *et al.,* 2017b).

With the threat of resistance growing, it is important to search for new isolates that will overcome resistance. It is also important to use baculovirus biopesticides as part of IPM programmes so as not to depend on them as the sole control method. Recently, Opoku-Debrah *et al.* (2013 & 2016) reported the identification of five new genetically distinct CrleGV-SA isolates, recovered from laboratory colonies of FCM from different geographical regions in South Africa. Restriction enzyme analysis (REN) of viral

genomic DNA and PCR amplification and sequencing of the *granulin* and *egt* genes enabled the classification of the new isolates and the two commercial isolates into two phylogenetic groups. Group I comprised of Cryptex®, CrleGV-SA Ado, CrleGV-SA Mbl, CrleGV-SA Cit, and CrleGV-SA MixC), while Group II is made up of Cryptogran® and CrleGV-SA Nels (Opoku-Debrah *et al.,* 2013). This is very important in the event that FCM develops resistance to the current isolates used in biopesticide formulations.

1.3.1.5 Ultraviolet radiation

Ultraviolet (UV) radiation is the biggest threat to the use of baculovirus biopesticides (Jacques, 1977; Shapiro, 1995). Although the OB protects the virion from various environmental factors, it does not offer protection against UV (Grzywacz, 2017; Mwanza, 2015). There are several ways in which UV is thought to cause loss of activity in baculoviruses. UV induces the formation of pyrimidine dimers by cross linking adjacent pyrimidine residues. The resultant dimers can cause the DNA to bend. This may inhibit the ability of the DNA replication complex to copy beyond the damaged site, or lead to the incorporation of incorrect nucleotides giving rise to lethal mutations, or inhibit the interaction of proteins involved in gene regulation (Tyrrell *et al.,* 1974; Rohrmann, 2013). Direct DNA damage is also characterised by deletions, strand breakage and the formation of labile sites on the DNA, while indirect effects are due to the formation of radicals (Ravanat *et al.*, 2001). A third possibility suggested is that DNA damage in baculoviruses is due to the formation of UV-generated reactive oxygen species such as peroxides, single oxygen, or hydroxyl radicals (Ignoffo & Garcia, 1978; Ignoffo *et al.,* 1989). Ignoffo and Garcia (1994) showed that the anti-oxidants, propyl gallate, ascorbic acid and phenylthiocarbamide as well as the oxidative enzymes catalase superoxide dismutase and peroxidase provided UV protection to the corn earworm NPV, Helicorvepa zea single-nucleopolyhedrovirus

(HzSNPV). This provided evidence for the hypothesize that UV generates reactive oxygen radicals that inactivate OBs. However, they pointed out that at the time, none of the materials they had used could be practically to provide UV protection at a commercial level.

Several studies have established that the medium wave or erythermal UV band (UVB, 280-320 nm) is the most severe component of UV to baculoviruses, with the near-UV region (UVA, 320-360 nm) being severe, yet slower in effect (David, 1969; Timans, 1982; Griego *et al.,* 1985; Burges and Jones, 1998). UVC (100-280 nm) is the least severe, because it is reflected by the ozone layer and clouds before reaching the earth's surface (Robberecht, 1989). Shapiro and Domek, (2002), used five different combinations of fluorescent combinations of UVA, UVB and white light to demonstrate effect of UV on the beet armyworm NPV, Spodoptera exigua multiple nucleopolyhedrovirus (SeMNPV) and HzSNPV. They used inexpensive UV lamps to come up with UVA/UVA, UVB/UVB, UVA/UVB, UVB/White and White/White light combinations. As expected the UVB/UVB combination produced the greatest amount of total radiation and subsequently led to the highest inactivation levels. This was recently corroborated in a study with CrleGV-SA, where UVB caused damage more rapidly than UVA (Mwanza, 2015). However, Shapiro and Domek (2002) found that the UVB/White light combination yielded a lower total radiation than the UVB/UVB combination but a greater virus inactivation than the UVA/UVB combination. This raised questions about the role of UVA in the inactivation of baculoviruses. It has however been shown that in bacteria, UVA caused DNA single-strand breaks (Tyrrell *et al.,* 1974). UVA is known to promote photosensitisation of DNA, activated by single oxygen radicals in photosensitisation type II and by electron abstraction in photosensitisation type I (Girard *et al.,* 2011). Hence it is highly plausible that UVA is

associated with oxidative DNA damage. Unlike UVB, UVA does not form cyclobutane pyrimidine dimers, pyrimidine (6-4) pyrimidone photoproducts and their Dewar valence isomers because DNA is not able to absorb UVA readily (Ridley *et al.,* 2009; Girard *et al.,* 2011).

The total amount of UV incident (flux) in a field will vary depending on the geography and season (Barker, 1968). Thus, some areas receive more UV than other because of the position on the earth as well as what time of the year it is. As a result, it is possible to predict when viruses are most likely to be degraded by using models that predict average fluxes in different areas and at different times of the year (Cutchis, 1982).

1.3.2 The effect of UV on baculoviruses

In laboratory experiments as far back as the 1950s, the link between UV irradiation and baculovirus inactivation was already being investigated (Watanabe, 1951, Aizawa, 1953). Granuloviruses were shown to be the most susceptible to UV, among the microbial control agents tested by Ignoffo *et al.,* 1977. *Bacillus thuringiensis* was shown to be the least sensitive in the same study while NPVs were only less sensitive than *Vairimorpha necatrix* a protozoa and the granulovirus. Early work showed that baculoviruses like Pieris brassicae granulovirus (PbGV) were susceptible to certain wavelengths of UV radiation and decreased in virulence when exposed to shorter wavelengths (David, 1969; Morris, 1971). Other baculoviruses have been shown to lose most of their activity within 24 hours of exposure to direct sunlight (David & Gardiner, 1967; Young & Yearian, 1974; Jacques, 1985). Ignoffo *et al*. (1977) showed that the half-life of PbGV was approximately 2 h and that after 4 h of UV exposure, the percentage original activity remaining (OAR) averaged 4.5. In comparison the

interpolated half-life of HzSNPV after 4 h UV exposure was approximately 2.2 h and the percentage OAR averaged 7.5. The *Spodoptera littoralis* NPV was shown to have inactivation rates higher than 90 % after 4 hours of exposure to sunlight irradiation, and close to 99 % after 8 hours of exposure (Jones *et al*., 1993). In the same study it was shown that wavelengths between 300 nm and 320 nm resulted in the most inactivation of the virus. Shapiro *et al,* (2002), showed that HzSNPV was more sensitive to UV than SeMNPV at all concentrations tested. It was noted that UV inactivation was inversely proportional to the virus concentration present and directly proportional to the time of exposure. Additionally, the degree of UV inactivation varies between different baculovirus species.

Under field conditions the half-life of baculoviruses, varies greatly from 10 hours to 10 days with the average half-life being around 24 hours in the absence of any form of UV protection (Jacques, 1985; Burges & Jones, 1998). This obviously varies from species to species as well as the feeding area of the target pest. It has been shown that the amount of UV reaching leaf under-surfaces in the lower canopy of trees is only 1 %, as compared to the top of cotton plants (Jones, 1988). Therefore, virus applications are targeted to leaf under surfaces to maximise the virus persistence as well. Additionally, the under surface of leaves is preferred feeding site for neonates and early instars which are the most problematic to crops and also most virus-sensitive stages of the pest life cycle (Grzywacz, 2017). Killick and Warden (1991), demonstrated that the NPV of the pine beauty moth, *Panolis flammea*, persisted for longer periods in the shaded parts of the pine canopy compared to the unshaded parts. Studies on the efficacy of CrleGV in the field have shown that degradation of the virus is more rapid on the northern (sun facing) side of the crop plant than on the southern side (Moore, 2002; Mwanza, 2015). Moore (2002) demonstrated CrleGV efficacy of

approximately 70 % was recorded approximately 17 weeks after application in citrus orchards. The study showed that at 21 days post spraying, efficacy had not declined on the southern side of the trees to the same level as on the northern side, where efficacy had dropped within 3-6 days. This is corroborated by Mwanza (2015) who recorded significantly lower LD_{50} on the southern side of citrus trees than on the northern side 21 days after spraying in the field. At 28 days after spraying the virulence on the northern side of the trees was so low that it was indeterminable, as opposed to the southern side where there was still a clear dose response. This good persistence is partly due to the architecture of citrus trees, that have significantly more shading than most crops on which baculovirus biopesticides are applied, and this confers extra protection to CrleGV (Moore *et al*., 2004). However, in some cases such as in the control of corn borer, *Ostrinia nubilalis* (Hübner). UV exposure is reduced by 93 % and 97 % in corn whorls and in leaf axils respectively, which are the feeding sites of the pest (McGuire *et al.,* 1994; Burges and Jones, 1998).

This has prompted a need to investigate ways of increasing tolerance to UV in baculoviruses. These include searching for UV tolerant strains as well as using UV-protectants such as dyes, fluorescent brighteners, lignin derivatives and plant extracts with antioxidant properties (Brassel & Benz, 1979; Shapiro & Robertson, 1990; Asano, 2005; Shapiro *et al*., 2009; Jeyarani *et al*., 2013).

While there is a great deal of research being conducted on the UV persistence of baculoviruses, there is variability in terms of experimental protocols researchers use (Shapiro *et al*., 2009; Lacey *et al*., 2015). For instance, some researchers prefer to evaluate natural sunlight exposure, which in itself has its own variables depending on prevailing conditions and location among others, while most studies make use of artificial UV sources that may not accurately represent natural sunlight or the incidence

of sunlight on leaf or fruit surfaces (Lacey *et al*., 2015). Coupled to this, there is variation in exposure distances, duration and choice of substrates. These variations in the experimental procedures make the evaluation of the research very complicated.

1.4 Improving the UV-tolerance of baculoviruses

According to Grzywacz & Moore (2017) the need for UV protection is determined by the plant architecture and where the pest feeds. Several other measures are taken to reduce the impact of UV irradiation. Since it is known that UV inactivates baculoviruses faster in wet suspension, most of the spraying in the field is done in the evening to reduce the impact of UV. In addition, several additives to the virus formulation have been tested in the laboratory and in the field to assess their UV-protective effect on baculoviruses. The main consideration in selecting UV-protectants is its ability to confer UV stability to the virus but in addition, the cost must be not be too high, it must not distort the natural appearance of the plant or its fruit, its storage conditions should not be incompatible with the virus and its required concentration should not be altered by factors such as high viscosity and blockage of spray filters (Lacey *et al.,* 2015).

1.4.1 Selecting for UV-tolerant baculoviruses

Most reports have focused on additives to the baculovirus formulation as a way of increasing UV-tolerance (Burgess & Jones, 1998; Hunter-Fujita *et al.,* 1998). Very few reports have looked at the possibility of the existence of virus strains within populations that have the inherent ability to resist the effects of UV (Witt & Stairs, 1975; Brassel & Benz, 1979; Witt & Hink, 1979; Shapiro & Bell, 1984; Sporleder *et al*., 2000; Jeyarani *et al*., 2013). As Witt and Stairs (1975) tested the effect of UV irradiation on the NPV of the greater wax moth, Galleria mellonella nuclear polyhedrosis virus (GmNPV) they discovered that within the virus population part of the virus was susceptible to low

doses of UV while another was susceptible to high UV dosage. This translated to almost a 1000-fold difference in susceptibility. They postulated that this heterogeneity in UV-response could be the result of genetic variability and if that was the case that it would be possible to select strains of virus that are UV-tolerant. Following up on these observations, Witt and Hink (1979) successfully isolated a near UV-tolerant strain of AcMNPV after 5 selection cycles. However, coupled with UV tolerance was the loss of virulence and they could not explain whether the loss of virulence was associated with the selection of UV-tolerance or if these where independent events. Brassel and Benz (1979) reported a six-step selection process that yielded a strain of CpGV with increased UV tolerance. Each cycle involved a UV exposure step followed by *in vivo* propagation of the virus. The strain isolated had a 5.6-fold increase in UV tolerance. In another study a 2.5-fold increase in virus persistence was recorded after 6 cycles of UV-exposure and propagation of the gypsy moth NPV, Lymantria dispar multiple nucleopolyhedrovirus (LdMNPV) (Shapiro & Bell, 1984). Sporleder *et al*. (2000) found that the half-life of Pthorimeae opercula (Zeller) granulovirus (PoGV) increased from 2.6 to 24 min after four UV exposure cycles at a total irradiation 1100 W/m^2. Lower irradiation levels resulted in a shorter half-life. More recently Jeyarani *et al*. (2013), subjected the cotton bollworm (*Helicoverpa armigera*; Hübner) NPV, HearNPV (Coimbatore isolate (CBE 1)) to a series of UV-exposure and *in vivo* propagation steps. They recorded increased tolerance to UV as well as retention of virulence from the third exposure cycle upwards. The isolated strain demonstrated a higher degree of persistence than the original strain. Persistence trials showed that HearNPV-CBE1 had 18 % and 26 % original activity remaining after 7 days under UV exposure and shaded conditions respectively (Jeyarani *et al*., 2013). If indeed genetically variable strains that have an inclination towards UV tolerance are present

in baculovirus populations, it would be possible as suggested by Witt and Stairs (1975) to develop a strain with field persistence and UV-tolerance.

It has also been demonstrated that there are differences in the UV-tolerance of different baculoviruses and of different isolates of the same baculovirus from different geographical regions (Shapiro *et al*., 2002; Akhanaev *et al.,* 2017). Shapiro *et al*. (2002) conducted experiments to determine the effect of virus concentrations and UV irradiation on the baculoviruses, SeMNPV and HzSNPV, and reported that SeMNPV was more UV-tolerant than HzSNPV. SeMNPV and HzSNPV were exposed to UV at the same concentration of 7.743 PIB/mm^2 for periods between 0 and 240 min. Although initially the percentage mortality recorded was similar, with 92.2 % for SeMNPV and 97.3 % for HzSNPV at 0 min, after 5 min the percentage mortality had decreased to 73.3 % and 21.7 % respectively. HzSNPV has also been shown to be more susceptible to UV compared to Trichoplusia ni multiple nucleopolyhedrosis virus (TnMNPV) (Gudauskas and Canerday, 1968). In addition, differences in UV tolerance have been recorded in different strains of the same virus. Akhanaev *et al*. (2017), compared the UV-tolerance of two strains of LdMNPV by measuring the relative rate of inactivation and virus half-life. The isolates, LdMNPV-27/0 and LdMNPV-45/0 were isolated from Western Siberia and North America respectively. After exposure to sunlight, it was observed that the North American strain, LdMNPV-45/0, previously shown to be more virulent towards *Lymantria dispar* larvae, was more sensitive to UV and lost its potency faster than the Asian strain, LdMNPV-27/0. A significant delay was recorded in LdMNPV-45/0 induced pathogenesis after 15 minutes sunlight exposure, while the LdMNPV-27/0 strain showed the same delay after 2 hours exposure to sunlight. Thus, the authors concluded that in regions of high UV loading, the effectiveness of the highly potent LdMNPV-45/0 could be significantly reduced.

Recently a new variant of Adoxophyes orana granulovirus (AdorGV) was isolated from *Adoxophyes spp*. larvae in the field (Nakai *et al.,* 2015). Morphological studies revealed that the new variant designated AdorGV-M, had significantly larger cuboidal OBs as opposed to the usual ovo-cylindrical shape associated with most granuloviruses. When tested against *Adoxophyes honmai* larvae, AdorGV-M was found to be equally pathogenic to an English isolate AdorGV-E. However, after UV irradiation the half-life of AdorGV-M was fivefold longer than AdorGV-E. The larger OBs of AdorGV were thought to contribute to this difference in UV-tolerance as the larger OBs meant there was a thicker layer of crystalline protein matrix than those of AdorGV-E.

1.4.2 Plant extracts as UV-protectants for baculoviruses

Various plant extracts have been tested for their potential as UV-protectants. Shapiro *et al*., (2009) tested 67 plant derived extracts, as UV-protectants for the beet armyworm nucleopolyhedrovirus, SeMNPV. Fifteen of the 67 extracts were found to provide good UV protection after exposure to UVB irradiation for 30 minutes. Four of the 15 were found to offer “excellent” (greater than 90 % OAR) protection after exposure to UVB for 300 minutes (Shapiro *et al*., 2009). Laboratory tests have shown several tea extracts to provide UV-protection to baculoviruses (Shapiro *et al*., 2008). A 1 % water extract of green tea provided UV-protection to SeMNPV in the laboratory, however, both 1 % and 5 % green tea extracts were ineffective under field conditions (Shapiro *et al*., 2008). Increased UV-protection was provided as the extract concentration increased from 10 % to 20 % and from 20 % to 30 % (Shapiro *et al*., 2008). A subsequent study revealed that black tea is a good UV protectant for SeMNPV providing almost 100 % UV protection for SeMNPV exposed to UV for over 5 hours (El Salamouny *et al*., 2009a). The unprotected SeMNPV had lost its efficacy

after 2 hours' exposure (El Salamouny *et al*., 2009a). Aqueous coffee and cocoa extracts were also found to provide UV-protection to SeMNPV to a degree that was comparable to that provided by green and black tea (El-Salamouny *et al*., 2009b). The OAR determined for all three ranged from 85-100 % after 300 minutes exposure. Tea and coffee extracts contain UV absorbing phenolics and are rich anti-oxidants (Radtke *et al.,* 1998; Scalbert & Williamson, 2000; Alemanno *et al.,* 2003; Lee *et al.,* 2003; Pellegrini *et al.*, 2003; Koshiro *et al.,* 2007). Their absorption spectra peak in the UV-region of the spectrum. Other plant extracts that have shown promise as UV-protectants include moringa and rice bran extracts (El-Helaly., 2013).

A number of publications have reported on lignin and its derivatives as potential UV-protectants for baculoviruses (Tamez-Guerra *et al*., 2000; Behle *et al*., 2003; Arthurs *et al*., 2006; Arthurs *et al*., 2008). Tamez-Guerra *et al.* (2000) reported that a spray dried formulation of the celery looper NPV, Anagrapha falcifera (Kirby) multiple nucleopolyhedrovirus (AfMNPV) containing pregelatinized corn flour and potassium lignate retained almost 100 % activity after 8 h exposure to simulated sunlight in the laboratory. When tested in the field, lignate formulations resulted in >50 % activity remaining after 48 h exposure. Lignin, a complex organic polymer, provided UV-protection to CpGV, but only at high dosages (3 x 10^{10} OB/L). This was 4.3 times higher than the recommended application dosage used in that region (Arthurs *et al*., 2006). A further field study demonstrated that a spray dried lignin formulation that contained CpGV (6.57 x 10^{12} OB/ha) significantly improved residual activity of CpGV in comparison to the granulovirus formulation alone. The effects were however short lived as after 7 days they could not be detected (Arthurs *et al*., 2008). In South Africa, Kirkman (2007) found that the advantage gained by adding lignin sulphate to CpGV

disappeared when the unprotected CpGV was sprayed in the evening instead of during the day.

1.4.3 Dyes and Optical brighteners as UV-protectants for baculoviruses

The use of dyes as UV-protectants is being extensively studied. The effect of the dyes is mainly attributed to their absorption properties in the wavelength region 280-400nm (Behle & Birthisel, 2014). Shapiro and Robertson (1990) tested 79 dyes as UV-protectants for the gypsy moth NPV, LdMNPV. The LdMNPV-dye combinations were exposed to artificial UV light for 1 h and the OAR then determined. Forty-one dyes from the 79 retained 11-50 % of original activity, while 18 dyes were labelled as "effective" for conferring greater than 50 % of OAR, while five dyes (lissamine green, acridine yellow, brilliant yellow, alkali blue, and mercurochrome) were said to be very effective (conferring >70 % OAR) and Congo Red was the only one that provided "complete" protection (100 % OAR).

Optical brighteners have also been tested as potential UV-protectants. Optical brighteners absorb UV radiation and transmit light in the blue region of the visible spectrum (Shapiro, 1992). Optical brighteners that have shown great promise include Tinopal LPW, Phorwhite AR, Intrawite CF, Leucophor BS, and Leucophor BSB. These optical brighteners were shown to cause larval mortality more quickly than the LdMNPV alone (Shapiro & Robertson, 1992). Tinopal LPW was shown to enhance mortality *T. ni, H. virescens* and Pieris brassicae larvae (Washburn *et al.,* 1998; Sood *et al*., 2013). The Tinopal LPW reduces the normal sloughing of infected midgut epithelial cells thus promoting cell-to-cell infection processes (Washburn *et al.,* 1998; Evans, 2000). This synergistic effect is very important and makes optical brighteners

a very attractive option for use as baculovirus UV protectants. The enhanced activity would enable the use of less virus and hence save costs.

1.4.4 Sunscreen active components as UV-protectants for baculoviruses

Other studies have investigated the potential of substances present in human sunscreen products as UV-protectants for baculoviruses. Asano (2005) evaluated the protective effect of a common sunscreen component, iron oxide on a commercial product, HamakiTendeki (Arysta LifeScience Co.). Iron oxide is used in cosmetic foundation powders and sunscreen products hence the author suspected it could be used as a protective agent for baculoviruses (Asano, 2005). HamakiTendeki is made up of two GV species, Homona magnanima granulovirus (HomaGV) and Adoxophyes orana granulovirus (AdorGV). It was observed that addition of 1-4 mg/ml of iron oxide to the product reduced UV inactivation to between one-eighteenth and one-sixth in comparison with the biopesticide product alone (Asano, 2005). The sunscreen agents, zinc oxide (ZnO) and titanium oxide (TiO_2) have been tested as UV protectants for CpGV (Wu *et al*., 2015). Both had a protective effect on the CpGV-ZY isolate at concentrations of up to 15 mg/ml. Infection rates did not increase significantly at higher concentrations. The lethal time of the GV was significantly reduced after addition of both substances as compared to the formulation without additives (Wu *et al*., 2015). The LT_{50} values were found to be 7, 6.64 and 8.71 days for ZnO, TiO_2 and CpGV-ZY alone respectively (Wu *et al*., 2015). These sunscreen agents are called reflectors and have the ability to reduce the effect of UV radiation by altering their molecular arrangements (size and shape) without changing the internal structure (Burgess & Jones, 1998; Wu *et al*., 2015). ZnO provides better protection against UVA while TiO_2 provides superior protection against UVB (Pinnell *et al*., 2000).While, TiO_2 reflects UV, it catalyses the formation of hydrogen peroxide in the presence of sunlight and water

and this was shown to reduce the activity of the NPV of the corn earworm, *Helicoverpa zea* (Boddie), HzSNPV (Farrar *et al.,* 2003). The use of photostabilized (coated) TiO_2 was found to prevent the formation of the hydrogen peroxide thus, provide better UV protection to the HzSNPV than the stabilised TiO_2 (Mitchnick *et al.,* 1999; Farrar *et al*., 2003; Sambandan & Ratner, 2011).

1.5 Cryptophlebia leucotreta granulovirus

In South Africa several baculovirus biopesticides have been registered for use against various crop pests (Table 1.1). The South African citrus industry in particular makes use of baculovirus biopesticides as part of its IPM strategy. Recently, another baculovirus, Cryptophlebia peltastica nucleopolyhedrovirus (CrpeNPV), was isolated from *Cryptophlebia peltastica,* and was shown to have a broad host range, infecting both *Cryptophlebia peltastica* and Cryptophlebia leucotreta (Marsberg *et al.,* 2018).

Table 1.1. Baculovirus biopesticides registered in South Africa.

Baculovirus	**Host Insect**	***Reg. Name (and Reg (L)number)**	**Crops**
CrleGV-SA	FCM	Cryptogram (L7598)	citrus, avocadoes, peppers, macadamias, ornamentals, etc.
		Cryptex (L8037)	Table grapes, citrus, pomegranates, persimmons.
		Gratham (L9038)	citrus
HearNPV	African Bollworm	Helicovir (L8484)	Wide variety of crops
		Bolldex (L8895)	All crops
		Graboll (9295)	Wide variety of crops
CpGV-M	Codling moth	Madex (L7950)	apples, pears
		Carpovirusine (L7275 & L8226)	apples, pears
CpGV-M	Codling moth and oriental fruit moth larvae	Madex Twin (L9781)	apples, pears stone fruit

Adapted from Knox *et al*, 2015 & Hatting *et al*., 2018

1.5.1 Discovery of CrleGV-SA

One of the baculoviruses used widely in South Africa as a biopesticide is *Cryptophlebia leucotreta* granulovirus (CrleGV). CrleGV was first described by Angélini *et al.* (1965) in infected FCM larvae from the Ivory Coast (IC). Two other different geographic isolates were then identified from infected laboratory reared FCM larvae, originally from South Africa (SA), at a facility in Germany and from infected larvae from Cape Verde (CV) (Fritsch, 1989). These isolates were distinguished by restriction enzyme (REN) analysis which identified small differences in the resultant restriction patterns (Jehle, 1992). Since then the genomes of CrleGV-CV3 isolate and CrleGV-SA have been sequenced and annotated (Lange & Jehle, 2003; Singh *et al*.,

2003; van der Merwe *et al.,* 2017). The overcrowding of FCM, led to the isolation of five new genetically distinct CrleGV-SA isolates (Opoku-Debrah *et al.,* 2013).

1.5.2 Genomic Characterization of CrleGV

Lange and Jehle (2003) sequenced the whole genome of CrleGV-CV3 isolate (Fig. 1.7) and deposited it into the NCBI's GenBank (Accession number NC_005068). This isolate was found to have 110.907 kbp, encoding for 129 open reading frames (ORFs). Out of the 129 ORFs, 62 were similar to other baculovirus' core genes and had homologues in the genomes of the GVs: Plutella xylostella granulovirus, Xestia c-nigrum granulovirus, Phthorimaea opercula granulovirus, and CpGV. Homologues were also identified in group I NPVs: AcMNPV, BmNPV, Epiphyas postvittana multiple nucleopolyhedrovirus, OpMNPV and Rachiplusia ou multiple nucleopolyhedrovirus, as well as group II NPVs: HearNPV (G4 & C1), HzSNPV and LdMNPV among others. A further 26 ORFs were found only among other GVs and five ORFs were specific to CrleGV only.

Of the 26 ORFs identified by Lange and Jehle (2003) to be specific to GVs, only two of them (Crle43 *mp-nase* and Crle106 *iap-5*) are known so far. Crle43 *mp-nase* was suggested to be involved in the breaking down of insect tissue during virus infection while Crle106 *iap-5* is part of the inhibitor of apoptosis gene family (Lange & Jehle, 2003). The five CrleGV-specific ORFs, Crle9, Crle18, Crle22, Crle48 and Crle49 were postulated to have been acquired by horizontal gene transfer. The functions of these ORFs unique to CrleGV are unknown.

Recently, the full genome sequence of CrleGV-SA was sequenced and compared to the CrleGV-CV3 sequence (van der Merwe *et al*., 2017). The genome was found to have 111 334 bp, containing 133 ORFs. Pairwise identity analysis revealed 96.6 %

similarity between the two isolates. The authors also discovered fusion events within the CrleGV-SA genome when they compared it to the CrleGV-CV3. These fusions events involved the ORFs, 27/28, 47/49 and 117/118. Additionally, a single ORF 73 in CrleGV-CV3 appeared as two distinct ORFs 73 and E. It was also observed that two other ORFs, 48 and 126, were truncated in CrleGV-SA. There was also nucleotide sequence variation between CrleGV-SA and CrleGV-CV3 in just about every ORF except for odv-e18 which was identical in both.

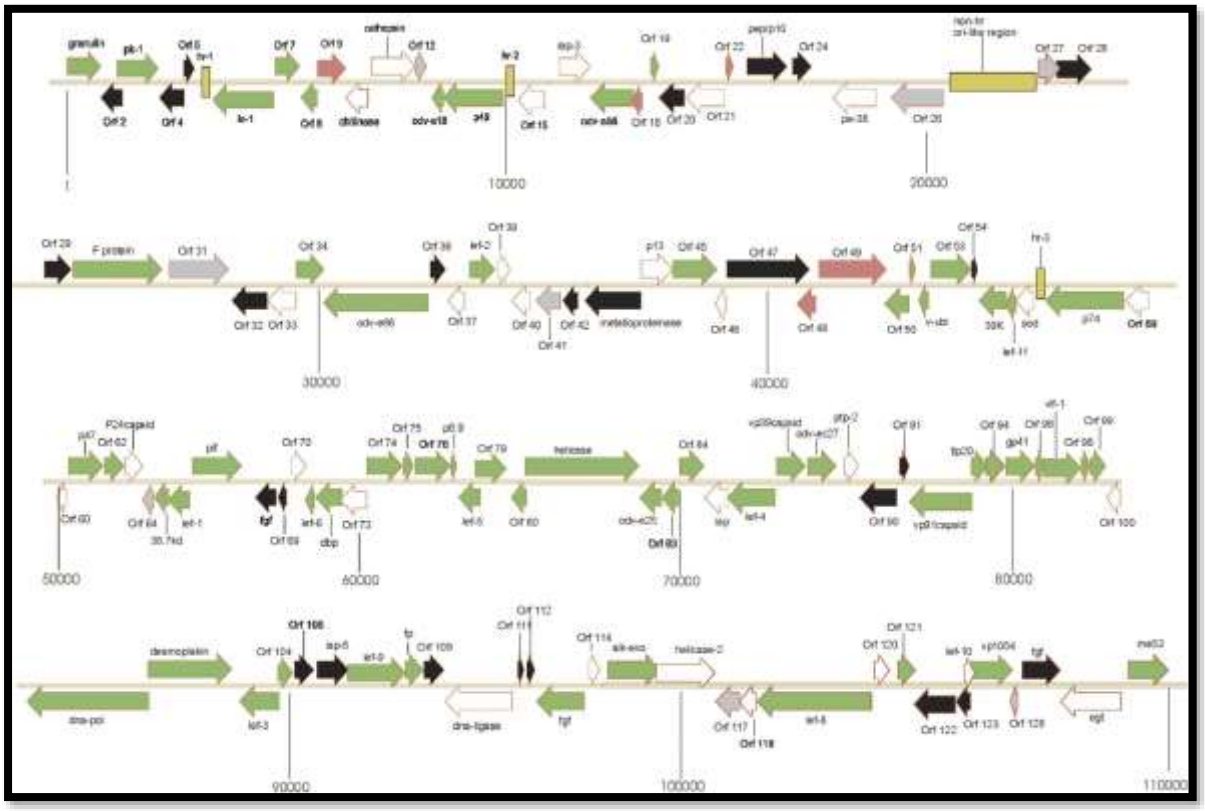

Figure 1.7: The CrleGV-CV3 genome. Arrows indicate ORFs and transcriptional direction. ORFs present in all baculovirus genomes sequenced at the time of publication are coloured in green; GV-specific ORFs are in black; ORFs only present within the genomes of CrleGV and CpGV are in grey; CrleGV unique ORFs are in red and ORF present in some NPVs and/or some GVs are in white. Repeat regions are coloured yellow (Lange & Jehle, 2003)

In their study, van der Merwe *et al* (2017) identified several CrleGV-SA ORFs, including ORF 10 which matched the CrleGV-CV3 ORF 10, a potential chitinase encoding gene. The ORF appeared truncated and non functional in both isolates. They also identified four novel ORFs, three of which were within the hrs regions identified by Lange and Jehle thereby suggesting that there the same non-coding ORFS as those already identified in CrleGV-CV3 (Lange & Jehle 2003; van der Merwe *et al.,* 2017).

1.6 The false codling moth

1.6.1 Taxonomy

The false codling moth, *Thaumatotibia leucotreta* (Meyrick) (Lepidoptera: Tortricidae) is an important citrus pest in Southern Africa (Moore *et al*., 2015a). It was first described by Fuller (1901) as the Natal codling moth *Carpocapsa* sp*.,* before Howard (1909) described it as an orange codling moth. It was then named by Meyrick (1912) as *Argyroploce leucotreta* (Eucosmidae, Olethreutidae) later Clarke (1958) moved it to the genus *Cryptophlebia*. It is currently classified as *Thaumatotibia leucotreta* (Lepidoptera: Tortricidae) (Komai, 1999).

1.6.2 Distribution and host crops

FCM is native to Sub-Saharan Africa and nearby islands in the Atlantic and Indian oceans close to Africa, such as Madagascar (Fig.1.8) (Erichsen and Schoeman, 1994; Newton, 1998). The pest has a wide range of wild and cultivated hosts (Venette *et al.* 2003; Stibick,2007). It occurs in many species, including citrus species, in South Africa, Mozambique, Zimbabwe and elsewhere (Jack, 1916a, 1916b; Hepburn, 1947; Stofberg 1954; Catling, 1969). Navel oranges are more susceptible to FCM attack than other citrus fruit, as more eggs are laid on this cultivar (Newton, 1998). It is believed

the greater acidity and excessive juice of lemons and limes prevents completion of larval development (Moore *et al.,* 2015b), while grapefruit and mandarins are less susceptible to FCM attack compared to oranges (Newton and Anderson, 1985; Newton, 1998).

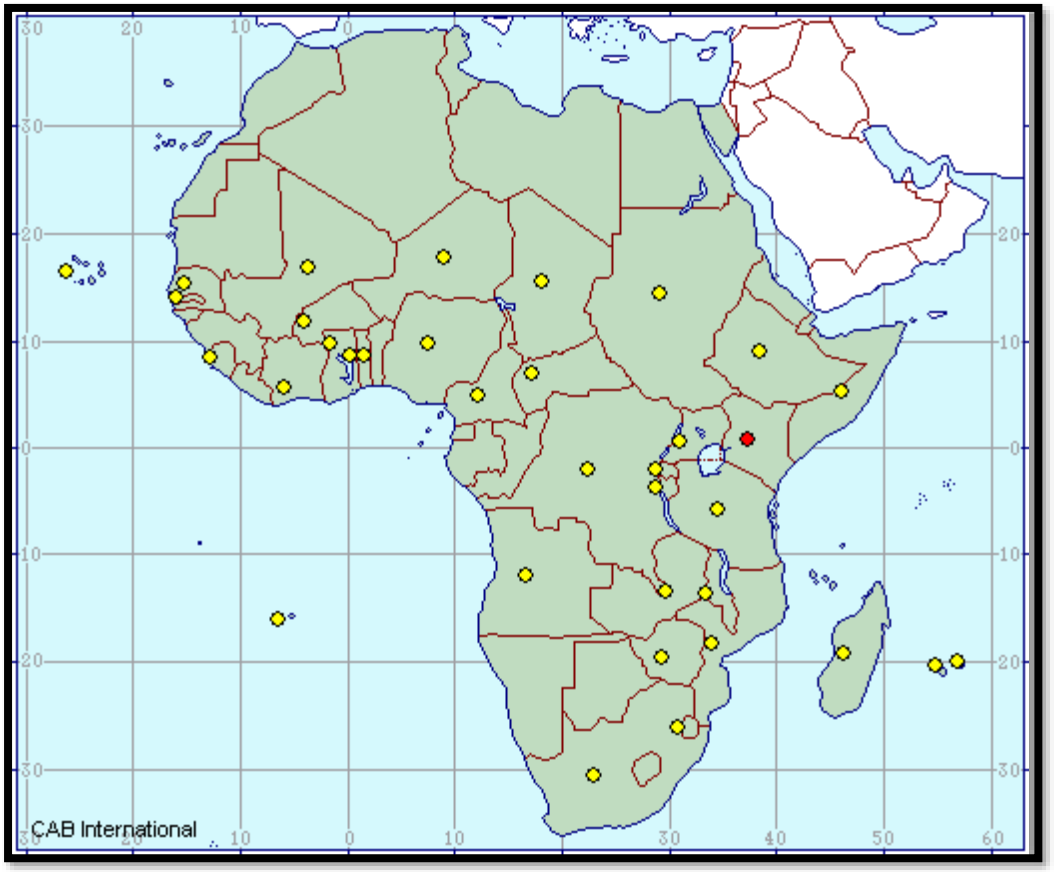

Figure 1.8: Geographic distribution of false codling moth (FCM) on the African continent. The yellow bullets indicate countries in which FCM is established. Adapted from Crop Protection Compendium (2006)

Other important host crops include avocado (*Persea americana*), corn (*Zea mays*), cotton (*Gossypium* spp.), macadamia (*Macadamia* spp.), and peach and plum (*Prunus* spp.) (Erichsen & Schoeman 1992; Newton 1998; Venette *et al*., 2003). In addition to cultivated crops FCM there is a wide variety of wild plants that host FCM in South Africa. These include wild plum (*Harphephyllum caffrum*), wild almond (*Brabejum*

stellatifolium), castor oil plant (*Ricinus lycioides*); jade plant (*crassula ovata*) and karoo boer-bean (*Schotia afra*) among many other. These could potentially act as natural reseirvors for FCM (Honiball, 2004; Kirkman & Moore, 2007; Stibick *et al.,* 2007).

1.6.3 Life Cycle

The FCM lifecycle follows the basic life cycle stages of egg, larva, pupa and adult. On citrus the time for total development is between 2.5-4 months in winter and 1.5- 2 months in summer (Newton, 1998). According to Schwartz (1981) it takes 23-26 days to develop from egg to adult under constant conditions of 27 °C and 70 % relative humidity. If uninterrupted, up to five generations can be completed on oranges in South Africa in a season (Venette *et al.,* 2003). Factors such as temperature, food availability and quality, photoperiod, humidity, latitude and the effect of predators and diseases determine the number of FCM generations that can succeed per year (USDA, 2010). On citrus, the eggs are laid in depressions of the rind and have a lifespan of 6-12 days (Stofberg, 1939). Newton (1989) observed that eggs are laid more on damaged or early ripening fruits than on healthy Navel or Valencia fruit. On damaged fruit, Newton (1988) regularly observed up to 12 eggs per fruit and less frequently up to a maximum of 20, although as many as 65 eggs per fruit have been found in a rare observation (Stofberg,1954). However, on healthy fruit, eggs are usually laid singly. Upon hatching the first instars are susceptible to a number of factors, in particular extreme temperatures (Newton 1998, Daiber, 1980). Larvae wander on the surface before burrowing their way into the fruit. In hosts that have soft rinds, such as citrus, the larvae will burrow into the rind from almost anywhere, although observations reveal preference for the navel end or an injured area of the rind (USDA, 2010). It takes between 12 and 33 days in warm weather, as opposed to

35 to 67 days in cooler conditions, for larvae to reach full development. Mature larvae (fifth instars) leave the fruit and drop to the ground leaving exit marks on the fruit. The larva then pupates in the soil before developing into a small inconspicuous moth, which is dark brown to grey in colour (Newton, 1998). The adult moth can live for one to six weeks and may live as long as 28 weeks under favourable winter conditions (Daiber, 1980, Couilloud, 1994).

1.6.4 Economic significance

The South African citrus industry exports approximately 70 % of its citrus fruit to various markets around the world (Citrus Growers' Association [CGA] 2013). In South Africa losses in the citrus industry due to FCM infestation are estimated to be over R100 million (Moore *et al*., 2004). FCM infestation results in fruit drop and consequently a reduction in yield. Added to this, infestation occurs just before fruit harvest and may not be detected before export, resulting in post-harvest decay of fruit. FCM has major economic significance due to its phytosanitary status, which means that the detection of a single larva in fruit marked for export could result in the entire consignment being rejected (Moore, 2002; Moore *et al.,* 2016; Moore *et al.,* 2017). As a result, of these stringent conditions imposed by export markets, there has been a concerted effort to control FCM at both the pre-and post-harvest stage.

1.6.5 FCM control with Cryptophlebia leucotreta granulovirus

There are various methods that are currently being used to control FCM on citrus as part of an IPM programme (Moore &Hattingh, 2012) (Table 1.2). These are chemical, cultural, biological (including microbial) and semiochemical techniques.

Table 1.2. Control measures against FCM.

Control Type	**Active ingredient**
Chemical	Fenpropathrin Cypermethrin Triflumuron Teflubenzuron Spinetoram Rynaxypyr Methoxyfenozide Emamectin benzoate
Cultural	Orchard Sanitation
Biological	*Trichogrammatoidea cryptophlebiae*
Mating disruption	E7-12AC, E8-12Ac, Z8/E8-12 E8-12Ac, Z8-12
Attract and kill	E7-12AC, E8-12Ac, Z8-12
Sterile Insect technique	Sterile FCM adult males
Microbial	CrleGV

* Adapted from (Moore & Hattingh, 2012)

Microbial control of FCM in South Africa is done with the baculovirus CrleGV. CrleGV was first isolated from infected FCM larvae from the Ivory Coast (Angélini *et al*., 1965). Subsequently CrleGV isolates were also obtained from Cape Verde (Mück, 1985) and from South African FCM larvae in laboratory culture isolates reared in a German laboratory (Jehle *et al*., 1992). The investigation of the potential and use of CrleGV-

SA as biopesticide for FCM has been reported since the early 2000s (Singh *et al.,* 2003; Moore *et al.,* 2004; Moore *et al.,* 2011; Moore *et al.,* 2015a).

Cryptogran is a registered CrleGV-SA biopesticide produced by River Bioscience, South Africa. Cryptogran was first registered to be used on citrus trees in 2004 and was registered for use on avocado trees in 2009 (Moore *et al*., 2004, Grove *et al.,* 2010). Cryptogran is formulated with a CrleGV-SA strain identified in an FCM colony reared by Citrus Research International (CRI) in Port Elizabeth, South Africa (Singh *et al*., 2003).

Extensive work has been conducted on the control of FCM using the *Cryptophlebia leucotreta* granulovirus, both in the laboratory and in the field for more than a decade, but the first report detailing a field trial using CrleGV on citrus was by Fritsch (1988) in the Cape Verde Islands (Moore *et al*., 2015a).

Moore (2002) reported the development of CrleGV-SA as a biopesticide for the control of FCM using a South African isolate from the Citrusdal region. In this initial study, LC_{50} and LT_{50} for CrleGV-SA were determined to be 4.095×10^3 OBs/ml and 4 days 22 h respectively, based on surface dose bioassays (Moore, 2002; Moore *et al*. 2011). Cryptogran (River Bioscience, South Africa), a CrleGV-SA based commercial biopesticide, was subsequently registered in South Africa to be used on citrus and was the first commercially available baculovirus produced in Sub-Saharan Africa (Singh *et al*., 2003; Moore *et al.,* 2004). Larval infestation of fruit was reported to decrease between 30 % to 92 %, while persistence at a level of up to 70 % for 17 weeks was demonstrated. Droplet-dose bioassays conducted with the five new CrleGV-SA isolates and two already existing isolates gave LD_{50} values that were between 0.79 and 3.12 (Opoku-Debrah *et al.,* 2016). Two other CrleGV formulations, Cryptex and

Gratham (both Andermatt, Switzerland) have been registered in South Africa (Kessler & Zingg, 2008; Moore *et al.,* 2015a). These CrleGV biopesticides form part of the IPM programme to control FCM in South Africa.

Moore (2002) reported that the OAR of CrleGV-SA on the northern (sun facing) aspect of the trees was reduced to 38 % within 3-6 days, while on the southern side it was reduced to 69 % after 21 days. This was confirmed in a recent study which showed that the LC_{50} of the commercial product Cryptogran in the field was reduced from 1.4 x 10^4 OBs/ml on the northern side of trees, and 2.08 x 10^3 OBs/ml on the southern side on day 1 of application, to 4.08 x 10^7 and 2.63 x 10^6 OBs/ml respectively after 21 days (Mwanza, 2015). Kirkman (2007) showed that molasses, a tank additive for Cryptogran when spraying, did not provide UV protection. Lignin was shown to provide the best protection in the laboratory although this did not translate to a significant difference to the unprotected CrleGV-SA when sprayed in the evening (Kirkman, 2007).

In laboratory experiments to determine the reapplication frequency of CrleGV-SA formulations, residual activity was recorded in bioassays conducted with CrleGV-SA exposed to UV under controlled conditions even when the virus samples were exposed to UV for 7 days (Mwanza, 2015). It is possible that this was due to inherent UV resistance in some of the virus population. This has previously been shown with CpGV, LdMNPV and HearNPV (Brassel and Benz, 1979, Shapiro and Bell 1984; Jeyarani *et al*., 2013). The selection of UV-tolerant virus strains would enable development of a biopesticide that will persist longer in the field.

1.7 Aim and Objectives

Susceptibility to UV radiation is one of the major challenges associated with baculovirus biopesticides, including CrleGV based biopesticides. CrleGV-SA biopesticides such as Cryptogran are registered for use in South Africa on citrus and avocado trees, as well as grapes, stone fruit, pomegranates and macadamia. As a result of the effect of UV radiation, farmers must respray up to three times per season between November and March.

The aim of this PhD project was to work towards developing a new commercial UV-tolerant CrleGV-SA biopesticide. This will focus firstly upon the selection of UV-tolerant CrleGV and secondly on testing the efficacy of different UV-protectants. A combination of these two approaches could produce a biological control agent with improved and prolonged activity, reducing reapplication costs. The production of a UV-tolerant CrleGV-SA biopesticide will benefit current users of CrleGV-SA biopesticides and will encourage more citrus farmers to use the biopesticide in place of chemical pesticides, with benefits for the environment and for export of produce to markets with stringent environmental requirements.

This aim builds on the findings of my previously completed Masters study that indicated that UV-tolerant CrleGV-SA strains spontaneously arise following prolonged UV exposure (Mwanza, 2015). This PhD study targeted the following objectives:

1. Isolation of UV-tolerant CrleGV from a laboratory source of CrleGV by repeated UV exposure and isolation of surviving virulent virus strains.

2. Genomic sequencing of UV-tolerant CrleGV-SA and sequence comparison with the unexposed virus isolate identify possible mutations to the virus DNA associated with UV-tolerance.

3. Identification of structural differences between UV irradiated virus, non UV-irradiated virus and the selected UV-tolerant virus using Transmission electron microscopy and Fourier Transform infrared spectroscopy.

4. Testing and comparison of three potential UV protectants.

5. Identification of the optimal combination of UV-tolerant virus and UV protectant for commercial use.

Chapter 2

Selection of UV-tolerant CrleGV-SA

2.1 Introduction

In South Africa, formulations of the South African isolate of Cryptophlebia leucotreta granulovirus (CrleGV-SA) have been used commercially for control of the false codling moth (FCM), *Thaumatotibia leucotreta* (Meyrick) (Lepidoptera: Tortricidae), in citrus since 2004, as part of the integrated pest management (IPM) programme (Moore & Hattingh, 2012; Moore *et al.,* 2015). As with other baculovirus biopesticides, ultraviolet (UV) radiation from sunlight, remains the major hurdle to the use of CrleGV-SA based biopesticides (Szewczyk *et al*., 2006). Various approaches to overcome or reverse the effects of UV have been investigated.

One approach which has not been extensively researched is the selection of UV-tolerant baculoviruses from wild virus populations or from laboratory populations. A few attempts to achieve this have been published (Brassel & Benz, 1979; Shapiro & Bell, 1984; Jeyarani *et al*., 2013). Brassel and Benz (1979) reported a 5.6-fold increase in UV tolerance of Cydia pomonella granulovirus (CpGV) after 6 UV exposure cycles, while Shapiro and Bell (1984) reported a 2.5-fold increase in UV tolerance of the gypsy moth NPV, Lymantria dispar multiple nucleopolyhedrovirus (LdMNPV) after a six step UV exposure cycle. Most recently Jeyarani *et al*. (2013), also recorded an increase in UV tolerance after subjecting the cotton bollworm NPV, Helicoverpa armigera Coimbatore Isolate I (HearNPV-CBE I) to 5 UV-irradiation cycles. UV experiments with

CrleGV-SA and other baculoviruses have shown that there is always residual activity after UV irradiation and it is possible that this could be a result of genetic variability within the population (Witt & Stairs,1975; Mwanza, 2015). In publications where selection of UV tolerant virus was reported, the working principle was that exposing the virus to UV, growing up the survivors *in vivo* and re-exposing these propagated survivors to UV would isolate and select for a UV-tolerant population from the original population (Brassel and Benz, 1979; Jeyarani *et al.,* 2013). The degree of UV tolerance was measured by analysing susceptibility of the relevant pest larvae to each selected virus population in bioassays (Brassel & Benz, 1979; Shapiro & Bell, 1984; Jeyarani *et al*., 2013). There have been no follow up publications to report on the molecular or morphological basis of the observed tolerance in the viruses tested.

The existence of such a strain would provide a platform for the development of UV tolerant baculovirus pesticides with longer field persistence. This in turn would lead to reduced frequency of applications and overall costs associated with tackling baculovirus susceptible pests (Jeyarani *et al.,* 2013).

In this chapter, the selection and isolation of a UV-tolerant strain of the CrleGV-SA is reported. To determine whether the selection of UV-tolerant virus after repeated UV-irradiation was successful, surface dose bioassays were conducted against neonate FCM larvae after each UV exposure cycle. Surface dose bioassays are designed to mimic the feeding patterns of insects that eat the fruit surface and burrow into the fruit (Jones, 2000). A known concentration of the test virus is spread on the surface of the diet and allowed to dry. A single insect is then placed on the diet and incubated. At the end of the incubation period, mortality of the larvae is checked, and the resultant data analysed by appropriate statistical procedure such as probit analysis (Hunter-Fujita *et al.,* 1998).

2.2 Materials and Methods

2.2.1 Virus Purification

Virus was purified from FCM larval cadavers that were previously inoculated with a known pure isolate of CrleGV-SA. The larval cadavers and FCM diet were provided by River Bioscience Pty (Ltd), Addo, South Africa. The FCM diet was prepared by mixing 800 g maize meal, 80 g wheat germ, 14.6 g powdered milk, 40 g brewers' yeast, 6 g nipagin and 2.6 g sorbic acid. The fifth instars were grown on baked FCM artificial diet, that was prepared by mixing 200 g diet with 200 ml sterile distilled water until a thick paste was formed in a 33 cm x 23 cm x 5.5 cm baking tray and baked at 180 °C for 15 min (Moore *et al*., 2014) This was inoculated with CrleGV-SA at the LC_{90} concentration for fifth instars (Moore *et al*., 2011). Larvae displaying infection symptoms were isolated and stored at -20 °C.

To isolate the viruses from larval cadavers and purify them from insect debris and other contaminants, the methods described by Hunter-Fujita *et al*. (1998) and Moore (2002) were followed. Using a pestle and mortar, 2 g infected larval cadavers was homogenised in 6 ml 0.1 % (w/v) SDS (Merck, SA) in double distilled water. The homogenate was passed through a muslin cloth to remove large particulate matter. An additional 4 ml 0.1 % SDS was added to the remaining homogenate and again passed through the muslin cloth. The resulting filtrate was split into two 50 ml Beckman JA20 centrifuge tubes and the tubes filled with 0.1 % SDS in water. The tubes were then centrifuged in a Sigma 3K30 bench top centrifuge (Sigma Laborzentrifugen GmbH, Germany) at 13000 g for 10 min. The supernatant was discarded, and the pellet resuspended in 0.1 % SDS and centrifuged again at 13000 g for 10 min. The process was repeated for a third time. The resultant pellet was resuspended in 1 ml

double distilled water and placed on top of a 30-80 % glycerol gradient that had been prepared 24 h prior to the purification. To prepare the gradient, different concentrations of glycerol were made with 0.1 % SDS in water. For a 30 % glycerol solution, 30 ml 100 % glycerol (Merck, SA) was added to 70 ml 0.1 % SDS. The 40 %, 50 %, 60 %, 70 % and 80 % glycerol solutions were prepared in a similar manner. The glycerol was then placed in 38 ml SW 28 Beckman Ultra clear tubes, starting with the 80 % solution at the bottom, followed by the 70 %, 60 %, 50 %, 40 % and the 30 % (least dense) solution at the top. These were placed at 4 °C overnight to allow the different bands to settle and an even gradient to develop. The CrleGV-SA pellets were loaded on top of the gradient and centrifuged in an Optima Ultracentrifuge Beckman L70 rotor (Beckman Coulter, USA) at 40572 g for 15 min. With the aid of a torch in a darkened room the virus band could be visually observed (Fig. 2.1).

Figure 2.1: A viral band prepared by ultracentrifugation in a glycerol gradient

Using a pipette, the band was transferred to clean 50ml JA20 tubes and topped up with double distilled water and centrifuged for 10 min in the Sigma 3K30 bench top centrifuge at 13000 g to wash and pellet the virus. The supernatant was discarded,

and the process repeated two more times. The pellet obtained was resuspended in 8 ml double distilled water at 4 °C.

2.2.2 Enumeration of OBs by dark field microscopy

To quantify the virus, the method described by Hunter-Fujita *et al.* (1998) was used. An aliquot of the virus sample was diluted 1 in 20 in double distilled water followed by a 1 in 10 dilution in 10 % SDS and sonicated before being diluted (1 in 5) in 0.1 % SDS, to give a final virus dilution of 1 in 1000. Using a micropipette (Gilson, USA), 5 µl of the virus suspension was placed onto a 0.02 mm deep Helber bacterial counting chamber (Hawksley, UK) which was then covered by a glass cover slip. The cover slip was placed gently from one side to ensure the volume of the suspension was exact and to eliminate air bubbles. Moving OBs were counted in four large squares, each consisting of 16 small squares, in the corners of the chamber and one randomly selected large inner square (Fig. 2.2) under dark field microscopy using an Olympus BX 51 TF microscope (Olympus, Japan) x40 objective and eyepiece magnification of x10, therefore 400x magnification.

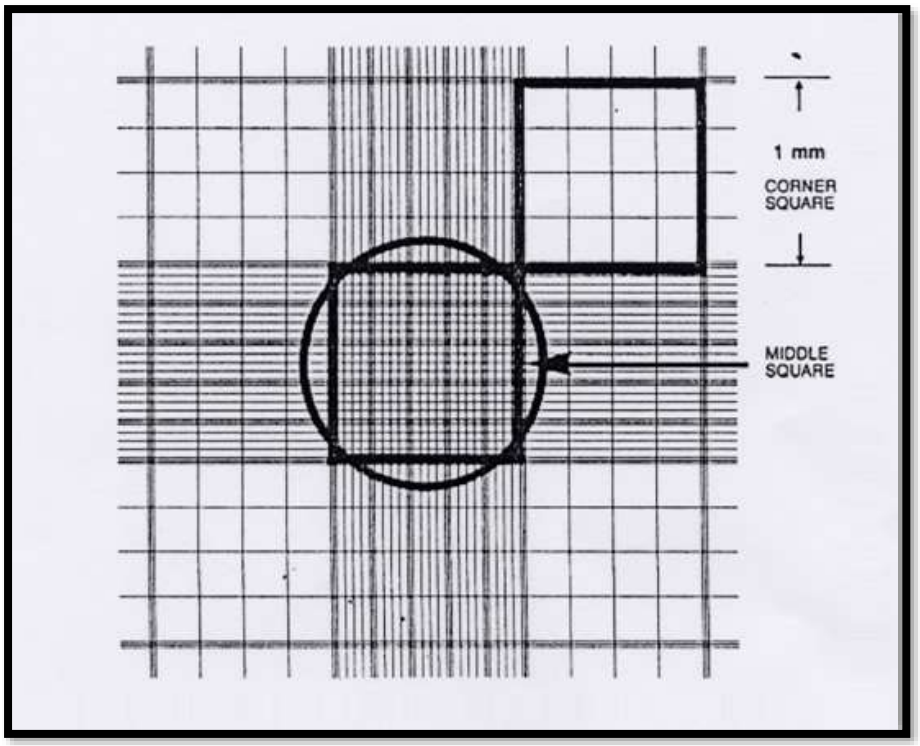

Figure 2.2: View of the Helber Thoma bacterial counting chamber under the light microscope. OBs found in the four large squares in the corners of the middle square (circled) and one random square in the centre of the middle square were counted. Source: www.hpacultures.org.uk/technical/ccp/cellcounting.jsp

All dark field enumeration was performed in triplicate. The mean counts were used to determine OB concentration, using the formula below:

$$OBs/ml = (dilution \times mean\ number\ of\ OBs) / (80 \times (5 \times 10^{-8}))$$

Where 80 is the number of small squares and 5×10^{-8} is volume in millilitres of the virus suspension within these squares.

2.2.3 Selection of UV-tolerant CrleGV-SA

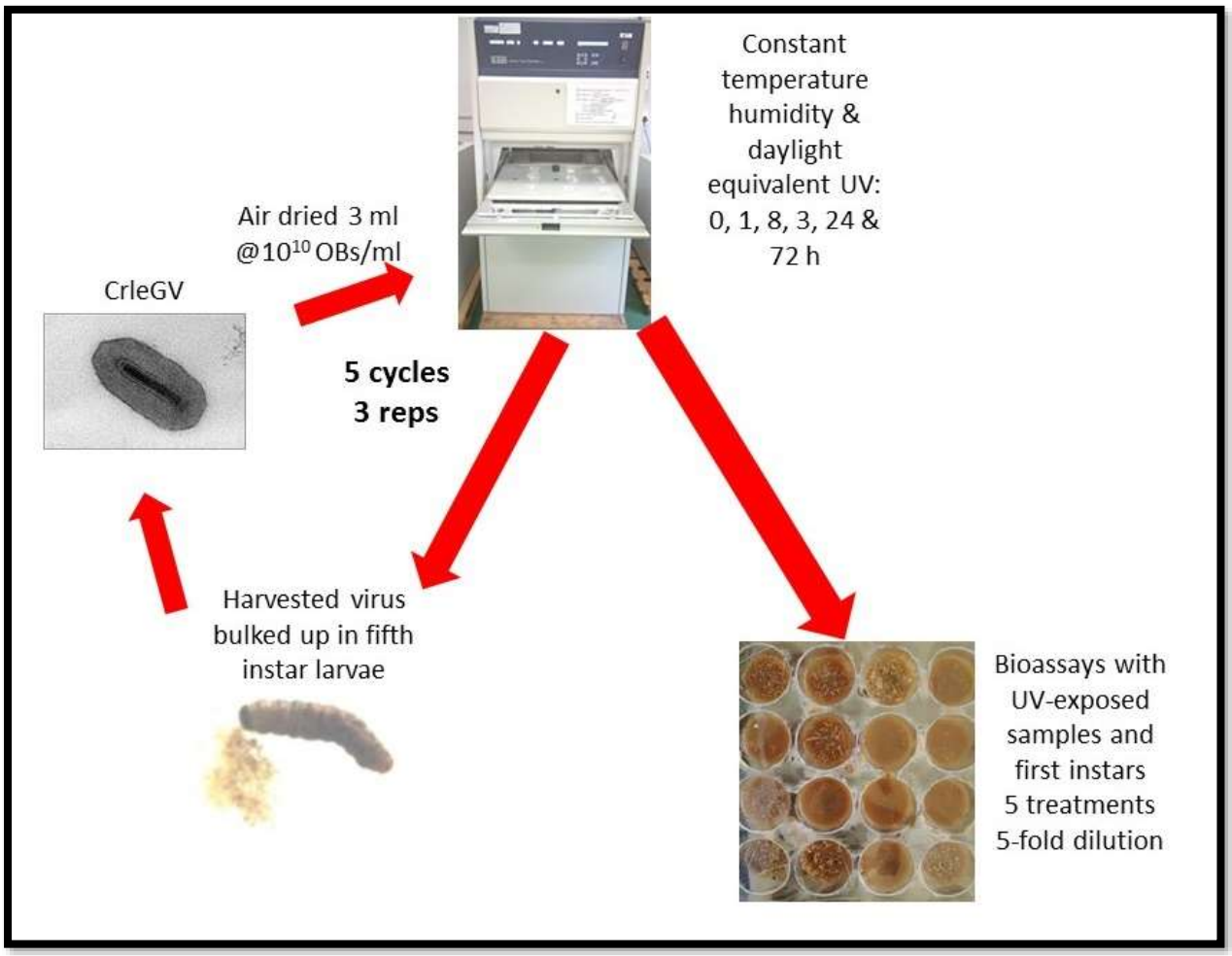

Figure 2.3: Outline of the selection process for UV-tolerant CrleGV-SA

FCM egg sheets (wax paper on which FCM females lay their eggs in the laboratory or at a rearing facility) and FCM fifth instars were provided by River Bioscience (SA) from their Addo (Eastern Cape, SA) insect rearing facility. To obtain FCM first instars, egg sheets in glass jars with lids, were incubated in a temperature-controlled room at 28 °C until they hatched. Eggs hatched within 24-48 h of incubation. First instars were then used in surface dose bioassays within 24 h of hatching. Fifth instars were provided in jars and used for the virus propagation step.

UV exposure was carried out in a Q-Sun Xe-3 HC test chamber (Q-lab, USA) housed at CSIR, Port Elizabeth (Fig. 2.3). This test chamber is fitted with three 100 W xenon arc lamps. Optical filters are used to provide the desired wavelengths of light. Other parameters such as temperature and humidity are also regulated in the chamber. The Daylight Q filter, which mimics UV conditions in normal sunlight, was used in this study. Temperature was set at 30 °C, irradiance at 300 Wm^{-2}, and relative humidity at 42 %. These conditions were based on averages collected over one summer period in the Sundays River Valley, Eastern Cape Province, an important citrus growing area (Linta Greef, Sundays River Citrus Company). Figure 2.3 gives an outline of the selection process. Purified CrleGV-SA aliquots of 3 ml at a concentration of 1 x 10^{10} OBs/ml were placed under a laminar flow hood overnight and allowed to dry in petri dishes and then placed in the UV test chamber for 1, 3, 8, 24, 72, 120 and 168 h on a 451 mm x 718 mm sample tray. However due to the very low larval mortality observed for samples exposed for 120 h and 168 h, these time points were discarded, and subsequent cycles went up to a maximum duration of 72 h. The UV exposed virus samples were then resuspended in 3 ml double distilled water, quantified and stored at 4 °C until they were needed for propagation of virus for the next cycle or for bioassays with FCM first instars.

2.2.4 Propagation of virus in fifth instars

In order to select for viruses that survived the first cycle of exposure, amplification was carried out within FCM fifth instars (Fig 2.3). The larvae were reared on artificial diet whose surface had been inoculated with the UV exposed CrleGV-SA. The diet was prepared in a tray covered with aluminium foil and baked in a preheated oven at 180 °C for 15 min. The baked diet was allowed to cool under a laminar flow hood for 30 min, before being cut with a knife into squares and placed in 24 or 25 well bioassay

plates with well dimensions of 20 mm x 20 mm x 17 mm deep. The surface of the diet was covered with 50 µl UV exposed CrleGV-SA, allowed to dry under the laminar flow hood for 30 min and a single FCM fifth instar placed in each well with the aid of an art paint brush (size 000). The plates were covered firmly and incubated at 30°C. Inspections were carried out routinely for 14 days to identify infected and/or dead larvae. These were placed in labelled containers and stored at -20 °C. Virus was then extracted and purified from the larval cadavers as described previously in section 2.2.1. Purified aliquots were kept at 4°C until they were needed for the subsequent exposure cycle or for analysis (this period ranged from 2 weeks to 6 months). The process of the exposure of CrleGV-SA to UV and the subsequent propagation of survivors in FCM fifth instars constituted one exposure cycle. In total five exposure cycles were carried out in this study.

2.2.5 Surface dose Bioassays

To evaluate the effect of UV irradiation at each cycle and time point as well as to evaluate the effect of UV re-exposure, surface dose-response bioassays were conducted on first instar FCM (Fig. 2.3). The assays were performed in 25 well bioassay plates with well dimensions of 20 mm x 20 mm x 17 mm deep. FCM eggs sheets supplied by River Bioscience were incubated in a temperature-controlled room at 28 °C between for 72 h after which they hatched. FCM diet was prepared as described in section 2.2.4. UV-exposed virus at each time point was adjusted to 1 x 10^9 OBs/ml and then serially diluted five-fold to give five concentrations at each time point, ranging from 3 x 10^7 OBs/ml to 3 x 10^3 OBs/ml (Fig. 2.4). Aliquots of 50 µl per well of a single virus concentration were spread on the surface of the diet by tilting the plate, and then allowed to dry under a laminar flow hood for 30 min. Each bioassay was carried out in triplicate using 25 larvae per concentration for each replicate.

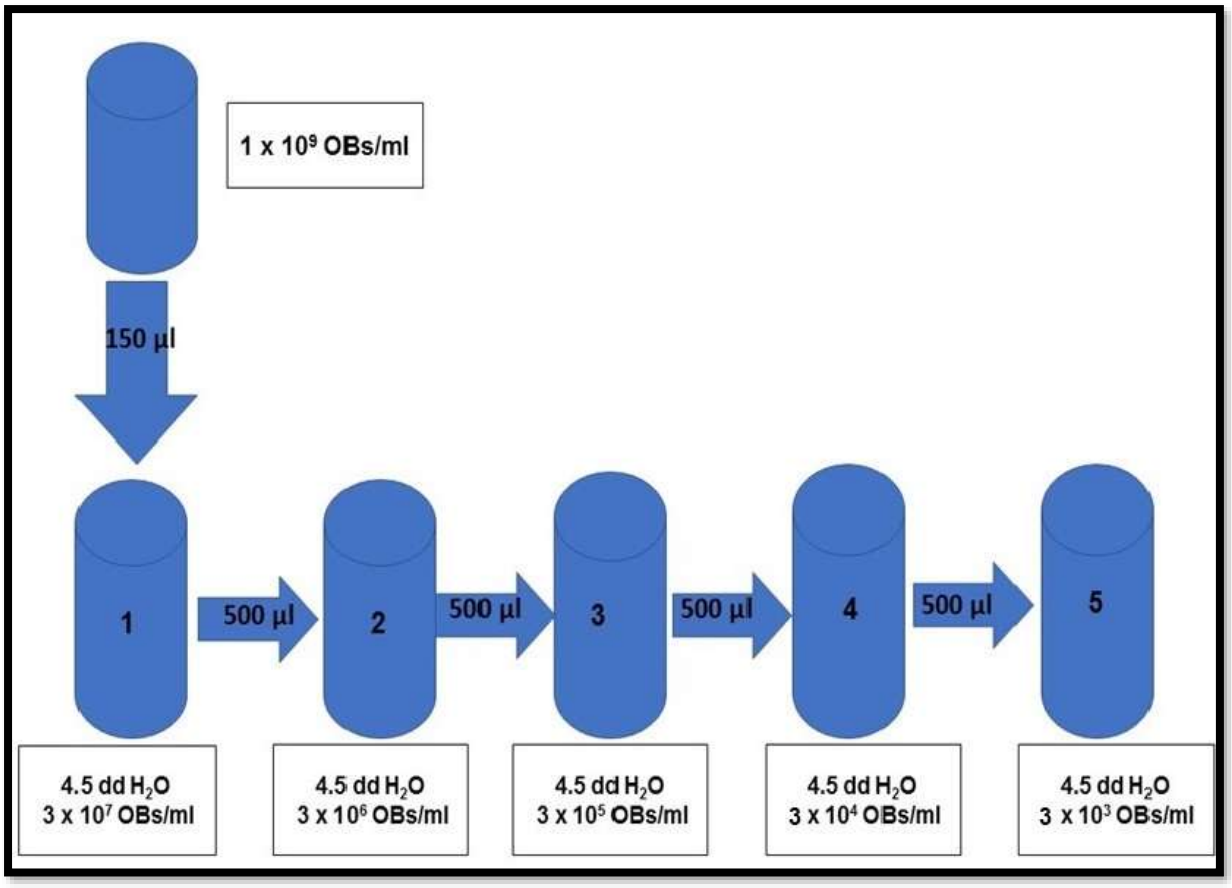

Figure 2.4: Outline of dilution series of CrleGV-SA for surface dose bioassays against FCM neonate larvae**.**

A single neonate larva was then picked up using a small art paint brush and placed on the surface of the diet in each well and each plate was covered with two layers of paper towel and a lid and incubated in a temperature-controlled room at 28 °C for 7 days. At the end of the incubation period, each well was inspected, and larval mortality was recorded. A larva was recorded as dead if upon being touched by a blade it did not move or it ruptured and was recorded as alive if it moved when touched by the blade. A control plate with sterile double distilled water instead of UV-exposed virus was also prepared. All bioassays were carried out in triplicate. Surface dose bioassays with unexposed CrleGV-SA were also conducted concurrently to provide a comparison. The mean mortality data obtained were subjected to probit analysis using

PROBAN, a statistical software programme used for analysis of bioassay data (Van Ark, 1995). This software takes into consideration the mortality of the treated larvae, and corrects this for mortality of control larvae, based on the Abbot formula (Abbott, 1925), giving a dose response curve from which the LC_{50} and LC_{90} values were determined at each exposure time. PROBAN transformed the doses to $\log_{10}$ and the percentage mortality response to empirical probits. Regression lines comparing responses at a particular time point across the five cycles were then determined based on this information. The slopes of the lines were compared and significant differences at $P \leq 0.05$ determined. Where lines were found to be parallel, relative potency comparisons were carried out. For each comparison at each time point, one sample from one time point was chosen as a reference (r) and compared against another sample (t) from a different cycle at the same time point (e.g. if at 3 h exposure, cycle 1 was chosen as r, then cycle 2 sample at 3 h exposure would be t). Where t was less than 1 ($t<1$) the test sample was more potent than the reference sample. Where the value of 't' equalled 1 ($t=1$) there was no difference in potency between the two samples being compared. A value of t which was greater than 1 ($t>1$) indicated that the test sample was less potent than the reference sample (Finney, 1965; Finney 1971; Dinse & Umbach 2011; van Ark 1995; Opoku-Debrah *et al.*, 2016). The Bartlett's test was used to compare the homogeneity of variances in the lines at $P \leq 0.01$.

2.3 Results

2.3.1 Surface dose-response bioassays after 1 UV exposure cycle

Virus samples exposed to the first cycle of UV irradiation for various time intervals, were subjected to bioassays as described in section 2.2.5. Surface dose-response bioassays with these samples from the first cycle of UV-irradiation, were used to determine a dose response relationship (Fig 2.5). Negative control mortality of all samples ranged from 0 % to 13 %. The regression lines fitted to the corrected data for all replicates were compared and the residual variances of the lines determined by Bartlett's test. The variances were determined to be homogeneous (X^2 = 0.763; DF = 5; P = 0.01) and thus comparisons of slopes and elevations could be carried out. The lines were determined to be parallel by the Chi-square test, and their elevations, were shown to be comparable (X^2 = 8.208; DF= 5; P = 0.05). The Bonferroni method was used to compare the elevations of the lines and determined that the elevations of the lines differed significantly from each other ($F_{5, 23}$ = 2.64; P = 0.05). This was corroborated by relative potency comparisons, which showed that the longer the sample was exposed to UV irradiation, the less potent it became (Table A1, Appendix I).

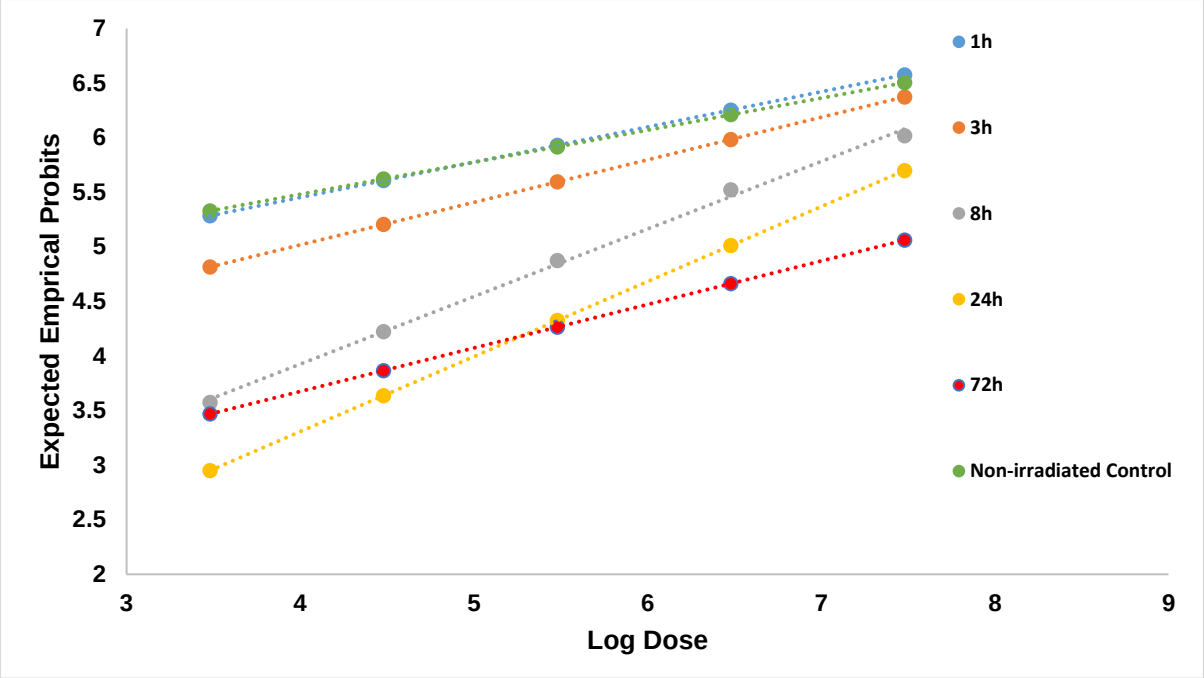

Figure 2.5: UV exposure cycle 1 log dose-probit regression lines for CrleGV-SA against neonate FCM larvae after UV irradiation for 0 h to 72 h time points in the Q-Sun test chamber.

As expected, following 1 cycle of UV exposure, the LC_{50} values increased from 3.96 x 10^4 OBs/ml for the non-irradiated control to 2.11 x 10^9 OBs/ml after 72 h of UV exposure at cycle 1 (Table 2.1).

Table 2.1: LC_{50} and LC_{90} values derived from bioassay data of samples exposed to UV in the first exposure cycle

Time (h)	LC_{50} (OBs/ml)	95 % Fiducial limits		LC_{90} (OBs/ml)	95 % Fiducial Limits		X^2	P
		Lower	Upper		Lower	Upper		
0	2.29×10^4	3.37×10^{-2}	4.73×10^4	5.30×10^8	5.30×10^7	2.63×10^{11}	0.613	0.892
1	3.96×10^4	1.00×10^0	6.00×10^5	3.71×10^8	4.37×10^7	3.79×10^{11}	0.285	0.958
3	8.97×10^5	2.75×10^4	4.60×10^7	1.75×10^9	2.29×10^8	2.96×10^{11}	1.229	0.750
8	4.73×10^7	1.48×10^7	1.39×10^8	4.46×10^9	1.00×10^9	8.44×10^{10}	0.302	0.955
24	2.89×10^8	8.44×10^7	1.17×10^9	2.11×10^{10}	3.58×10^9	2.49×10^{12}	1.089	0.783
72	2.11×10^9	3.64×10^8	1.69×10^{11}	3.50×10^{12}	6.87×10^{10}	1.39×10^{18}	1.629	0.657

X^2-Chi square goodness of fit, DF degrees of freedom for chi-square=3. P- Probability of a greater chi-square

2.3.2 Surface dose-response bioassays after 2 UV exposure cycles

Survivors of the first UV exposure cycle were propagated in FCM fifth instars before being exposed to UV for the second exposure cycle in the Q-Sun test chamber under the same conditions as the previous cycle. The mortality of neonate larvae was related to the dosage of all six time points (Fig 2.6). Control mortality of all samples ranged from 4 % to 8 %. The regression lines fitted to the corrected data for all replicates were compared and the residual variances of the lines determined by Bartlett's test. The variances were determined to be homogeneous ($X^2 = 0.214$; DF = 5; P = 0.01) and thus comparisons of slopes and elevations could be carried out. The lines were determined to be parallel by the Chi-square test, and their elevations were shown to be comparable ($X^2 = 4.642$; DF= 5; P = 0.05). The Bonferroni method was used to compare the elevations of the lines and determined that the elevations of the lines differed significantly from each other ($F_{5, 23} = 2.64$; P = 0.05). This agreed with relative potency comparisons, which showed that the longer the sample was exposed to UV the less potent it became (Table A2, Appendix I).

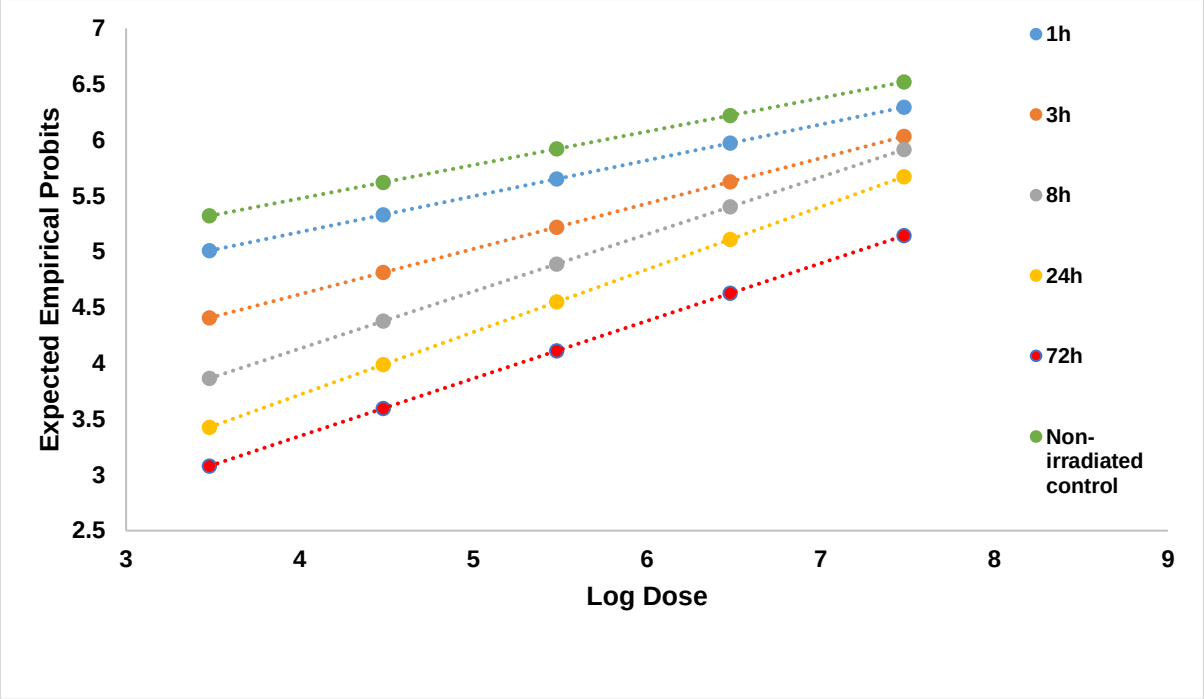

Figure 2.6: UV exposure Cycle 2 log dose-probit regression lines for CrleGV-SA against neonate FCM larvae after UV irradiation for 0 h to 72 h time points in the Q-Sun test chamber.

There was a steady increase in the LC_{50} values from 0 h, (2.57 x 10^4 OBs/ml) to 72 h (1.59 x 10^9 OBs/ml) in cycle 2 (Table 2.2). Relative potency determination showed that with increased exposure to UV the virus became less potent (Table A2, Appendix I). When cycle 1 and cycle 2 were compared (Fig 2.10), time point against corresponding time point, it was recorded that at the 1 h time point the LC_{50} increased slightly though not significantly, and relative potency comparison showed cycle 2 to be more potent than cycle 1(Table A6, Appendix II). All other UV exposure time points for cycle 1 and 2 showed a similar trend, where the cycle 2 LC_{50} value was more potent than the cycle 1 LC_{50} value.

Table 2.2: LC_{50} and LC_{90} values derived from bioassay data of samples exposed to UV in the second exposure cycles.

Time (h)	LC_{50} (OBs/ml)	95 % Fiducial limits		LC_{90} (OBs/ml)	95 % Fiducial Limits		X^2	P
		Lower	Upper		Lower	Upper		
0	2.57×10^{4}	9.24×10^{-3}	5.54×10^{5}	4.80×10^{8}	4.63×10^{7}	4.98×10^{12}	0.267	0.961
1	2.83×10^{5}	4.55×10^{2}	2.42×10^{6}	2.74×10^{9}	2.39×10^{9}	7.63×10^{12}	0.116	0.985
3	8.67×10^{6}	1.01×10^{6}	3.81×10^{7}	1.23×10^{10}	1.20×10^{9}	4.59×10^{12}	0.252	0.964
8	4.93×10^{7}	1.27×10^{7}	1.89×10^{8}	1.56×10^{10}	2.13×10^{9}	1.33×10^{12}	0.256	0.963
24	1.91×10^{8}	5.58×10^{7}	8.72×10^{8}	3.67×10^{10}	4.67×10^{9}	5.04×10^{12}	0.333	0.949
72	1.59×10^{9}	3.66×10^{8}	5.27×10^{10}	4.82×10^{11}	2.27×10^{11}	3.51×10^{16}	0.159	0.978

2.3.3 Surface dose-response bioassays after three UV exposure cycles

Survivors of the second UV exposure cycle were propagated in FCM fifth instars before being exposed to UV for the third UV exposure cycle in the Q-Sun test chamber under the same conditions as in the previous two cycles. The mortality of neonate larvae was related to the dosage for all six UV exposure time points (Fig 2.7). Control mortality of all samples ranged from 4 % to 8 %. The regression lines fitted to the corrected data for all replicates were compared and the residual variances of the lines determined by Bartlett's test. The variances were determined to be homogeneous (X^2 = 1.382; DF = 5; P = 0.01) and thus comparisons of slopes and elevations could be carried out. The lines were determined to be parallel by the Chi-square test and their elevations were shown to be comparable (X^2 = 3.773.; DF = 5; P = 0.05). The Bonferroni method was used to compare the elevations of the lines and determined that the elevations of the lines differed significantly from each other ($F_{5, 23}$ = 2.64; P = 0.05). The control line was significantly different from all the lines from 1 h to 72 h (P=0.0033). This was further corroborated by relative comparative values that showed the non-irradiated control to be the most potent compared with the other five samples

(Table A3, Appendix I). The lines for the 1 h and 3 h samples were both significantly different to the 72 h sample.

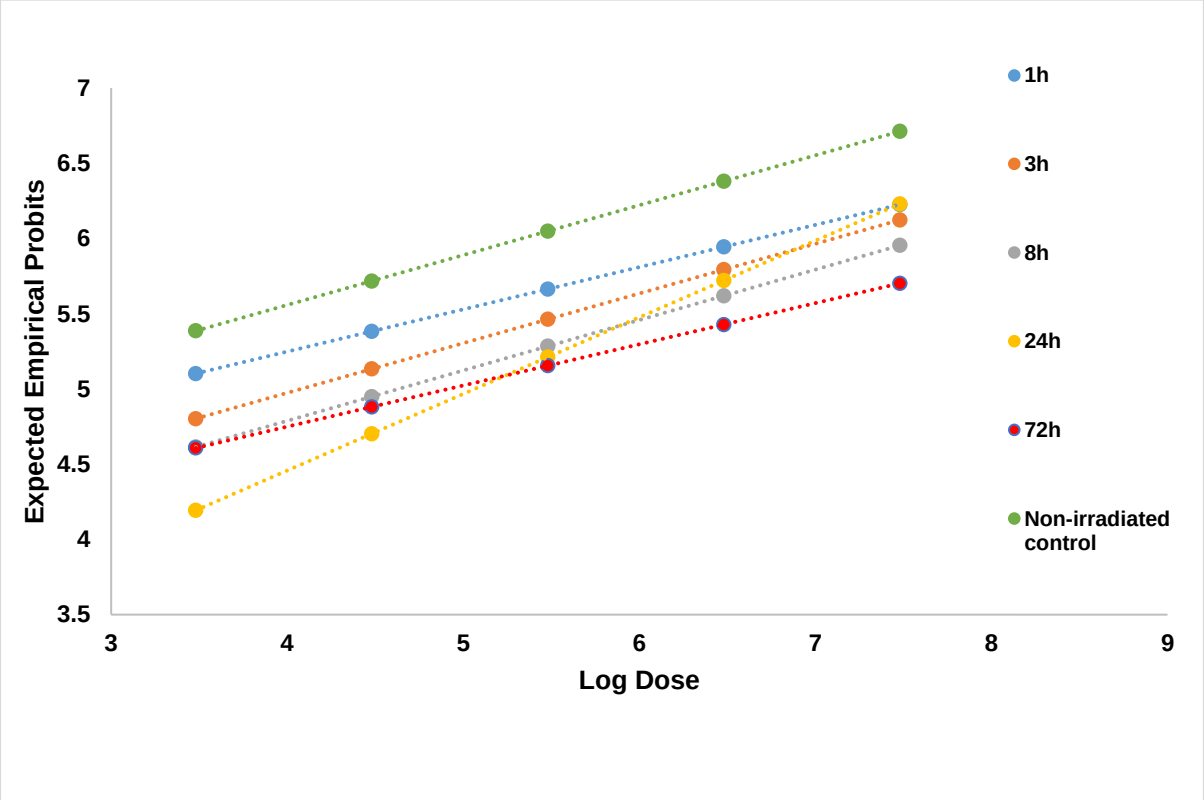

Figure 2.7: UV exposure cycle 3 log dose-probit regression lines for CrleGV-SA against neonate FCM larvae after UV irradiation for 0 h to 72 h time points in the Q-Sun test chamber.

Unlike the first two cycles, the change in LC_{50} values in cycle 3 was not a steady increase. The LC_{50} values from cycle 3 increased from 2.06 x 10^4 OBs/ml for the non-irradiated control to 1.18 x 10^6 OBs/ml for virus exposed to UV for 3 h (Table 2.3). The LC_{50} for the 8 h exposure sample then decreased to 4.26 x 10^5 OBs/ml, before increasing to 1.15 x 10^7 OBs/ml after 24 h exposure and then finally decreasing to 8.18 x 10^6 OBs/ml after 72 h UV exposure. Despite the uneven trend with LC_{50} values, relative potency determination showed that for all the samples, the longer the virus was exposed to UV the less potent it became. However, when time points in cycle 3

were compared to corresponding time points in the previous cycles, patterns began to emerge (Fig. 2.10). There was no significant difference between the 1 h samples, although relative potency comparisons showed the cycle 3 sample to be more potent than the cycle 2 sample (t=1.189), but less potent than the cycle 1 sample (t=0.152) (Table A6, Appendix II).

When the LC_{50} for the 3 h samples in both cycle 1 (LC_{50}=8.97 x 10^5 OBs/ml) and cycle 2 (LC_{50}=8.67 x 10^6 OBs/ml) were compared to the corresponding sample from cycle 3 (LC_{50}=1.19 x 10^6 OBs/ml) (Fig 2.10), it was recorded that after cycle 3 the LC_{50} value was significantly higher (P=0.00333) than the cycle 2 value, but not significantly different from the cycle 1 value. Relative potency comparisons showed the 3 h CrleGV-SA sample for cycle 3 to be more potent than the corresponding cycle 2 sample (t=5.576), but less potent than the cycle 1 sample (t=0.453) (Table A7, Appendix II). Although there was no significant difference between the 8 h samples, relative potency comparisons showed that the cycle 3 sample was more potent than both cycle 1 (t=7.485) and cycle 2 (t=9.075) samples (Table A8, Appendix II). Relative potency comparisons for the 24 h samples showed the cycle 3 sample is much more potent than the cycle 2 (t=25.551) and cycle 1 sample (t=36.551) (Table A9, Appendix II). Similarly, relative potency comparisons for the 72 h samples showed the cycle 3 sample is much more potent than the cycle 2 (t=302.722) and cycle 1(t=239.781) samples (Table A10, Appendix II).

Table 2.3: LC_{50} and LC_{90} values derived from bioassay data of samples exposed to UV in the third exposure cycles.

Time (h)	LC_{50} (OBs/ml)	95 % Fiducial limits		LC_{90} (OBs/ml)	95 % Fiducial Limits		X^2	P
		Lower	Upper		Lower	Upper		
0	2.06×10^4	3.69×10^{-2}	4.04×10^5	1.52×10^8	1.88×10^7	1.07×10^{11}	0.065	0.991
1	1.30×10^5	4.42×10^{-1}	1.73×10^6	4.75×10^9	2.85×10^8	$6.06x\ 10^{14}$	0.502	0.916
3	$1.18 x10^6$	1.62×10^4	$7.35x\ 10^6$	$9.08 x10^9$	6.61×10^8	2.96×10^{13}	0.135	0.982
8	4.26×10^5	1.99×10^5	2.30×10^7	2.86×10^{10}	1.67×10^9	1.49×10^{14}	1.064	0.788
24	1.15×10^7	2.71×10^6	3.75×10^7	3.79×10^9	6.68×10^8	1.29×10^{11}	0.233	0.967
72	8.18×10^6	1.97×10^5	6.64×10^7	3.91×10^{11}	6.89×10^9	$8.25x\ 10^{18}$	0.501	0.916

2.3.4 Surface dose-response bioassays after four UV exposure cycles

Survivors of the 3rd UV exposure cycle were propagated in FCM fifth instars before being exposed to UV for the 4th UV exposure cycle in the Q-Sun test chamber under the same conditions as the previous three cycles. The mortality of neonate larvae was related to the dosage of all six time points (Fig 2.8). Control mortality of all samples ranged from 0 % to 8 %. The regression lines fitted to the corrected data for all replicates were compared and the residual variances of the lines determined by Bartlett's test. The variances were determined to be homogeneous ($X^2 = 0.237$; DF = 5; P = 0.01) and thus comparisons of slopes and elevations could be carried out. The lines were determined to be parallel by the Chi-square test and their elevations were shown to be comparable ($X^2 = 0.602$; DF = 5; P = 0.05). The Bonferroni method was used to compare the elevations of the lines and determined that the elevations of the lines differed significantly from each other ($F_{5, 23} = 2.64$; P = 0.05). At P=0.0033, the control line was significantly different from all the lines from 1 h to 24 h, but not significantly different from the 72 h line (P=0.0033).

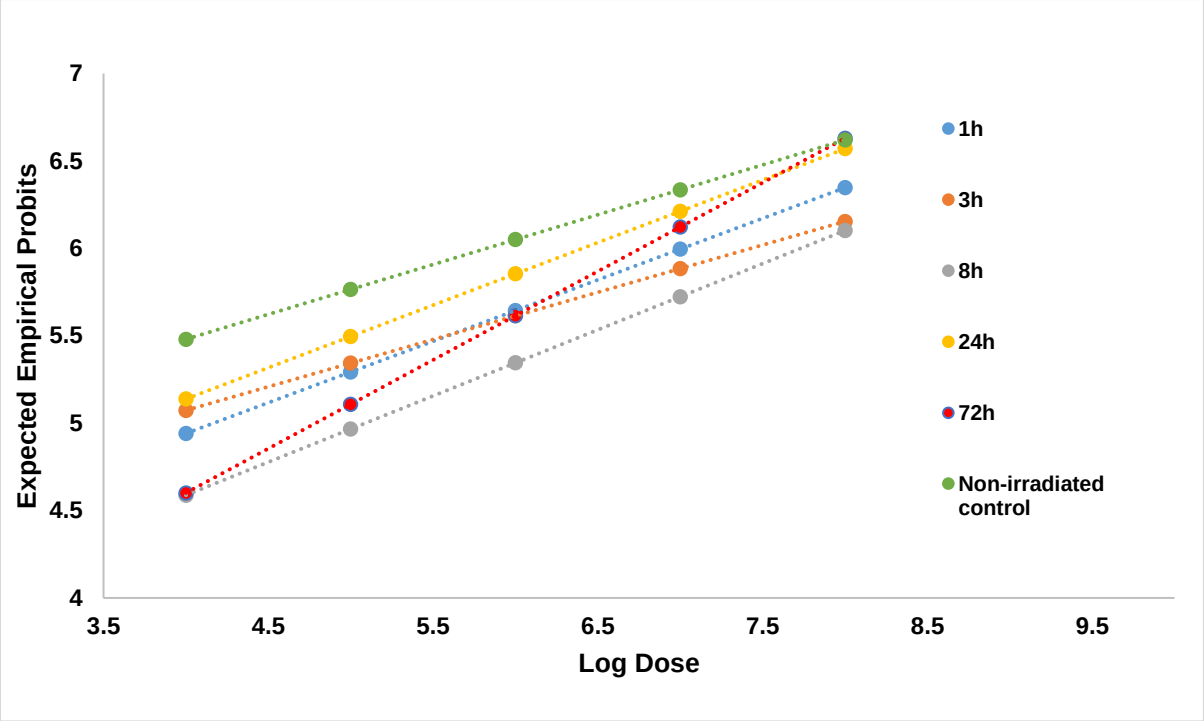

Figure 2.8: UV exposure Cycle 4 log dose-probit regression lines for CrleGV-SA against neonate FCM larvae after UV irradiation for 0 h to 72 h UV exposure time points in the Q-Sun test chamber.

As observed in cycle 3, the change in LC_{50} values in cycle 4 was not a steady increase. The LC_{50} values from cycle 4 increased from 2.08 x 10^4 OBs/ml for the non-irradiated control to 1.47 x 10^6 OBs/ml for the 3 h exposure sample (Table 2.4). The LC_{50} for the 8 h sample then decreased to 5.36 x 10^5 OBs/ml before increasing to 1.22 x 10^7 OBs/ml after 24 h exposure and then finally decreasing to 6.12 x 10^6 OBs/ml after 72 h exposure. Relative potency comparisons were carried out for the samples in cycle 4 (Table A4, Appendix I). As in the previous cycles, the general trend observed with relative potency values was that the virus became less potent with increased time under UV exposure. Comparisons between corresponding time points in the cycle 4 and the previous cycle were also carried out (Fig 2.10). The LC_{50} of the 1 h sample from cycle 3 was 1.30 x 10^5 OBs/ml, this increased to 1.47 x 10^6 OBs/ml after 1 h UV

exposure in cycle 4. This was not significantly different (P=0.00333), with the relative potency comparisons showing the cycle 3 sample to be more potent than the cycle 4 sample (t=4.469) (Table A6, Appendix II). The LC_{50} at 3 h in cycle 3 was 1.19 x 10^6 OBs/ml and decreased to 5.36 x 10^5 OBs/ml at cycle 4. Relative potency comparison showed that the two time points were only slightly different in potency (t=1.063 at cycle 3) (Table A7, Appendix II). While there was no significant difference between the 8 h samples at cycle 3 and 4, the relative potency values, showed that the cycle 3 samples were almost twice as potent as the cycle 4 virus samples (t=2.0384) (Table A8, Appendix II). There was a significant difference between the 24 h samples at cycle 3 (LC_{50}=1.15 x 10^7 OBs/ml) and cycle 4 (LC_{50}=4.13 x 10^5 OBs/ml) and this was corroborated by relative potency comparison that showed the cycle 4 sample to be more potent than the cycle 3 virus sample (t=13.876) (Table A9, Appendix II). Relative potency values also showed that the 72 h sample at cycle 4 was more potent than the 72 h exposure sample at cycle 3 (t=4.875) (Table A10, Appendix II).

Table 2.4: LC_{50} and LC_{90} values derived from bioassay data of samples exposed to UV in the fourth exposure cycles.

Time (h)	**LC_{50} (OBs/ml)**	**95 % Fiducial limits**		**LC_{90} (OBs/ml)**	**95 % Fiducial Limits**		**X^2**	**P**
		Lower	**Upper**		**Lower**	**Upper**		
0	2.08 x 10^4	1.89 x 10^{-6}	8.32 x 10^5	6.49 x 10^8	6.22 x 10^7	1.02 x 10^{13}	0.206	0.971
1	1.47 x 10^6	1.35 x 10^4	9.60 x 10^6	6.51 x 10^9	7.33 x 10^8	2.77 x 10^{13}	1.186	0.760
3	5.36 x10^5	2.18 x 10^1	6.90 x 10^6	2.96 x10^{10}	1.47 x 10^9	1.21 x 10^{16}	0.291	0.957
8	1.22 x 10^7	8.16 x 10^5	5.75 x 10^7	2.99 x 10^{10}	2.81 x 10^9	1.54 x 10^{13}	1.222	0.751
24	4.12 x 10^5	7.42 x 10^2	3.59 x 10^6	1.57 x 10^9	2.20 x 10^8	3.30 x 10^{11}	0.320	0.952
72	6.12 x 10^6	7.37 x 10^5	2.18 x 10^7	2.07 x 10^9	4.36 x 10^8	5.00 x 10^{10}	0.588	0.898

2.3.5 Surface dose-response bioassays after 5 UV exposure cycles

Survivors of the fourth UV exposure cycle were propagated in FCM fifth instars before being exposed to UV for the fifth UV exposure cycle in the Q-Sun test chamber under the same conditions as the previous four cycles. The mortality of neonate larvae was related to the dosage of all six time points (Fig 2.8). Control mortality of all samples ranged from 0 % to 8 %. The regression lines fitted to the corrected data for all replicates were compared and the residual variances of the lines determined by Bartlett's test. The variances were determined to be homogeneous (X^2 = 0.237; DF = 5; P = 0.01) and thus comparisons of slopes and elevations could be carried out. The lines were determined to be parallel by the Chi-square test and their elevations were shown to be comparable (X^2 = 0.602; DF = 5; P = 0.05). The Bonferroni method was used to compare the elevations of the lines and determined that the elevations of the lines differed significantly from each other ($F_{5, 23}$ = 2.64; P = 0.05).

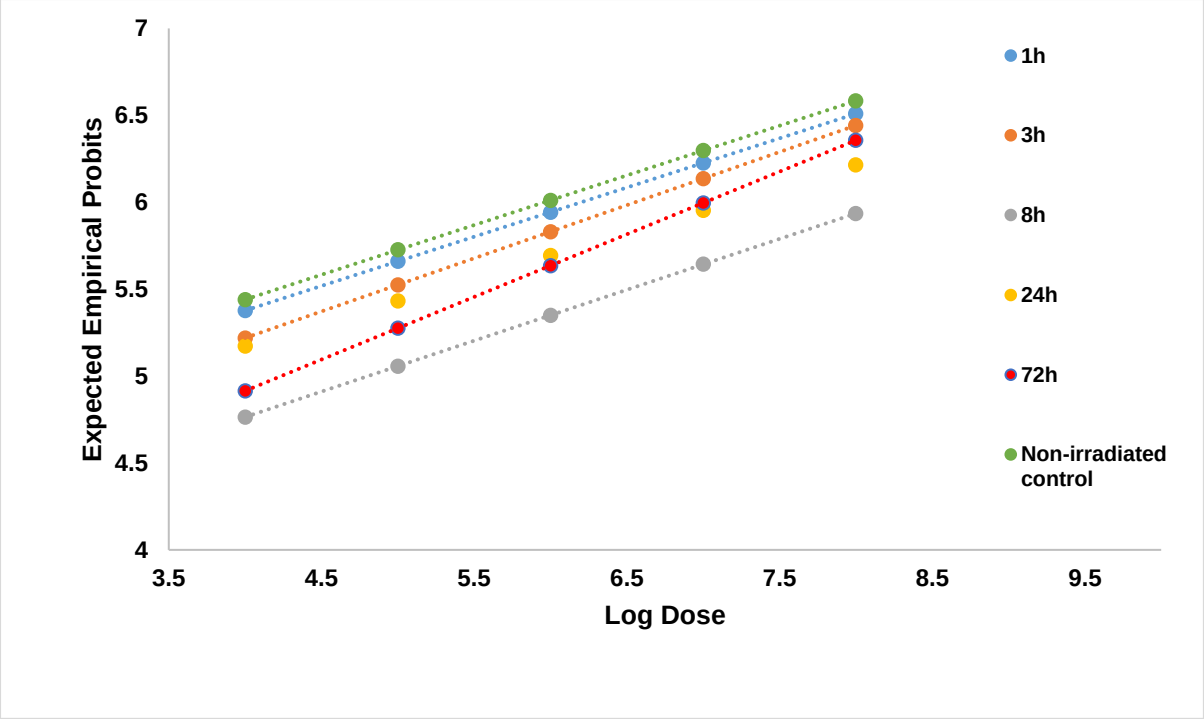

Figure 2.9: UV exposure Cycle 5 log dose-probit regression lines for CrleGV-SA against neonate FCM larvae after UV irradiation for 0 h to 72 h UV exposure time points in the Q-Sun test chamber.

LC_{50} values in cycle 5 increased from the non-irradiated control (2.87×10^4 OBs/ml) to the 8 h UV exposure sample (6.38×10^6) and then decreased for the 24 h (2.16×10^5 OBs/ml) and the 72 h (1.73×10^6 OBs/ml) virus samples (Table 2.5). Comparisons between corresponding time points in cycle 5 and cycle 4 (Fig. 2.10) revealed that samples at cycle 4 were less potent compared to those at cycle 5 (Table A10, Appendix II).

Table 2.5: LC_{50} and LC_{90} values derived from bioassay data of samples exposed to UV in the fifth exposure cycles.

Time (h)	LC_{50} (OBs/ml)	95 % Fiducial limits		LC_{90} (OBs/ml)	95 % Fiducial Limits		X^2	P
		Lower	Upper		Lower	Upper		
0	2.87×10^{4}	1.70×10^{-5}	9.37×10^{5}	8.83×10^{8}	8.86×10^{7}	6.92×10^{12}	0.829	0.829
1	4.64×10^{4}	2.07×10^{-3}	1.27×10^{6}	1.57×10^{9}	1.48×10^{8}	2.34×10^{13}	0.508	0.915
3	1.93×10^{5}	1.80×10^{1}	2.57×10^{6}	2.99×10^{9}	3.10×10^{8}	5.34×10^{12}	0.861	0.836
8	6.38×10^{6}	4.14×10^{4}	4.61×10^{7}	1.53×10^{11}	5.72×10^{9}	4.14×10^{16}	0.642	0.886
24	2.16×10^{5}	2.19×10^{-1}	3.96×10^{6}	1.82×10^{10}	9.33×10^{8}	2.79×10^{16}	0.448	0.927
72	1.73×10^{6}	1.60×10^{4}	1.12×10^{7}	6.22×10^{9}	7.01×10^{8}	2.87×10^{12}	0.296	0.956

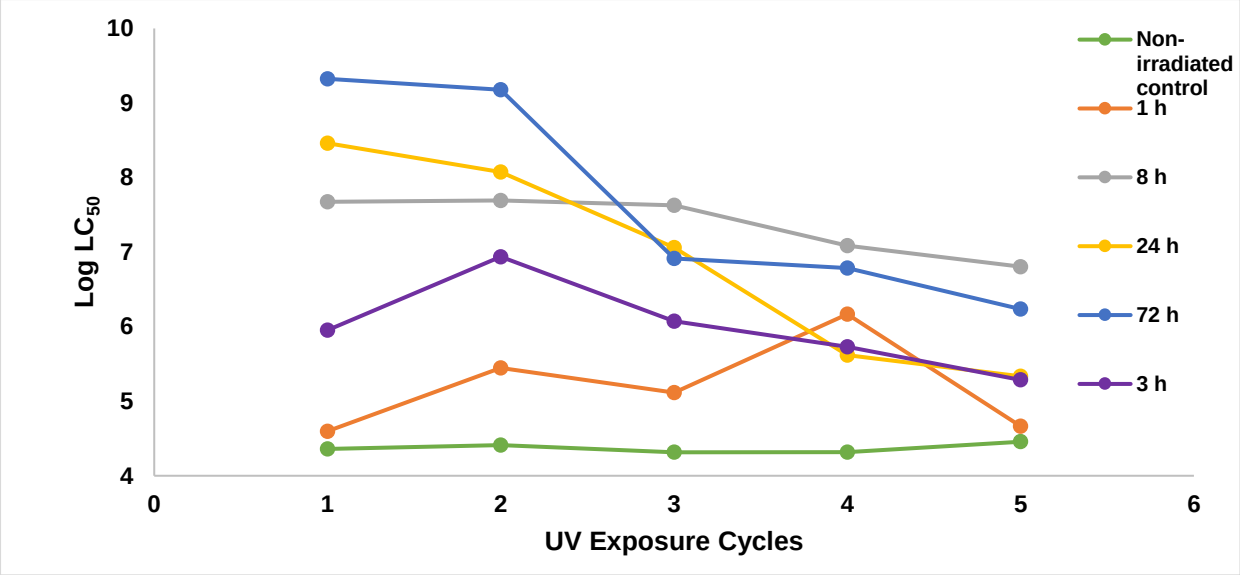

Figure 2.10: Change in LC_{50} at each UV exposure time point over five UV exposure cycles

2.4 Discussion and Conclusion

The damaging effect of ultraviolet radiation remains one of the main challenges facing the use of baculoviruses as biopesticides (Szewczyk *et al*., 2006). As such it is important that ways to improve the persistence of the virus are investigated. In this chapter, the selection of UV-tolerant viruses and generation of a UV-tolerant virus population was explored. To select for UV-tolerant CrleGV-SA, repeated UV exposure for various time periods and propagation in fifth instars was carried out. Analysed bioassay data from both UV exposure cycle 1 and cycle 2 indicated a gradual increase in LC_{50} as UV exposure time increased. This increase is likely to be due to the detrimental effect of UV on baculovirus survival and virulence, which intensifies with UV exposure time and is consistent with previous findings (Shapiro & Domek; 2002; Shapiro *et al*. 2002; Arthurs *et al.*, 2008; Mwanza 2015). However, from cycle 3 onwards the effect of increased exposure recorded in cycle 1 and 2 was not clear. This can be attributed to the fact that at this point, the selection process resulted in more tolerant virus being present and its contribution to the virulence of the virus population becoming more pronounced.

LC_{50} values for the 1 h UV exposure time point had an irregular pattern, with no clear trend. The LC_{50} increased and decreased after every subsequent cycle. This could be because the virus was not exposed to UV for long enough to select for UV-tolerant baculoviruses. As a result, the 1 h exposure samples were considered as having been unsuccessful in selecting UV-tolerant virus throughout the five cycles of UV exposure. Similarly, bioassay data obtained from the 8 h time points across the five UV exposure cycles was quite irregular and, as a result of this irregular progression in LC_{50}, the 8 h time point was discarded and not probed further.

Bioassay data from 3 h UV exposure showed that the LC_{50} increased from cycle 1 (8.97×10^5 OBs/ml), to cycle 2 (8.67×10^6 OBs/ml). However, in subsequent cycles the LC_{50} decreased, suggesting that the virus was regaining its potency, with cycle 5 3 h UV exposure samples being the most potent in the grouping. This suggests that the cycle 5 virus sample had become more UV-tolerant after being passaged through several cycles of UV exposure. Thus, for the samples exposed to UV for 3 h, a UV-tolerant virus population was selected after the fifth cycle. Relative potency comparisons determined that the cycle 3 (t=3.936) and cycle 4 (t=4.276) samples were both less potent than the cycle 5 sample. The cycle 1 (t=1.805) sample was also less potent than the cycle 5 sample, suggesting that this cycle 5 sample had become more UV-tolerant after being passaged through five cycles of UV exposure. Thus for the samples exposed to UV for 3 h, UV-tolerant virus was selected for after the fifth cycle.

The LC_{50} for the 24 h UV exposure samples decreased from cycle 1 (2.89×10^8 OBs/ml) to cycle 5 (2.16×10^5 OBs/ml) (Fig 2.10). Relative potency comparisons showed how each sample in successive UV cycles became more potent than the samples in the preceding cycle. When the cycle 5 sample was made the reference, cycle 1 (t=223) and cycle 2 (t=156) samples were found to be significantly less potent. A significant decrease was recorded when comparing with cycle 3 (t=6.107), suggesting the virus population was becoming less susceptible to UV after cycle 3, as compared to the previous cycles. Although, the cycle 4 (t=0.440) sample was more potent than the cycle 5 sample, this was not significantly different and indicated selection of the UV-tolerant virus at this point.

Similar to the 24 h UV exposure samples, the LC_{50} for the CrleGV-SA samples exposed to UV for 72 h decreased from cycle 1 (2.11×10^9 OBs/ml) to cycle 5 (1.73×10^6 OBs/ml). Relative potency determination showed how the selected CrleGV-SA

samples in cycle 5 were more potent than the samples in cycle 1 and cycle 2 (both t>1000). Like the 24 h samples, the relative potency value dramatically changed at cycle 3 (t=5.992) showing that the virus had become less susceptible to UV irradiation at this stage. The CrleGV-SA sample at cycle 5 was slightly more potent than the sample at cycle 4 (t=1.227). Thus, using the 72 h sample, a UV-tolerant virus sample was successfully selected.

The data in this study followed the trend recorded by Jeyarani *et al*. (2013) with HearNPV-CBE I. After an initial loss in virulence, they recorded an overlap in the LC_{50} values of the original strain and UV exposed strain in the final three cycles, in UV tolerance selection tests. They concluded that this indicated retention of virulence. Brassel and Benz (1979) also established that the decisive selection took place in the third and fourth cycles and, although they proceeded to a sixth cycle, there was no further improvement in the UV-tolerance of CpGV. In contrast to the findings in this study, Shapiro and Bell (1984) recorded that the original activity of LdMNPV declined for the first 5 cycles, increased at the sixth cycle and remained stable up to the tenth cycle. In all UV selection studies, a critical cycle was reached after which UV-tolerant strains were selected.

In the present study there was a 4.65-fold decrease in the LC_{50} value after 3 h UV exposure, from cycle 1 to cycle 5. In comparison, Brassel and Benz (1979), found that after six UV exposure cycles (10 min exposure time per cycle) there was a 5.6-fold increase in UV tolerance of CpGV, while Shapiro and Bell (1984) reported a 2.5-fold increase in the activity of LdMNPV after 6 exposure cycles (60 min exposure time). Witt & Hink (1979) reported a six-fold difference in the sensitivity of AcMNPV after 5 selection cycles (exposure time between 0-600 min), with an additional 5 cycles not yielding any further significantly increased tolerance compared to the fifth cycle. In

the present study the fold difference in LC_{50} was even higher for the 24 h UV exposure (1338-fold difference) and 72 h exposure (1220-fold difference) CrleGV-SA samples. These fold differences following longer exposure time periods were much higher than what has been previously reported for other viruses. This is attributed to the presence of UV-tolerant CrleGV-SA with better selection after longer periods of UV exposure, which were not tested in the reported studies. Over the duration of the study, the non-irradiated control remained relatively stable, thus indicating both the reproducibility of the system as well as stability of untreated (control) CrleGV-SA during serial passaging.

The virulence of the selected CrleGV-SA was similar to that of the unexposed virus and this is comparable to findings by Jeyarani *et al.* (2013). However, this contrasts with findings by Witt and Hink, (1979), who reported that the virulence of selected AcMNPV was reduced compared to the wild type virus. It was not determined whether the loss in virulence and increase of UV tolerance were a result of the same mutation or if there were independent events.

In conclusion, bioassay data from UV exposure cycle 1 confirmed that UV-induced deactivation increases with increase in exposure time. Bioassay data also showed that UV-tolerant virus was successfully isolated. The next step was to sequence the whole genome of the UV–tolerant virus selected after five cycles and compare it with the sequence of the original non-tolerant CrleGV-SA, and to investigate any morphological differences between the UV exposed and unexposed samples using transmission electron microscopy.

Chapter 3

Genome sequencing and analysis of CrleGV-SA after cycle 1 and cycle 5 UV exposure

3.1 Introduction

The selection and isolation of potentially UV-tolerant CrleGV-SA was described in Chapter 2. To identify molecular differences between the UV-susceptible and UV-tolerant CrleGV-SA, next generation sequencing (NGS) was conducted on CrleGV-SA samples from UV exposure cycle 1 and cycle 5. The resultant sequences were compared with the published sequence for CrleGV-SA.

NGS is a high-throughput non-Sanger sequencing method that generates millions of sequences at once (Shucter, 2008; Hall, 2007). The sequence reads generated are short and vary in size (35-250 bp or 650-800 bp) depending on the sequencer used and are used in *de novo* assembly of a complete genome sequence (Mardis, 2007; Liu *et al.*, 2011). The most commonly used NGS platforms are Roche 454 pyrosequencing (454 Life Science), Illumina MiSeq and HiSeq (Solexa) sequencing, Nanopore sequencing (Oxford Nanopore Technologies) and Solid sequencing (ABI Biosystems) (Liu *et al.*, 2011; Shokralla *et al*., 2012). While each sequencing platform may have its own sequencing bias, sequence reads from NGS, generally avoid cloning bias issues that may affect genome representations (Mardis, 2007).

NGS has been employed to sequence and characterise complete baculovirus genomes. Presently there are approximately 84 full baculovirus genomes that have been sequenced, of which 54 are in the genus *Alphabaculovirus* (lepidopteran NPVs), 26 are in the genus *Betabaculovirus* (lepidopteran GVs), 3 are in the genus *Gammabaculovirus* (hymenopteran NPVs) and 1 in the genus *Deltabaculovirus* (dipteran NPV) (GenBank, 2019). NGS data have been used to construct and determine phylogenetic relationships of baculoviruses. Previously, the polyhedrin/granulin gene was used to determine these relationships (Bidesh *et al.,* 2000). When other genes such as the *DNA polymerase, lef-2, ecdysteroid UDP-glucotransferase cathepsin* and *chitinase* genes were used, differences in the resultant phylogenetic trees were noted, especially for polyhedrin, which disagreed with other gene phylogenies (Bulach *et al.,* 1999; Chen *et al.,* 1997; Chen *et al.,* 1999; Clarke *et al.,* 1996; Kang *et al.,* 1998). However, the use NGS data for whole genome sequences, has proved to be more advantageous than the use of the sequence data of single genes (Herniou *et al.,* 2001). In addition to the assembly of whole genome sequences and determination of phylogenetic relationships of baculoviruses, NGS has been used to identify and quantify the genetic composition of resistance-breaking commercial isolates of Cydia pomonella granulovirus and in the identification of singe nucleotide polymorphisms present in CpGV isolates (Alletti *et al.,* 2017; Wennmann *et al*., 2017). One of the advantages of NGS analysis is that it can be used to detect single nucleotide polymorphisms (SNPs) quicker than traditional methods (Hyten *et al*., 2010). SNPs represent the most common type of genetic variation in genetic sequences.

In this chapter the sequences of CrleGV-SA obtained after exposure to UV in cycle 1 and cycle 5 were assembled and mapped to the CrleGV-SA genome and compared to find variation that could have given rise to the UV tolerance property.

3.2 Materials and methods

3.2.1. CTAB DNA extraction

CrleGV-SA samples obtained from UV-tolerance experiments described in section 2.2 were used to prepare genomic DNA for sequencing. A CrleGV-SA virus sample from cycle 1 (referred to as CrleGV-SA C1 from here onwards) of exposure to UV for 72 h and a sample from cycle 5 (referred to as CrleGV-SA C5) from here onwards) of UV exposure for 72 h were amplified in FCM fifth instars. OBs were extracted, purified (as described in section 2.2.1) and diluted to a concentration of 1 x 10^8 OBs/ml. Genomic DNA was extracted from the virus samples using a CTAB extraction method modified by Singh *et al*. (2003) and by Goble (2007). Aliquots of 80 µl 1 M Na_2CO_3 were added to 200 µl of each virus sample in 1.5 ml Eppendorf tubes and incubated at 37 °C for 30 min. After incubation, 120 µl 1 M Tris-HCl (pH 6.8), 90 µl 10 % SDS and 75 µl 20 mg/ml proteinase K (20 mg/ml) (Inqaba Biotech, SA) were added and the samples incubated for 60 min at 56 °C. The samples were then centrifuged (Eppendorf, Germany) at 13400 g for 3 min, the resultant supernatants transferred to new 1.5 ml tubes and the pellets discarded. To each supernatant, 500 µl CTAB buffer (100 mM Tris-HCl (pH8), 1.4 NaCl, 20 mM EDTA and 2 % CTAB) was added and incubated at 70°C. After incubation, 500 µl ice cold ultra-pure chloroform held at -20 °C was added and the mixture centrifuged in an Eppendorf microfuge at 10000 g. The DNA layer was transferred to a new Eppendorf tube, 400 µl ice cold isopropanol added and the sample left to stand at -20°C overnight. The sample was then centrifuged at 13400 g

for 30 min in an Eppendorf microfuge. The resultant pellet was resuspended in 1 ml ice cold 70 % ethanol, centrifuged for 10 min at 13400 g in an Eppendorf microfuge and the ethanol poured off. The pellet was air dried and resuspended in 50 µl RNase-free, DNase-free ultrapure water and stored at -20°C.

3.2.2 DNA Sequencing

Approximately 200 ng genomic DNA extracted from CrleGV-SA samples from UV exposure cycle 1 and cycle 5 as described in section 3.2.1 were sent for sequencing by Inqaba Biotech, SA. The sequencing was performed using next generation DNA sequencing technology on the MiSeq desktop sequencer (Illumina, USA). The reads obtained for each sample were paired and ends trimmed using the soft trimming function in Geneious R11 (Biomatters Ltd, New Zealand). The *de novo* assembly was then run in Geneious R11 . The CrleGV-SA genome (GenBank Accession number MF974563; van der Merwe *et al.,* 2017) was used as the reference sequence for mapping and the two samples were mapped against it. The CrleGV-SA isolate sequenced by van der Merwe *et al.* (2017) was the same one used in this study. For the assembly of the reads, medium sensitivity was used and single consensus sequences generated for CrleGV-SA C1 and CrleGV-SA C5. Pairwise multiple alignments were performed on the consensus sequences, and thereafter predicted ORFs were mapped against the reference CrleGV-SA published sequence. The Find SNPS/Variants tool was used to search for SNPs in both CrleGV-SA cycle 1 and CrleGV-SA cycle 5 and these were exported in a table to Microsoft Excel 2016 in csv format for further analysis.

3.2.3 *In-silico* restriction endonuclease analysis of CrleGV-SA genomes from OBs exposed to UV in cycle 1 and cycle 5.

Full CrleGV-SA genomes extracted from OBs exposed to UV in exposure cycle 1 and exposure cycle 5 were subjected to *in silico* restriction endonuclease analysis in Geneious R11 using the Restriction Cloning tool. The appropriate sequence was selected in the document pane of the software and the Cloning tab, followed by the Find Restriction sites tab used for the selection of a subset of enzymes commercially available, with known restriction sites contained in the CrleGV-SA genome. Based on publications by Opoku-Debrah *et al*. (2013 & 2016) the following restriction enzymes were selected; *BamH*I, *EcoR*I, *Kpn*I, *Hind*III, *Xba*I, *Sal*I and *Xho*I. The resultant restriction profiles for each enzyme and for each genome sequence were then compared.

3.3 Results

In addition to functional differences measured by bioassay data, genome sequencing was used to provide evidence that UV-tolerant viruses had been selected by the series of exposure and re-exposure to UV irradiation.

Sequencing of CrleGV-SA from UV exposure cycle 1 generated 278 938 paired reads, of which 278 399 reads were used to produce 470 contigs. The largest contig was 115 445 bases long and was assembled from 272 009 sequences. The CrleGV-SA cycle 1 genome was assembled into a contiguous sequence with a length of 111 334 bp (Fig 3.1) and with a GC content of 32.6 % and 99.9 % identity to the CrleGV-SA genome (van der Merwe *et al*., 2017).

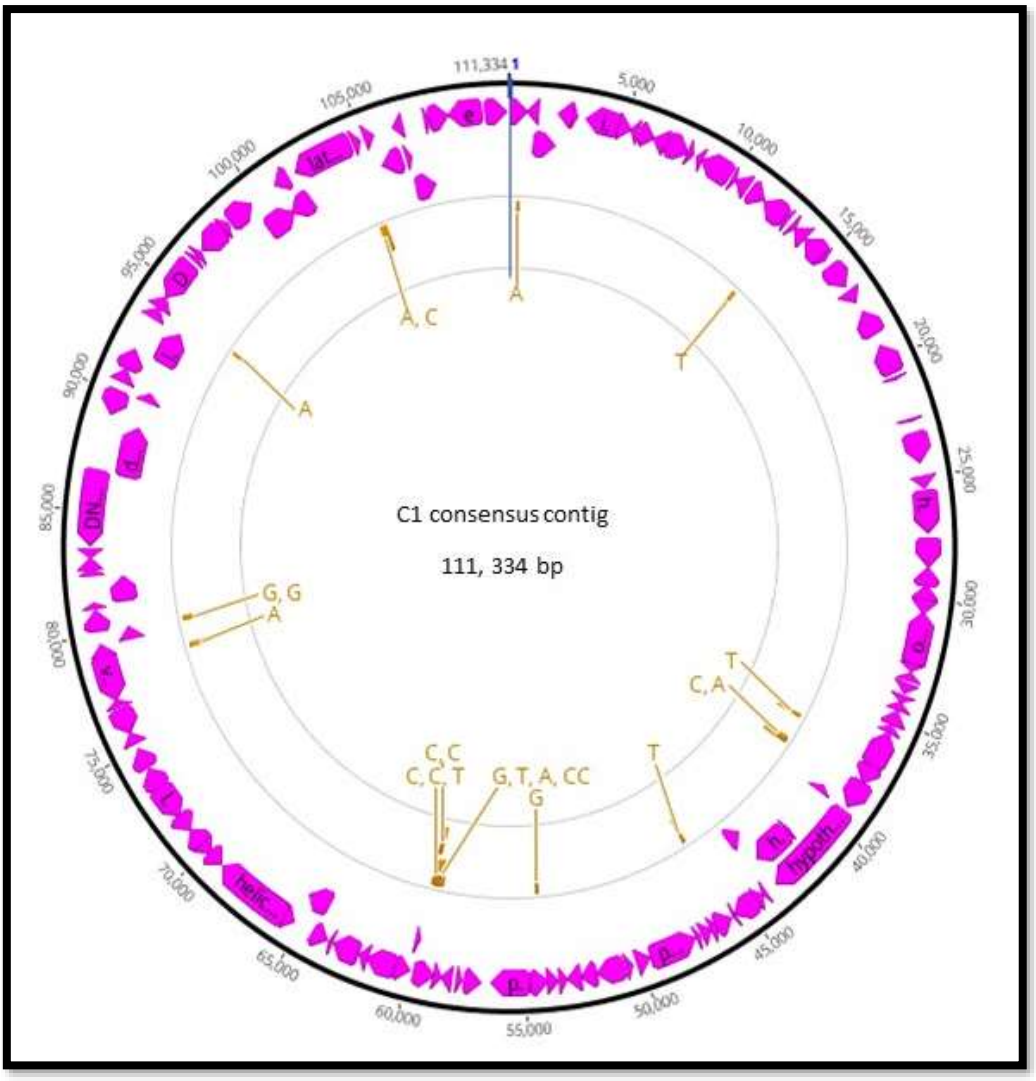

Figure 3.1: CrleGV-SA genome from UV exposure cycle 1 (C1) after annotation, using the published CrleGV-SA sequence as the reference. ORFs are in pink and because of the genome size cannot be individually labelled fully. The blue line indicates where the first position of the first nucleotide. The brown letters represent points were SNPs occurred. Included are SNPs that resulted in no change in amino acids. The numbers on the outside represent nucleotide positions.

Sequencing of CrleGV-SA from UV exposure cycle 5 generated 1 030 337 paired reads, of which 1 035 796 reads were used to produce 3901 contigs. The largest contig was 56825 bases long and was assembled from 492215 sequences. The CrleGV-SA

cycle 5 genome was assembled into a contiguous sequence with a length of 113730 bp (Fig 3.2) and the resultant nucleotide alignment had a GC content of 32.6 % and 99.99 % identity to the CrleGV-SA genome.

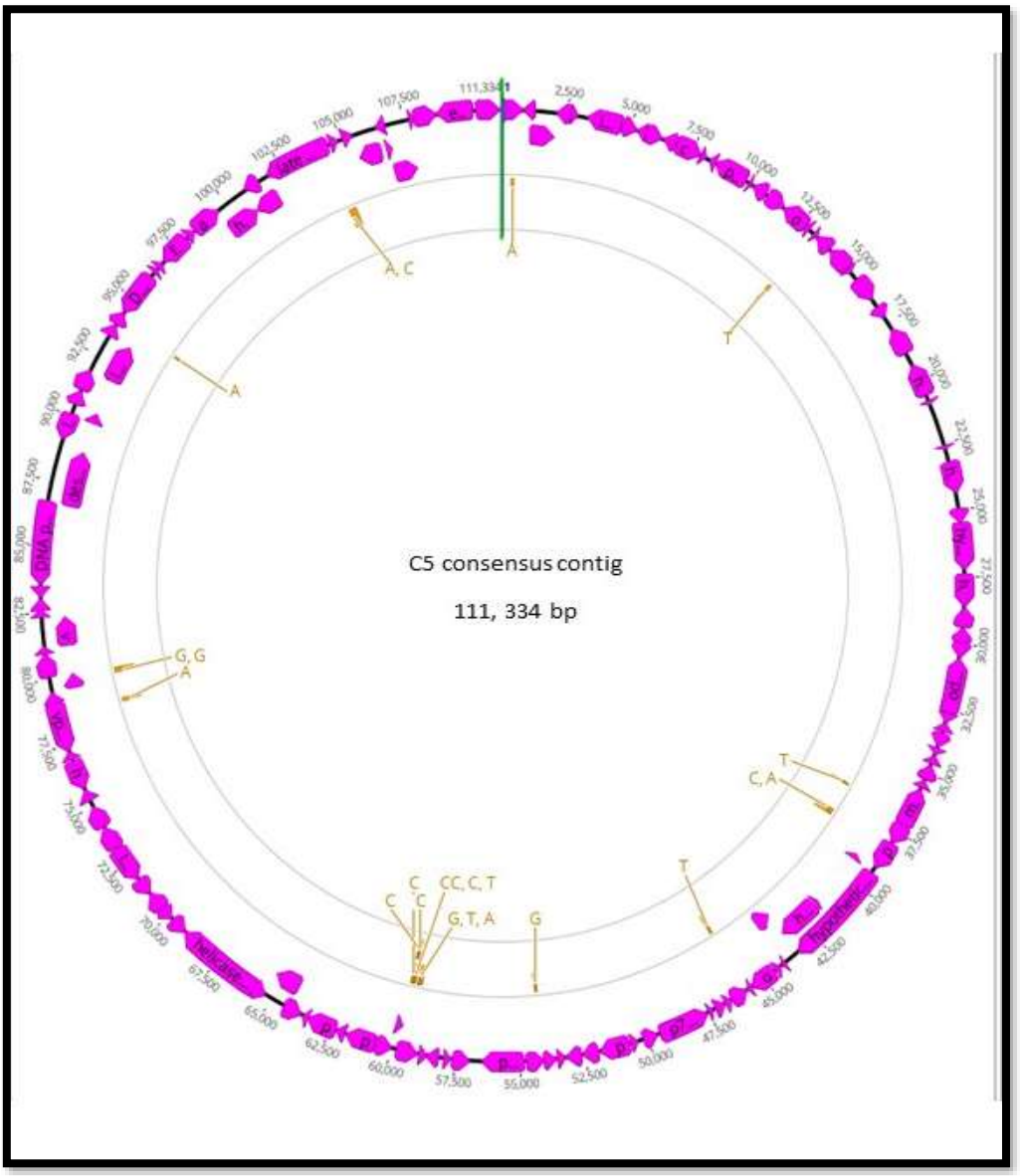

Figure 3.2: CrleGV-SA genome from UV exposure cycle 5 (C5) after annotation using the published CrleGV-SA sequence as the reference. The blue line indicates where the first position of the first nucleotide. The brown letters represent points were SNPs

occurred. Included are SNPs that resulted in no change in amino acids. The numbers on the outside represent nucleotide positions.

The genome sequence of the CrleGV-SA exposed to UV in cycle 1 was mapped to the published unexposed CrleGV-SA genome sequence (van der Merwe *et al*., 2017) and seven SNPs were detected in the consensus sequence from the surviving population (Table 3.1). These SNPs were present in the population but not necessarily in each virus. The first SNP detected was a SNP transition, where the nucleotide guanine was changed to adenine in the granulin gene. This would have resulted in a change in amino acid from the sulphur-rich cysteine to the acidic tryptophan. Another SNP was detected at position 36843, where a transversion takes place from adenine, replaced by thymine in the metalloproteinase Coding Sequence (CDS). This SNP resulted in a change of amino acid from the aromatic phenylalanine to the aliphatic isoleucine. At nucleotide position 38194 a SNP transition from thymine to cytosine was detected, which resulted in the change of amino acid from isoleucine to the hydroxylic threonine. At position 45853, a SNP transition from cytosine to thymine was detected and this resulted in the amino acid changing from the aliphatic valine to the sulphur containing methionine. A SNP transition at position 79840, resulted in the change of amino acid from valine to leucine. Another amino acid change from the acidic glutamic acid to the basic lysine took place as a result of a SNP transition from guanine to adenine at position 94086. The last SNP was detected at position 104574, where thymine was replaced by cytosine and this resulted in the change of amino acid from methionine to threonine and hence the loss of a start codon in a hypothetical CDS.

The CrleGV-SA sequence obtained after exposure to UV in cycle 5 was mapped to the published sequence of the unexposed CrleGV-SA genome (van der Merwe *et al*., 2017). A total of 14 SNPs were detected. Of these, 7 had already been identified in

the cycle 1 sequence and the other 7 were unique to the cycle 5 sequence (Table 3.2). The first of these SNPs, unique to the cycle 5 sequence, was at position 13168 where a cytosine was replaced by thymine, which led to the amino acid change from alanine to valine. At position 59709-59710, two thymine residues were replaced by two cytosine residues, leading to the amino acid change from isoleucine to valine. At 59734, adenine was replaced by thymine and this led to the change in amino acid from aspartic acid to glutamic acid. At 59752, a SNP transversion was detected where an adenine residue was replaced by a cytosine residue and this resulted in the change in amino acid from the basic histidine to the amidic glutamine. At 59779, a thymine was replaced by a cytosine, which led to the amino acid change from the hydroxylic serine to the aliphatic serine. At 78522, a guanine was replaced by an adenine and consequently a serine amino acid was replaced by a phenylalanine.

Table 3.1: Common SNPs detected in both of CrleGV-SA genome consensus sequences from virus exposed to UV in cycle 1 and cycle 5.

Name	Nucleotide Positions	Amino Acid Change	Change	Codon Change	Polymorphism Type	Protein Effect	Protein
A	434	C -> Y	G -> A	TGT -> TAT	SNP (transition)	Substitution	Granulin
A	94086	E -> K	G -> A	GAA -> AAA	SNP (transition)	Substitution	Hypothetical protein CDS
C	38194	I -> T	T -> C	ATT -> ACT	SNP (transition)	Substitution	PIF factor-2
G	79840	L -> V	T -> G	TTG -> GTG	SNP(transversion)	Substitution	Hypothetical protein CDS
T	45853	V -> M	C -> T	GTG -> ATG	SNP (transition)	Substitution	39K protein
T	36843	F -> I	A -> T	TTT -> ATT	SNP(transversion)	Substitution	Metallo-proteinases CDS
C	104574	M -> T	T -> C	ATG -> ACG	SNP (transition)	Start Codon Loss	Hypothetical protein CDS

Table 3.2: SNPs unique to the CrleGV-SA cycle 5 genome consensus sequence.

Name	Nucleotide position	Amino Acid Change	Change	Codon Change	Polymorphism Type	Protein Effect	Protein
A	78522	S -> F	G -> A	TCT -> TTT	SNP (transition)	Substitution	Hypothetical CDS
C	59752	H -> Q	A -> C	CAT -> CAG	SNP(transversion)	Substitution	Hypothetical CDS
C	59752		A -> C		SNP(transversion)	Extension	Hypothetical CDS
C	59779	S -> G	T -> C	AGT -> GGT	SNP (transition)	Substitution	Hypothetical CDS
CC	59709	LI -> LV	TT -> CC	ATT -> GTT	Substitution	Substitution	DNA binding protein
T	13168	A -> V	C -> T	GCT -> GTT	SNP (transition)	Substitution	Hypothetical CDS
T	59734	D -> E	A -> T	GAT -> GAA	SNP(transversion)	Substitution	DNA binding protein

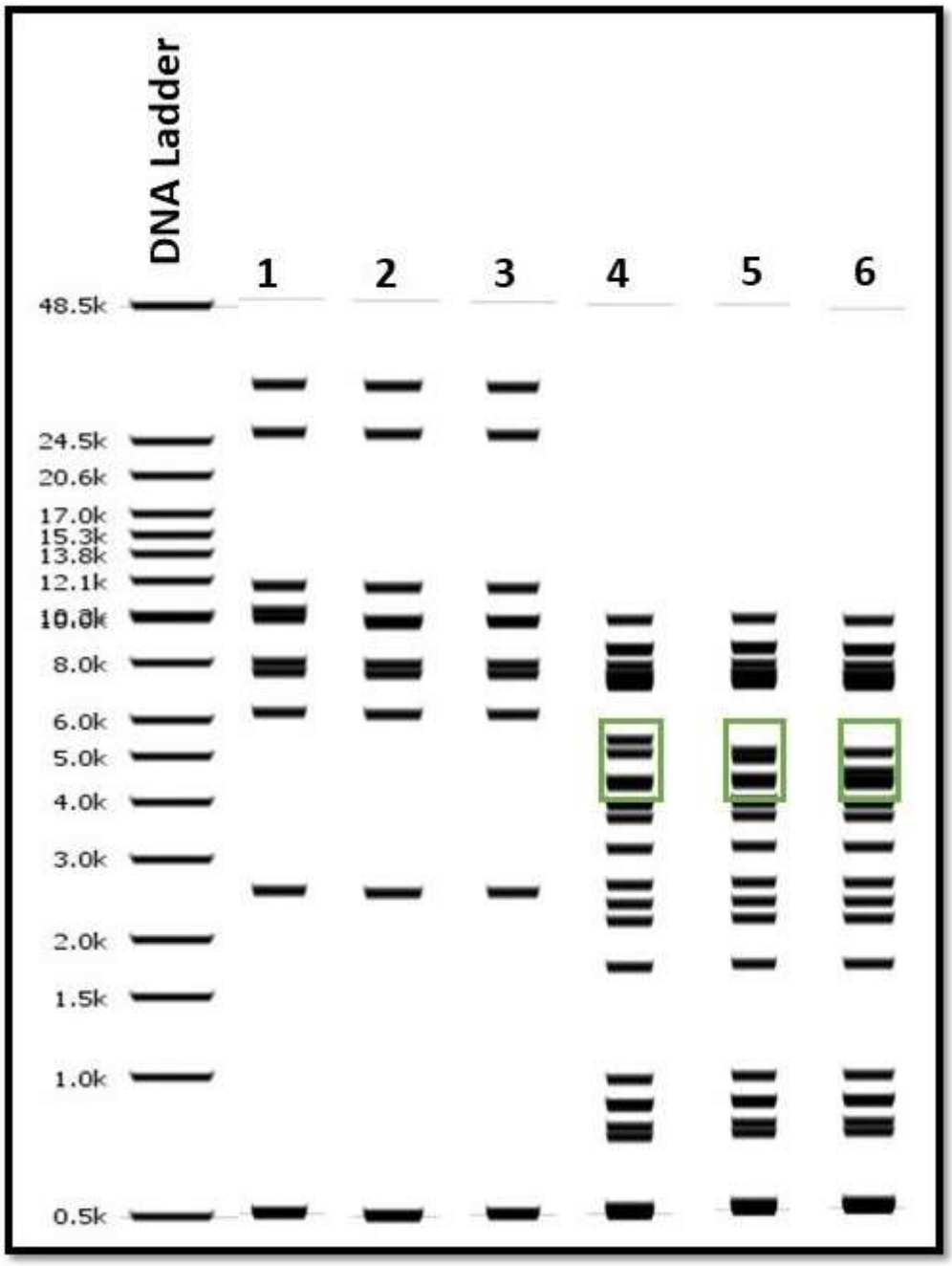

Figure 3.3: *In-silico* digestion of CrleGV-SA genomes from UV exposure cycle 1 (C1) and cycle 5 (C5) with the restriction enzymes *Bam*HI and *Eco*RI. The lane marked DNA ladder contains the DNA marker whle lane 1-original CrleGV-SA (BamHI), lane 2-CrleGV-SA C1 (BamHI), lane 3-CrleGV-SA C5 (BamHI), lane 4-original CrleGV-SA (EcoRI), lane 5- CrleGV-SA C1 (EcoRI) and lane 6- CrleGV-SA C5 (EcoRI). The highlighted areas in green boxes show differences in the restriction profiles obtained

with EcoR1. There was no difference in the in silico profiles obtained using the restriction enzyme BamHI.

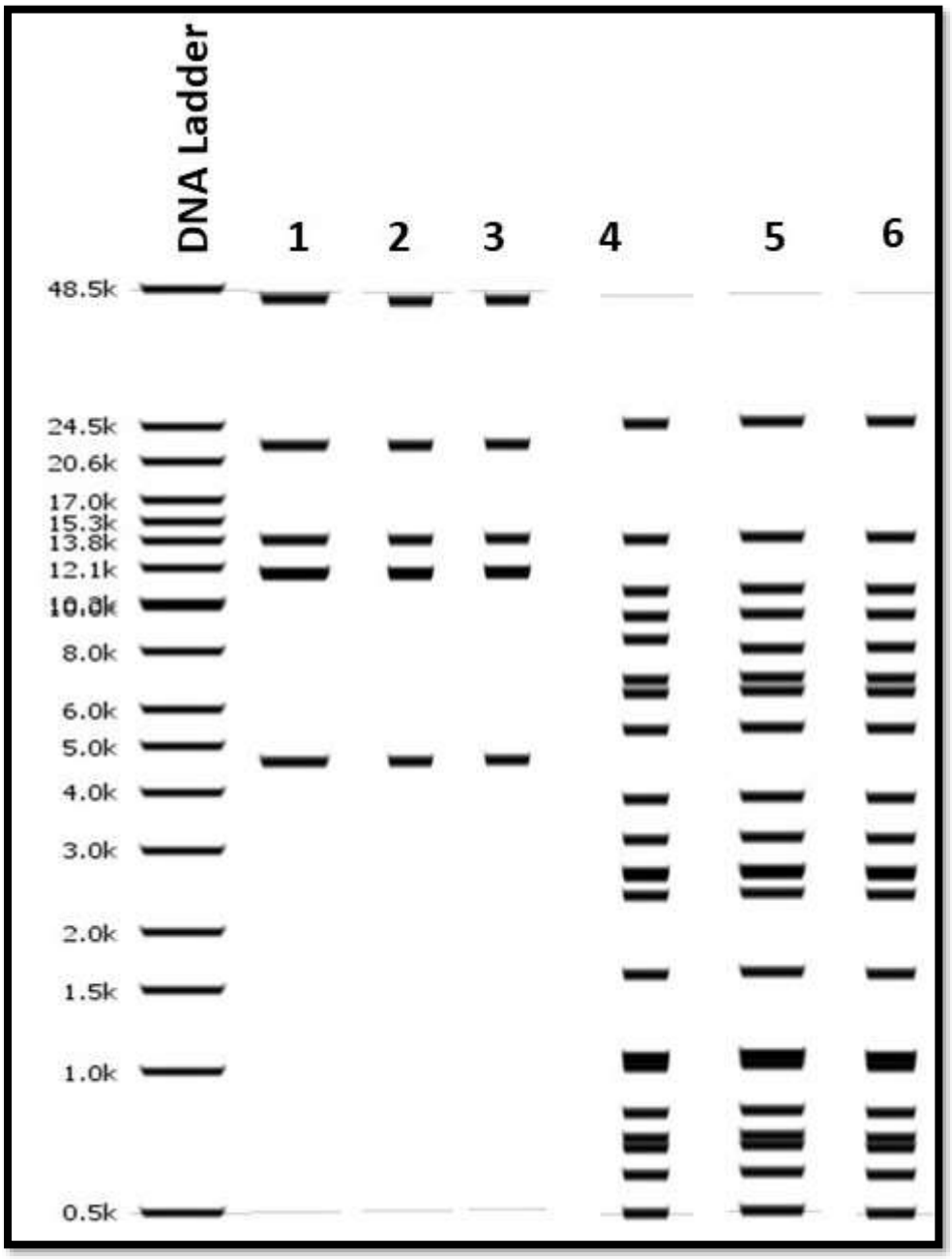

Figure 3.4: *In-silico* digestion of CrleGV-SA genomes from UV exposure cycle 1 (C1) and cycle 5 (C5) with the restriction enzymes XhoI and HindIII. The lane marked DNA ladder contains the DNA marker whle lane 1-original CrleGV-SA (XhoI), lane 2-CrleGV-SA C1 (XhoI), lane 3-CrleGV-SA C5 (XhoI), lane 4-original CrleGV-SA

(HindIII), lane 5- CrleGV-SA C1 (HindIII) and lane 6- CrleGV-SA C5 (HindIII). There was no difference in the restriction profiles obtained from these two restriction enzymes.

In-silico restriction enzyme profiles for the unexposed CrleGV-SA , CrleGV-SA C1 and CrleGV-SA C5 genomes were generated using the enzymes BamHI and EcoRI (Fig 3.3), XhoI and HindIII (Fig. 3.4), KpnI, XbaI and SalI (not shown). For 6 of the 7 enzymes used there was no difference in the *in-silico* profiles obtained for the three genomes. However, the EcoRI *in-silico* profiles showed differences in fragments obtained between 4000 kb and 6000 kb. One fragment of size 5500 kb was present in the original CrleGV-SA genome but absent in both the CrleGV-SA C1 and CrleGV-SA C5 genomes (Fig. 3.3, lanes 4, 5 & 6). Additionally, in the same region, the 5000 kb fragment for the original CrleGV-SA and CrleGV-SA C5 appeared as a single band while for the CrleGV-SA there were two bands very close to each other. Lastly, the original CrleGV-SA and CrleGV-SA C1 gave fragments approximately 4300 kb which appeared to be two closely spaced bands, whereas at the same position for CrleGV-SA the thickness suggested three bands closely spaced.

3.4 Discussion and Conclusion

Genomes of CrleGV-SA OBs exposed to UV for 72 h in cycle 1 and cycle 5 of selection were sequenced, mapped and assembled using the published sequence of CrleGV-SA as the reference (van der Merwe *et al*., 2017). The full CrleGV-SA genome sequence was recently published and deposited into the GenBank database and was used in this study, as the test samples were derived from the same strain (van der Merwe *et al*., 2017). The cycle 1 sample generated less number of reads compared to the cycle 5 sample. This is most likely due to the difference in quantity of surviving

virions. Seven SNPs were detected in the genome of the surviving CrleGV-SA isolated from cycle 1 exposure, while 14 SNPs were detected in the genome of surviving CrleGV-SA isolated from cycle 5.

The differences observed in the sequence of the cycle 1 isolate appear to have been introduced into the population after UV irradiation, otherwise they would have been detected in the original CrleGV-SA published by van der Merwe *et al*. (2017). It is possible that pre-existing gene sequences helped the virus survival after UV irradiation. However, it is difficult to say whether the detected SNPs alone or in combination with other unaltered genes conferred UV survival to the virus. It would be of interest in further studies to sequence the genomes unirradiated virus samples from both cycle 1 and cycle 5 and compare them with the CrleGV-SA genome in GenBank to assess whether any mutations are acquired during the passage.

Several of the mutations detected in the genome of the survivors from both cycle 1 and cycle 5, were in protein coding sequences whose proteins are known and their genes form part of the baculovirus core genes. These are *granulin*, *pif*-2, *39K protein* gene and the metalloproteinases coding sequence. Granulin is the main OB protein and was therefore originally thought to confer protection to the virion. However, it has been established that this protection is limited when it comes to UV irradiation (Witt & Stairs, 1975). It is possible that a mutation in the *granulin* gene in combination with others elsewhere in the genome may improve the UV-tolerance of the virus. PIF-2 is known to form a stable complex with PIF-3 on the surface of AcMNPV and plays an important role in the initial stages of infection (Peng *et al.*, 2010). Therefore, a mutation in *pif-2* could result in improved oral infection of the larvae, which would counter the negative effects of UV irradiation. The 39K protein (also known as pp31) has been demonstrated in experiments to have both an early promoter and late promoter and is

involved in both late and early transcription (Guarino *et al.,* 1986; Rohrmann, 2013). The deletion of pp31 in AcMNPV and of its homolog in BmNPV resulted in reduction of late gene transcription, a 100-fold reduction in budded virus and improper formation of the virogenic stroma (Guarino *et al.,* 1992; Gomi *et al.,* 1997; Yamagishi *et al.,* 2007). Thus, a mutation in this gene could promote an increase in late gene transcription and in the production of budded virus, resulting in increased virulence of the virus. Among the SNPs detected only in the cycle 5 sequence, all except two occurred in hypothetical protein CDS regions. The two known sequences occurred in the DNA binding protein (DBP). DBP can anneal and unwind DNA and, in BmNPV, it preferentially binds to ssDNA and destabilizes dsDNA in a non-polar manner (Mikhailov *et a*l., 1997 & 2003). AcMNPV mutants lacking a *dbp* gene produce defective nucleocapsids (Mikhailov *et al*., 2007). Therefore, a mutation in *dbp* gene could potentially expedite the DNA replication and therefore contribute to the efficiency of the infection process. This could explain the decreased LC_{50} values recorded after UV irradiation after the third cycle.

The severity of the mutation is determined by the position of the nucleotide change in the codon. If a wobble base is mutated, it is likely that it will not influence the amino acid and resultant protein. However, where the nucleotide change forces an amino acid change, several considerations must be made. Where an acidic amino acid replaces another acidic amino acid the effect may be negligible (conservative substitution), compared to when an acidic amino acid replaces a basic or aliphatic acid. Similarly, the size of the amino acids being exchanged matters. Where the amino acids are the same type and size, there may be no effect, compared to when the type is the same but the size different. This may affect the rigidity of the protein. While the nature of some amino acids remained unchanged in the isolated UV-tolerant virus,

changes occurred at nucleotide position 434, where the sulphur rich cysteine was replaced by acidic tryptophan; at position 36843 the aromatic phenylalanine was replaced by the aliphatic isoleucine; at 94086 a basic amino acid replaced an acidic amino acid. Such changes would have a greater impact if there is a large difference in the hydration potentials of the amino acids and would lead to changes in the crystallization and folding of the proteins and may therefore confer different or enhanced efficiency in the protein.

The SNPs detected in the cycle1 exposed CrleGV-SA were retained in the cycle 5 exposed CrleGV-SA. This suggests that these could have been critical in establishing UV tolerance. However, additional SNPs were observed in the cycle 5 sequence, which were not present in the cycle 1 virus isolate. These new SNPs were associated with greater virulence, as highlighted by the low LC_{50} values in bioassays after the fifth cycle of UV exposure (recorded in chapter 2.3.5), as well as UV-tolerance. Thus, there is a relationship between the introduction of these new SNPs and increased tolerance to UV. It would be interesting to identify at what stage the additional SNPs observed in cycle 5 appear. This could be achieved by PCR amplification and sequencing regions of the genome where these SNPs were detected in samples from cycle 2 to cycle 4.

While most of the restriction enzymes used in this study did not give differences in fragments obtained, EcoRI cleavage resulted in fragments that were different from the original CrleGV-SA between the sizes 4000-6000 kb. This suggests that the some of the SNPs observed were lying in EcoRI restriction sites. This could be confirmed by PCR amplification and sequencing of the regions were EcoRI sites occur in the CrleGV-SA genome. One fragment that was present in the original CrleGV-SA was absent in both CrleGV-SA C1 and CrleGV-SA C5 and this could possibly be

associated with the establishment of UV tolerance as it is present only after UV-irradiation and maintained in the UV-tolerant population. An additional fragment was also identified in CrleGV-SA C5 but was not present in the original CrleGV-SA and CrleGV-SA C1. It is possible that this band could be as a result of one or some of the SNPs unique to CrleGV-SA C5. It is envisaged that in future work, *in vitro* profiles will be generated to support the *in silico* data. It is expected that in vitro profiles may reveal different patterns due to the mixed genotype nature of baculoviruses.

The main goal of the work reported in this chapter was to identify differences between the CrleGV-SA sequences obtained after UV exposure in cycle 1 and cycle 5, using the published CrleGV-SA genomic sequence as the reference sequence. SNPs were observed in both sequences which were thought to be responsible for establishing UV-tolerance. Additional SNPs were detected only in the cycle 5 sequence and are thought to enhance the UV-tolerance, as well as improve the virulence of the UV-tolerant population. Thus, the work reported in this chapter, further confirmed the bioassay data obtained in chapter 2. In the following chapter, the effect of UV irradiation on the morphology of the CrleGV-SA OB will be reported.

Chapter 4

The effect of ultraviolet radiation on the morphology of Cryptophlebia leucotreta granulovirus

4.1 Introduction

In the preceding chapters, potential UV-tolerant Cryptophlebia leucotreta granulovirus (CrleGV-SA) was isolated and analysed by surface dose bioassays and next generation sequencing with subsequent analysis of the genome data. In this chapter the effect of UV radiation on the integrity and structure of the occlusion body (OB) and nucleocapsid will be reported. Transmission electron microscopy (TEM) and attenuated total reflection Fourier transform infrared spectroscopy (ATR-FTIR) were employed to achieve this goal.

Electron microscopy has been applied extensively in the study of baculoviruses (Bergold, 1947; Ignoffo, 1973; Dhladhla *et al*., 2018). The capsule like structure of the baculovirus OB was first discovered and reported by Bergold (1947), following electron microscopy studies. In the same study and in subsequent studies electron microscopy, particularly TEM, provided evidence that the OB structure was crystalline in nature (Arnott & Smith, 1968). Burgess (1977) reported on the estimation of the molecular weight of DNA of various baculoviruses by electron microscopy. In the years that followed, when a new baculovirus has been discovered, electron microscopy has been used to characterise the baculovirus morphology and size correctly (Akermann &

Smirnoff, 1983; Grasela *et al*., 2008; Bayramoglu *et al.,* 2018). In addition to morphology, TEM has been used to identify and differentiate between single (SNPVs) and multiple (MNPVs) nucleopolyhedroviruses, based on the number of virions enclosed in the OB (Hughes & Addison, 1970; Akermann & Smirnoff, 1983). Matilainen *et al*. (2005) employed electron microscopy to investigate the mechanism of baculovirus entry into hepatoma cells with Autographa californica multiple nucleopolyhedrovirus (AcMNPV), as a case study. In a related study Au *et al*. (2010) used conventional electron microscopy and immunogold electron microscopy to evaluate microinjection of *Xenopus laevis* oocytes as a system for studying nuclear transport of AcMNPV. Scanning electron microscopy is also used for baculovirus enumeration (Evans & Shapiro, 1997; Hunter-Fujita, 1998). Dhladhla *et al*. (2018) showed that scanning electron microscopy could be used as a quantification tool for CrleGV-SA, using latex beads as a reference standard and demonstrated that the method was comparable to enumeration with dark field light microscopy. However, electron microscopy has rarely been used in UV tolerance studies on baculoviruses. One of the earliest instances in which electron microscopy was used in baculovirus UV tolerance studies is described by Brassel and Benz (1979), where the morphology and density of OB protein of a selected UV-tolerant strain of the Cydia pomonella granulovirus (CpGV) was assessed. They postulated that the selection of UV-tolerant virus would be a result of larger OBs or denser nucleocapsids. However, this was not so, as there was no difference in the morphology of the selected UV tolerant strain and the original strain.

The granulovirus OB matrix protein granulin shares 60 % amino acid sequence similarity with the NPV matrix protein polyhedron (Gati *et al*., 2017). Polyhedrin has a body centred cubic crystal lattice with a 103 A unit cell and has a solvent content of

only 20 % (Anduleit *et al.,* 2005; Coulibaly *et al.*, 2009; Gati *et al.* 2017). This confers exceptional stability to the OB in the environment. X-ray diffraction studies on CpGV granulin protein revealed that the granulin lattice is highly ordered. These studies established that granulin makes up approximately 60 % of the OB volume. Using both TEM and coupled with Fast Fourier transform (FFT) analysis is a good way to visualize the crystallinity of a protein. Where crystalline lattice exists, the faceting can be seen in a TEM image and as Bragg spots following FFT analysis. The extent to which the faceting is visualized depends on whether the zone axis is perpendicular or not to the electron beam (Zhou & Greer, 2016). Appearance of Bragg spots after FFT processing of TEM images gives an idea of the type and quality of crystals present. The higher the number of Bragg spots the more ordered the lattice crystals would be (Stevenson *et al.,* 2016).

While electron microscopy allows for visual analysis of UV damage to the OB, vibrational spectroscopic techniques such as Raman spectroscopy and Fourier Transform Infrared spectroscopy (FTIR), allow for analysis of the surface molecular structure of the baculovirus OBs after UV irradiation. Raman spectroscopy has previously been used to show small changes in the Amide III, Amide I and S-H stretch regions of the Raman spectrum after CrleGV-SA was exposed to UVA and UVB in the laboratory (Mwanza, 2015). However, Raman spectroscopy was not available for this study due to a breakdown in the equipment. Instead ATR-FTIR was used to observe molecular changes in the OB after UV irradiation. The major functional difference in the two techniques is that Raman spectroscopy is dependent on the change in polarizability of a molecule while ATR-FTIR being an infrared spectroscopy technique relies on the change in dipole moments of a molecule (Wilson & Walker, 2010). However, both methods can be combined with microscopic techniques.

Infrared (IR) active molecules have bonds that have an electric dipole that can change by atomic displacement due to natural vibrations (Baker *et al.,*2014). These vibrational modes can be measured and quantified by IR spectroscopy. IR spectroscopy has a wide range of applications that provide molecular information for molecules varying from amino acids, small peptides, isolated proteins and enzymes to peptide protein complexes, membrane bound proteins and entire membranes (Fabian & Mantele, 2002). FTIR is a type of IR spectroscopy that is used frequently to obtain information about proteins including determination of secondary structure by various computational techniques such as curve fitting and pattern recognition-based techniques (Hering *et al*., 2004; Hansen *et al.,* 2015). Preparation for FTIR spectroscopy is non-destructive to the material used, requires only small amounts of material and minimum sample preparation. In addition, it is simple and easily reproducible and non-destructive to the material used (Movasaghi *et al.,* 2008). FTIR Spectra can be obtained in three different experimental configurations, namely transmission, reflection-absorption and attenuated total reflection (ATR), which was used in this study (Lima *et al.,* 2015). In comparison to the other configurations, ATR-FTIR provides a single spectrum, which is an average signal from the sample that light passed through and offers a high signal to noise ratio (Sukuta & Bruch, 1999; Kazarian & Chan, 2013). ATR-FTIR uses the total internal reflection phenomenon. The sample is placed on an optically dense crystal with a high refractive index, onto which an IR beam is directed, resulting in total internal reflection of the beam (Minnes *et al.,* 2017). The internal reflectance generates an evanescent wave that extends beyond the surface of the crystal and penetrates the sample on the crystal surface. This wave interacts with the sample, attenuating the IR beam of light exiting the crystal, which is then directed towards the detector (Glassford *et al*., 2013). For protein FTIR spectra,

three regions are of importance. These are the fingerprint region (600-1450 cm^{-1}) which correspond to bending and fingerprint carbon vibrations, the amide (I/II) region (1500-1700 cm^{-1}) and lastly, the high-wavenumber region (2550-3500 cm^{-1}) which corresponds to stretching vibrations such as the S-H and O-H groups (Baker *et al.*, 2014).

The aim of this chapter is to report on the effect of UV irradiation on the morphology of CrleGV-SA OBs as analysed by TEM and ATR-FTIR. This was done to gain an understanding of whether UV damages viral DNA only or if it also damages the OB ultrastructure.

4.2 Materials and Methods

4.2.1 Transmission electron microscopy

Virus suspensions obtained from the selection of UV-tolerant virus described in section 2.2 were used. A 72 h UV-exposed CrleGV-SA at cycle 1, a 72 h UV-exposed CrleGV-SA at cycle 5 and an unexposed CrleGV-SA virus sample were each diluted with double distilled water to give 1 ml aliquots at a concentration of 1 x 10^8 OBs/ml and prepared for TEM imaging. A modified method described by Wolff *et al.* (2002) was used to prepare the OB samples for TEM. The 1 ml samples were centrifuged at 3500 g for 5 min in a microfuge (Eppendorf, Germany) and the supernatant was discarded. The pellets were fixed overnight in Karnovsky's fixative made up of 2.5 % glutaraldehyde, 2 % paraformaldehyde in 0.05 M pH 7.2 phosphate buffer and 0.001 M calcium chloride. The samples were then centrifuged and the fixative removed. The sample was washed with buffer three times for 5 min. The samples were post fixed in 1 % osmium tetroxide for 1 h at room temperature. Care was taken to mix the osmium tetroxide into the pellets before leaving the samples to stand. Following post-fixation

the samples were centrifuged as before, the osmium tetroxide removed and the samples washed with double distilled water three times for 5 min and were spun down for 1 min in between washes. The samples were then dehydrated in acetone as follows, 30 % acetone, twice for 5 min; 50 % acetone, twice for 5 min; 75 % acetone, twice for 5 min; and 100 % acetone, twice for 10 min. The samples were then embedded in Spurr's low viscosity resin. This was achieved by first adding a 1:2 ratio of resin to acetone to the sample for 45 min. After this, the 1:2 mixture was removed using a pipette and replaced with a 1:1 mixture. This was left to infiltrate overnight. The following day the 1:1 mixture was replaced using a pipette with a 3:1 mixture and left to infiltrate overnight. Eppendorf tube lids were left open and the tops sealed with parafilm that had a single hole made by poking them with a pipette tip to allow the acetone to evaporate. After this the resin-acetone mixture was pipetted out and the pellet transferred to a new capsule where 100 % resin was added and left to stand for 5 h at room temperature. The capsule was then placed in an oven at 60 °C overnight to allow the resin to set. The resin block was then removed and sectioned using a Leica Ultracut ultramicrotome (Leica, Germany). Sections 70 nm thick were placed on a 300 mesh carbon coated copper grid and stained with drops of 4 % uranyl acetate for 2 min, followed by lead citrate for 1 min. The grids were allowed to dry and placed in a vacuum desiccator for at least 1 h. The sections were then examined in a JOEL JEM-2100 TEM (JOEL, Japan) set in secondary electron (SE) mode. The micrographs were taken at an accelerating voltage of 200 kV at a low probe current to prevent damage to the specimen.

For statistical analysis of each sample group (control, cycle1 and cycle 5), 100 OBs in the longitudinal orientation from randomly selected images were counted and

classified as intact or damaged. The percentages of intact and damaged OBs were recorded and compared among the three groups.

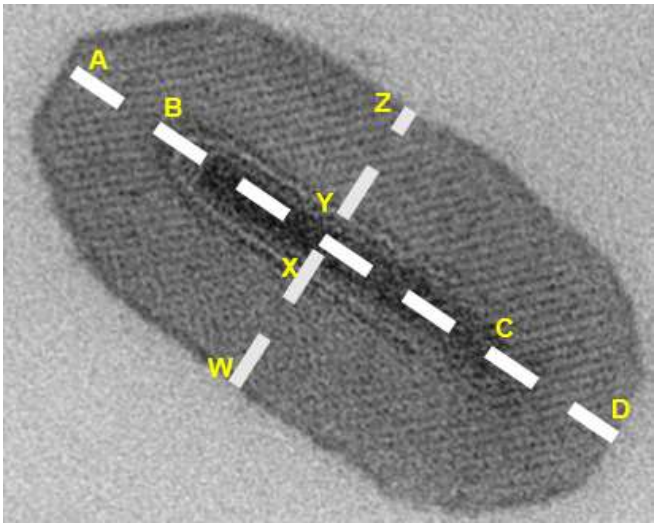

Figure 4.1: Measurements carried out in ImageJ®. The distance ABCD represents OB length, WXYZ represents OB width, BC and XY represent nucleocapsid length and width respectively. For all OBs measured, the NC:OB ratio was determined using the formula, Distance XY ÷ Distance WXYZ.

Measurements of each of the 100 OBs were taken along the length and width of the OB and nucleocapsid cavity using the image processing software ImageJ® (National Institutes of Health, USA) (Fig 4.1). The mean and standard error of the mean of each of these measurements were calculated in Microsoft Excel 2016. To compare if there were significant differences between the means of the unexposed control and cycle 1, control and cycle 5, and cycle 1 and cycle 5 samples, a paired student's t test (two-tailed) at $P \leq 0.05$ was conducted in Microsoft Excel 2016. To determine whether UV exposure and section of viable virus resulted in a change in the size of the area around the nucleocapsid cavity, the nucleocapsid to OB width ratio (NC:OB) was calculated for the OBs in a longitudinal orientation. The mean and standard error of the mean of the ratio was then compared pairwise between the three groups using a

student's t test in Microsoft Excel 2016 to elucidate whether UV radiation had an effect on it.

The same CrleGV-SA suspensions used for TEM analysis were used for mid-ATR-FTIR spectroscopy analysis. The aim was to identify any difference in the spectra of the OB in the UV irradiated and non-irradiated samples. 30 µl of each sample was pipetted onto the diamond crystal surface. The IR spectra were acquired in absorbance mode using a Bruker V70x spectrometer (Bruker Optik, Germany). A background absorption using double distilled water was taken to correct for the medium containing the OBs. The diamond crystal was washed with 70 % ethanol in-between analyses. The absorbance spectra were obtained at 4 cm^{-1} resolution and an average of 2000 scans per sample were collected.

4.3 Results

4.3.1 Morphological studies on Unexposed CrleGV-SA using TEM

The unexposed control samples observed under TEM displayed the typical crystalline faceting associated with baculovirus OB, the nucleocapsid and the double layered envelope of the nucleocapsid (Fig 4.2a & c). The corresponding FFT image indicates the crystalline nature of the OB (Fig 4.2b). Most OBs observed using TEM contained a single nucleocapsid, although occurrences of OBs with double nucleocapsids were recorded.

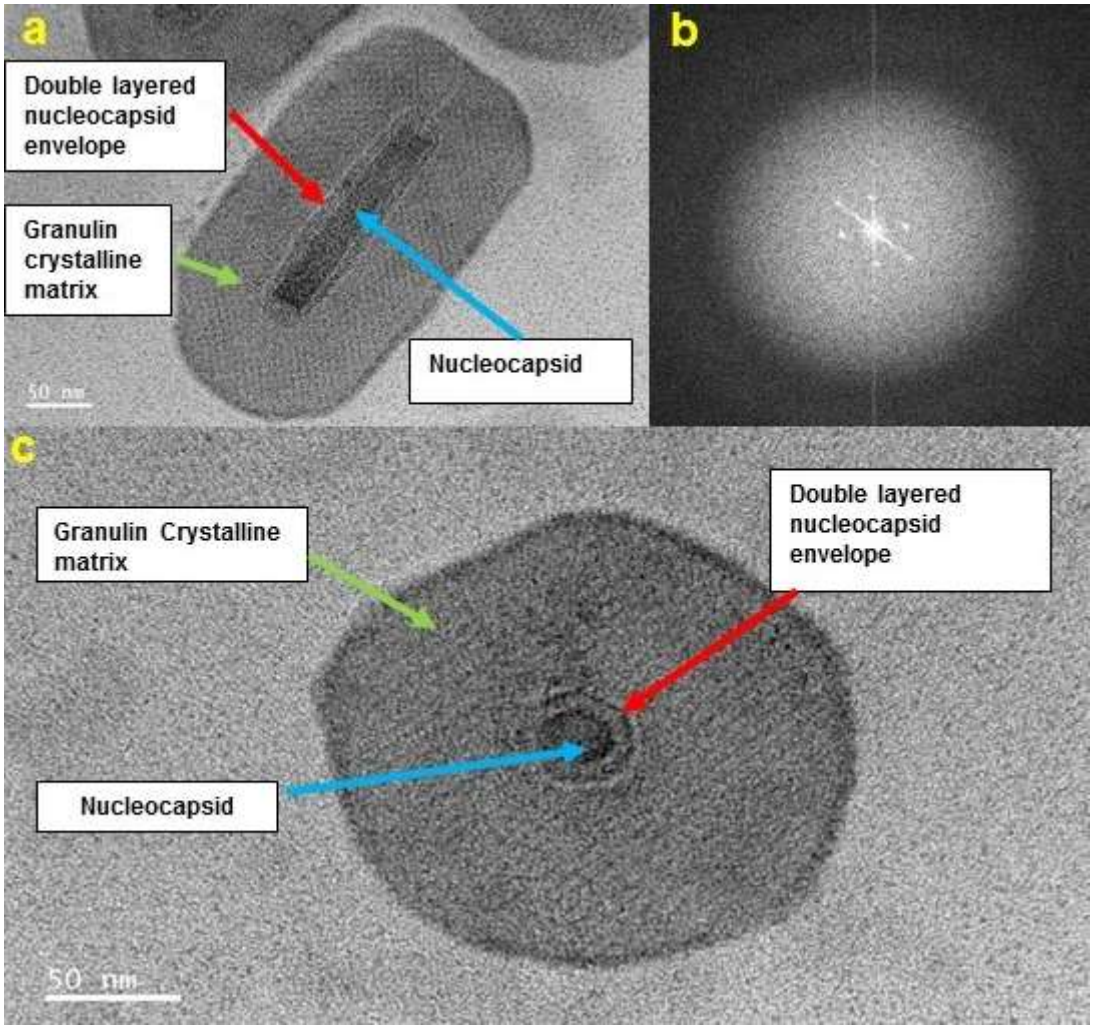

Figure 4.2: a) TEM SE longitudinal section of unexposed CrleGV-SA OB with OB nucleocapsid (blue arrow) and double layered envelope of the nucleocapsid (red arrow) indicated; **b)** The corresponding crystal lattice FFT structure; **c)** TEM SE transverse section of unexposed CrleGV-SA OB.

4.3.2 UV Exposed CrleGV-SA for 72 h in cycle 1

CrleGV-SA samples exposed to UV for 72 h in cycle 1 showed signs of damage. The nucleocapsids of affected OBs appeared thin, distorted, and in some cases altogether disintegrated (Fig 4.3a & c). In comparison, the nucleocapsids in the unexposed control were thick and of regular shape (Fig 4.2). In addition, the double-layered envelope of the nucleocapsid appeared disintegrated in TEM images of UV exposed

OBs. (Fig 4.3a & c). In others, the proteinaceous OB was shown to disintegrate from the interior outwards (Fig 4.3c, brown arrows). The damaged OBs were found to be amorphous and did not show evidence of crystalline faceting when analysed using FFT analysis (Fig 4.3b & d). There is visual evidence to support the suggestion that the UV damage is progressive as seen in Fig 4.4a, where OB 1 is at an early stage of degradation and OBs 2 and 3 are at more advanced stages of degradation. Despite the severity of the damage observed in most TEM images, several intact OBs were also observed among the damaged ones (Fig 4.4b, green arrow) with crystalline faceting present (Fig 4.4d).

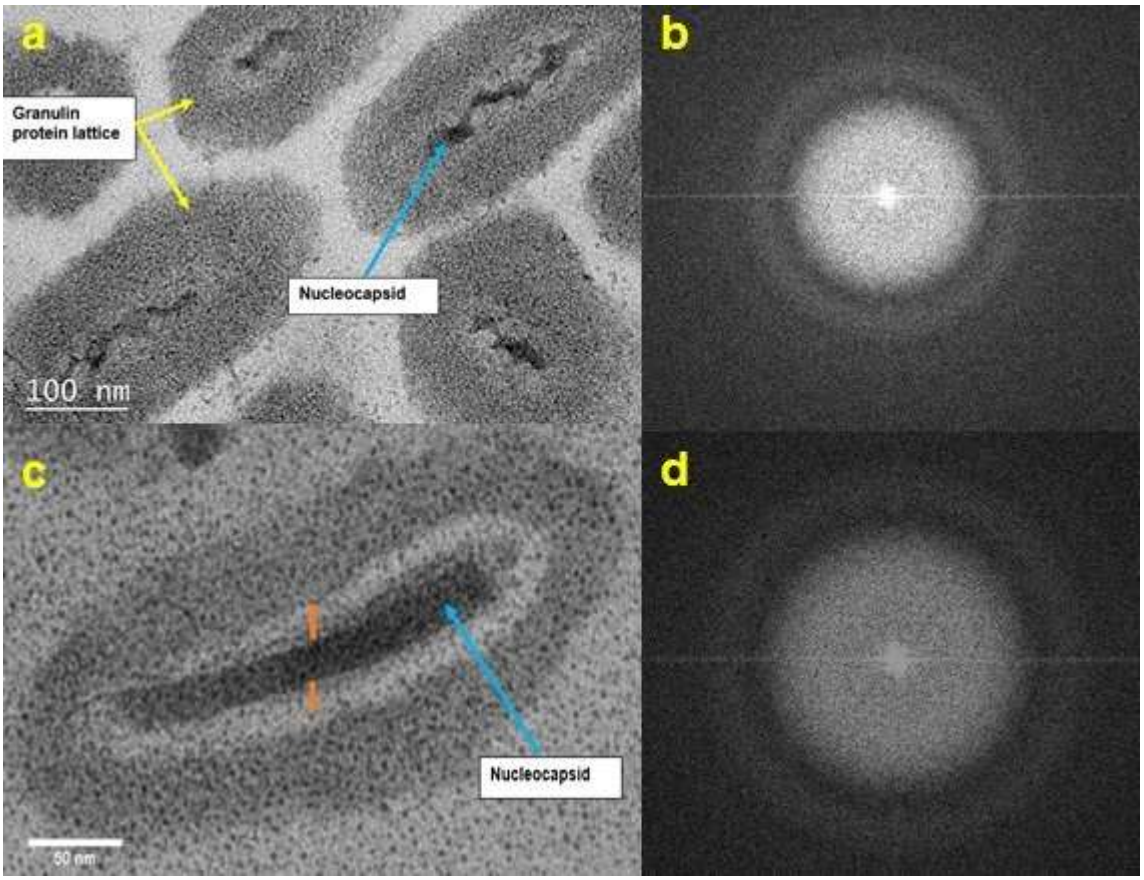

Figure 4.3: TEM SE sections of UV damaged CrleGV-SA OBs after exposure to UV for 72 h in UV exposure cycle 1, **a)** The crystalline structure of the OB (yellow arrows) is not visible and the nucleocapsid (blue arrow) appears thinner and disintegrated.

Nucleocapsid double envelope is not visible; **b)** The corresponding FFT image shows no pattern implying no crystalline lattice structure; **c)** The OB appears to be disintegrating outwards as indicated by the brown arrows and **d)** the corresponding FFT image to c) shows no pattern implying no crystalline lattice structure.

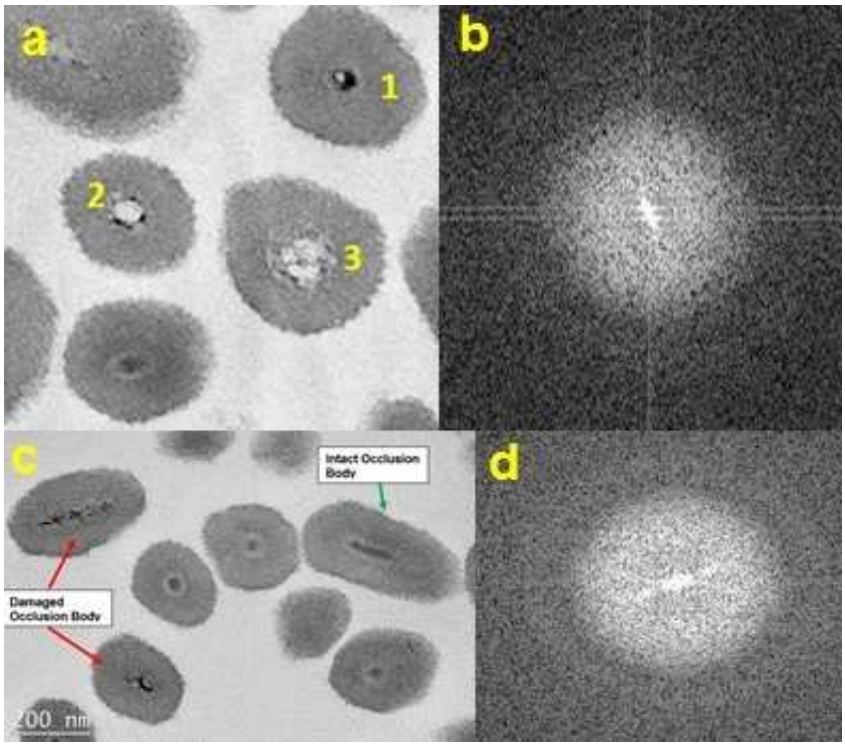

Figure 4.4: CrleGV-SA OBs exposed to UV for 72 h in UV exposure cycle 1, indicating **a)** Progressive degradation of the nucleocapsid (from 1-3); **c)** FFT verification of crystalline lattice structure of intact OBs. **c)** Presence of an intact OBs (green arrow) among damaged OBs and **d)** FFT confirmation of crystalline lattice structure in intact OBs in c).

4.3.3 UV Exposed CrleGV-SA for 72 h in cycle 5

As described in section 2.2, CrleGV-SA OBs were subjected to a series of UV exposure and re-exposure experiments for five exposure cycles. Bioassays were then conducted to assess whether any UV-tolerant CrleGV-SA had been selected during the process. Bioassay results of samples exposed to UV up to cycle 5 showed

retention of viral activity. The sample exposed to UV for 72 h at cycle 5 was used to investigate if any morphological differences existed in the OBs. The TEM images obtained showed that most of the OBs were intact (Fig 4.5a), with the crystalline faceting of the OB visible (Fig 4.5a & b), as well as the regular nucleocapsid enclosed within an intact double envelope. However, a few (11 %) damaged OBs were observed in the population (Fig 4.5c & d), with the crystalline faceting present in some OBs showing damage but absent in others. However, unlike in cycle 1 where the damage to the virion also meant the nuclear envelope had broken down in some of the cycle 5 damaged OBs the nuclear envelope could still be seen to be intact.

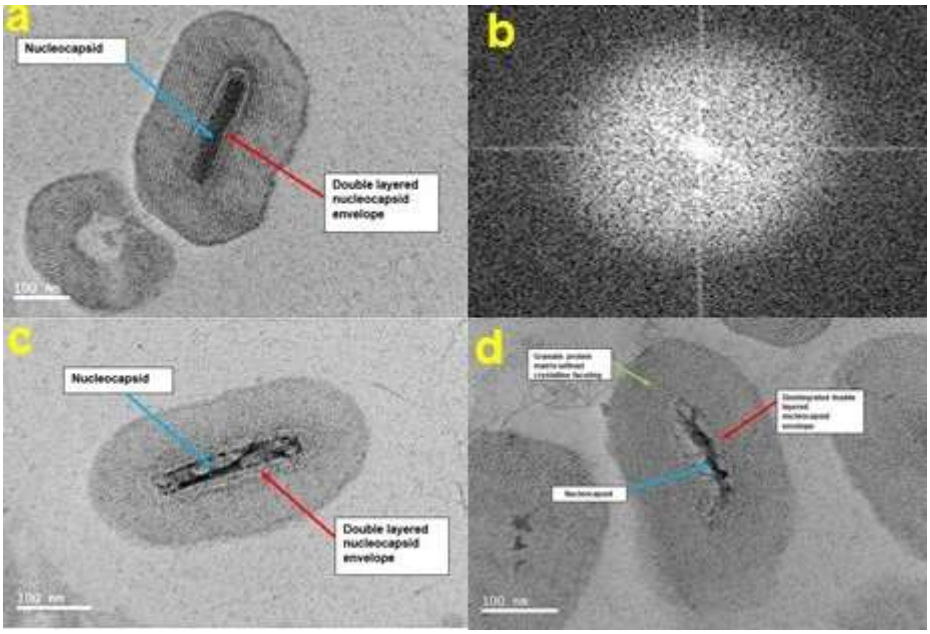

Figure 4.5: TEM SE section of CrleGV-SA OBs exposed to UV for 72 h in UV exposure cycle 5 indicating **a)** OB crystalline structure intact even after UV exposure and nucleocapsid (blue arrow) also intact as well as nucleocapsid envelope (red arrow) with **b)** showing FFT confirmation of crystalline lattice structure in OBs; **c)** Damaged CrleGV-SA OB with the nuclear envelope (red arrow) still visible; the nucleocapsid (blue arrow) appears damaged and **d)** damaged OB with the nuclear envelope and virion damaged

4.3.4 Measurements of OB dimensions from TEM images after UV irradiation

When 100 OBs were randomly counted from TEM images obtained from different TEM sections, it was calculated that 11 % of the OBs were damaged in the cycle 5 exposure in comparison to 82 % in cycle 1. Additionally, a higher proportion of multi-capsid OBs were recorded in cycle 5 than in the cycle 1 samples.

Table 4.1: Mean (± SEM) OB and nucleocapsid dimensions of unexposed CrleGV-SA and UV exposed CrleGV-SA OBs for 72 h in cycle 1 and cycle 5.

Dimension	Control	Cycle 1	Cycle 5
OB length (nm)	365.31 ± 4.91†[a]	301.30 ± 6.03[b]	347.29 ± 4.62[c]
OB width (nm)	213.47 ± 3.16[a]	184.03 ± 3.60[b]	215.86 ± 2.78[a]
NC length (nm)	210.16 ± 3.89[a]	182.76 ± 5.56[b]	180.35 ± 4.97[b]
NC width (nm)	48.87 ± 4.89[a]	58.57 ± 1.11[b]	53.37 ± 0.90[c]

†Different letters in the same row indicate statistically significant differences between sample types at $P \leq 0.05$

The mean length and width (±SEM) (longitudinal section) of the unexposed OBs was 365.31 ± 4.91 nm and 213.47 ± 3.16 nm respectively. The mean length and width recorded for the nucleocapsids was 210.16 ± 3.89 nm and 48.87 ± 0.97 nm respectively (Table 4.1). In comparison, the mean length of the cycle 1 OBs (301.30 ± 6.03 nm) and nucleocapsid cavities (182.76 ± 5.56) were significantly smaller ($t(198) = 1.65$, $p = 1.27 \times 10^{-14}$ for OB length and $p = 1.76 \times 10^{-5}$ for nucleocapsid length) than those of the unexposed control OBs. The mean nucleocapsid cavity width (58.57 ± 1.11) of the UV exposed cycle 1 OBs was significantly larger ($t(198) = 1.65$, $p = 8.89 \times 10^{-12}$) than the unexposed control OBs. The mean of the cycle 5 OB length (347.29 ± 4.62) was significantly smaller than the mean OB length of the unexposed OBs (t

(198) =1.65, *p* =0.004). However, there was no significant difference between the mean of the OB width of the unexposed control and the mean width of cycle 5 UV exposed OBs (t (198) =1.65, *p* =0.24). When dimensions of cycle 1 OBs were compared to cycle 5 OBs, they were significantly different except in the case of nucleocapsid cavity length (cycle1=182.76 ± 5.56 nm, cycle 5=180.35 ± 4.97 nm) where there was no significant difference (t (198) =1.65, *p* =0.50).

The mean NC:OB ratio for the cycle 1 samples was 0.33 ± 0.007 and this significantly differed from both the compared unexposed control ratio of 0.23 ± 0.004 (t (198) =1.65, *p* =1.015 $x10^{-24}$) and the cycle 5 ratio of 0.25±0.005 samples (t (198) =1.65, *p* = $1x10^{-17}$) (Fig 4.6). Thus, UV exposure resulted in thinning of the OB. The NC:OB ratio of cycle 5 OBs was also significantly larger (t (198) =1.65, *p* =0.002) than the unexposed control OBs.

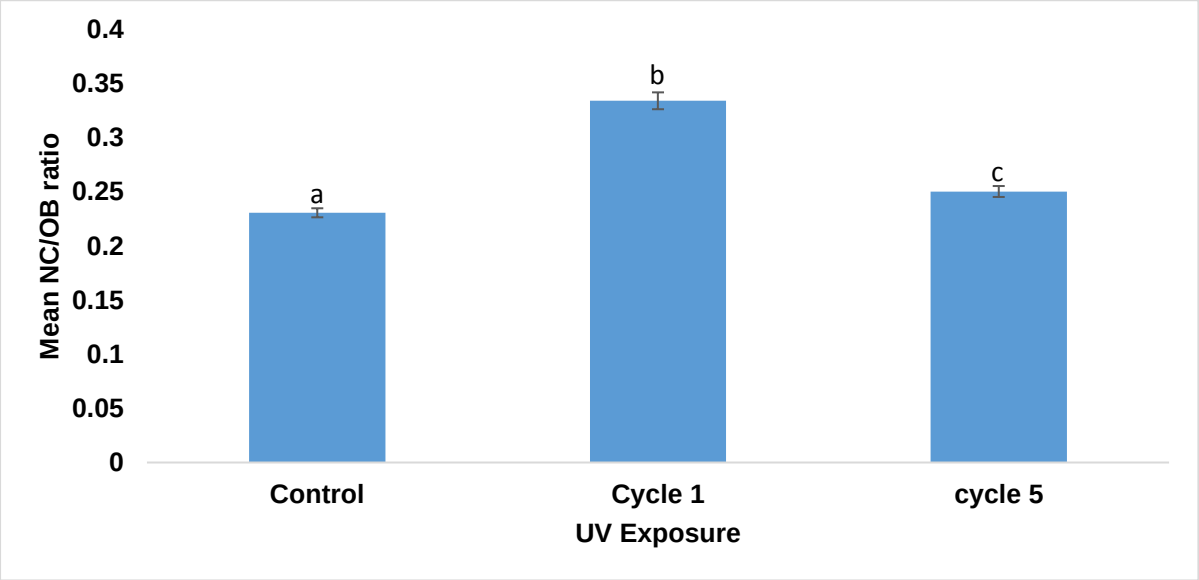

Figure 4.6: A comparison of the mean NC: OB width ratio. The error bars represent standard deviation (SEM). For each treatment n=100 OBs from randomly selected images. Bars with different letters (a, b & c) are significantly different at P≤0.05

4.3.4 Representative ATR-FTIR spectroscopic analysis of UV irradiated CrleGV-SA

ATR-FTIR was used to identify differences in the OB protein after UV irradiation. There were minor differences in the spectra obtained before UV irradiation and after UV irradiation, although there was no difference in the spectra of the cycle 1 and cycle 5 UV irradiated samples (Fig 4.7). Several peaks were found to have emerged or disappeared after UV irradiation in the fingerprint region and near the high wavenumber region. The first difference appeared at 669.26 cm^{-1} where a peak in the unexposed sample was absent in the irradiated samples. At 902.63 cm^{-1} a peak was present in the irradiated samples, but not in the unexposed control and this was followed by what appears to be a peak shift from 1010.64 cm^{-1} in the unexposed control to 1075 cm^{-1} in both the irradiated samples. Peaks that were present in the control samples spectra were absent in the irradiated samples at 1191.94 cm^{-1} and 2362.67 cm^{-1}. At 1259.44 cm^{-1}, 2900.78 cm^{-1} and 2983.71 cm^{-1} peaks present in the irradiated samples' spectra were absent in the unexposed sample spectra. The expected and easily identifiable Amide I, II and III peaks, between 1300 cm^{-1} and 1700 cm^{-1} were not distinct in the spectra. This is most likely because of the water in which the viruses were suspended, which absorbs strongly in this region. Despite blanking with water and accounting for the blank, these regions were still not clear enough.

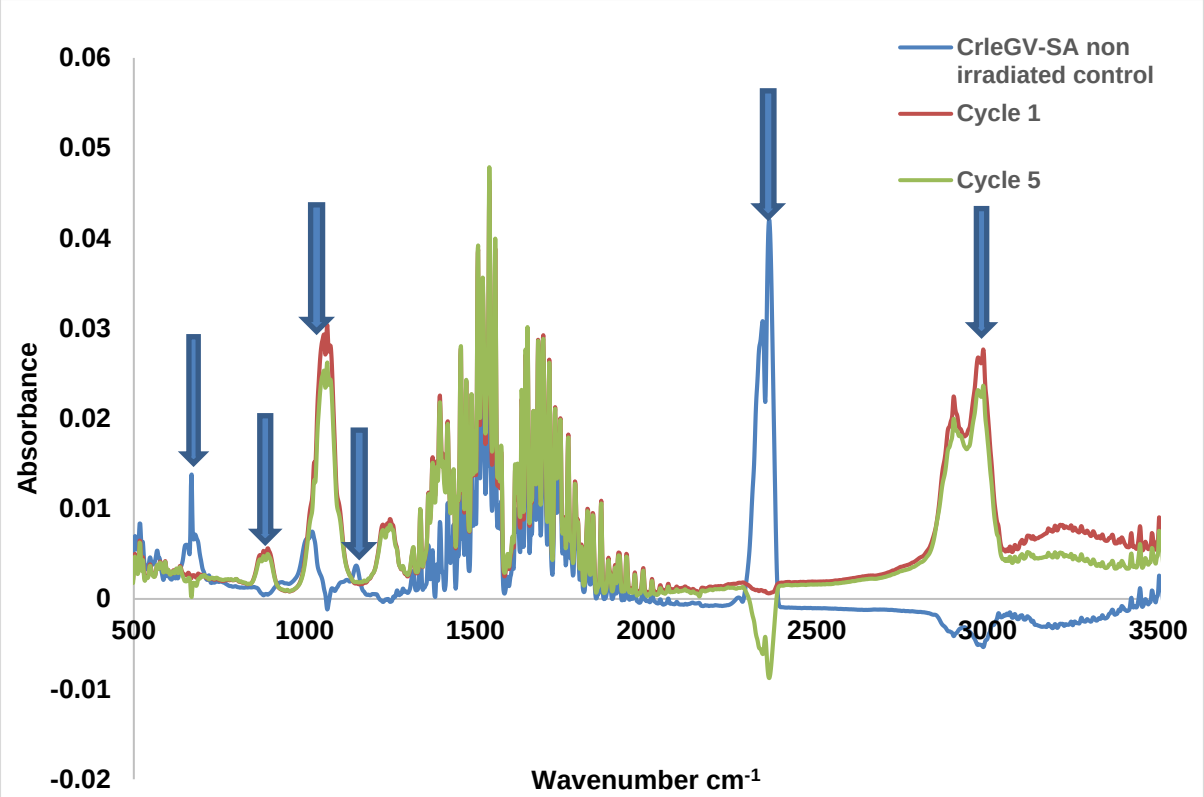

Figure 4.7: FTIR-ATR Spectra of CrleGV-SA OBs exposed to UV for 72 h at cycle 1 and cycle 5. Arrows indicate spectral regions with differences after UV irradiation.

4.4 Discussion and Conclusion

In this study TEM imaging and FTIR analysis were used to detect damage caused by UV irradiation on CrleGV-SA OBs. This is the first time that such an observation made by TEM has been recorded for any baculovirus. Dhladhla (2012) previously described the use of TEM to determine the crystalline structure of the CrleGV-SA OB. This crystalline structure is formed by the OB protein, granulin (Rohrmann, 1992). While granulin, protects the OB from harsh environmental conditions and allows for the OB to persist for a long time in the soil or such protected environment, it has been shown

that it cannot provide sufficient protection to the nucleocapsid against UV irradiation (Rohrmann, 1986; Mwanza, 2015).

The dimensions measured for the unexposed CrleGV-SA OBs and nucleocapsids were consistent with the CrleGV-SA OB measurements made by Dhladhla (2012) and generally consistent with dimensions of other granuloviruses, which have OBs ranging from 300-400 nm in length and 120-300 nm in diameter, and the virions ranging from 200-300 nm in length and 30-60 nm in diameter (Akermann & Smirnoff, 1983; Herniou *et al*., 2011). The FFT images for the control OBs revealed the expected crystalline structure in the protein matrix. It has previously been shown by X-ray diffraction that NPV polyhedra have a body centred cubic lattice with unit cells that have 123 symmetry and that CpGV, which is closely related to CrleGV, has 123 symmetry (Anduleit *et al.,* 2005; Coulibaly *et al.*, 2009; Gati *et al.* 2017). X-ray diffraction analysis would be required to confirm the appropriate crystal space group for the granulin CrleGV-SA OB used in this study.

The OBs from UV exposure cycle 1 offered the best representation of UV damage, as this is the scenario present in the field. In this study, damage to the CrleGV-SA OBs was observed to take various forms, suggesting it could be a stepwise process. The first type of damage observed in cycle 1 OBs exposed to UV for 72 h was the thinning of the nucleocapsid. This could be an earlier stage of damage before the nucleocapsid envelope breaks down, leading to the OB losing its structural integrity and disintegrating from the inside out. Studies have shown that UV exposure causes DNA damage (Ignoffo & Garcia, 1978; Ignoffo *et al.,* 1989; Ravanat *et al.*, 2001; Rohrmann, 2013). Hence, it is possible that the DNA damage results in the nucleocapsid losing its integrity and therefore disintegrating. Another effect of the UV irradiation is the disappearance of the nucleocapsid envelope. At this stage it is not clear whether the

nucleocapsid envelope collapses first, or if the nucleocapsid disintegrates first. There is also evidence to suggest that the disintegration of the nucleocapsid does not occur in one step but rather as a stepwise process as evidenced by TEM images showing cross sections of OBs with varying amounts of nucleocapsid remaining. Some OBs were without the nucleocapsid envelope but with a relatively intact virion. Further analysis of these same images showed that the crystalline faceting of the granulin OB was absent. The NC:OB ratio obtained for cycle 1 UV exposed OBs agrees with the suggestion that the OB was disintegrating from the centre, progressing outwards. On average the OBs from cycle 1 were at least 65 nm shorter than the control OBs and 47 nm shorter than the cycle 5 OBs. It is possible that the increased size of the cycle 5 OBs could have contributed to their UV-tolerance properties. This would seem to agree with the original postulation put forward by Brassel and Benz (1979), where they expected the isolated UV-tolerant CpGV to be larger than the unexposed wild type, although that was not the case in their study. Larger OBs may mean more granulin is present in the OB and therefore provides better UV protection compared to a smaller OB. Granulin content can also be increased if the shape of the OB is altered. Nakai *et al*. (2015) isolated a new variant of the Adoxophyes orana granulovirus from *Adoxophyes* spp. larvae in the field. This new isolate, AdorGV-M, was found to be equally pathogenic as the wild type English isolate, AdorGV-E, but retained more virulence after UV irradiation than AdorGV-E. Electron Microscopic observations of the morphology of AdorGV-M revealed that it had significantly larger cuboidal OBs, instead of the ovo-cylindrical shape normally associated with granuloviruses. With very little sequence divergence between the two species it was possible that the cuboidal shape increased the amount of granulin and therefore conferred a greater degree of UV tolerance to AdorGV-E. Given the the decrease in damaged OBs from cycle 1 (82

%) to cycle 5 (11 %), it could also be argued that intact viruses were selected for following the repeated exposures. However, these samples were imaged immediately after UV exposure and without being passaged in FCM larvae. Therefore, the most likely reason for increase in intact OBs after each cycle would be the selection of tolerant virus.

A characteristic that was distinct in the experiments in this study, was the loss of the crystalline faceting after UV exposure. This results in the OB becoming amorphous and one could even suggest that this loss of crystalline faceting would allow UV irradiation to reach the nucleocapsid more freely and cause DNA damage. An interesting observation was the retention of the crystalline structure in the cycle 5 OBs that were damaged, whereas in most instances the cycle 1 OBs that were damaged presented an amorphous OB.

ATR-FTIR did not identify any major changes in the OB surface molecular structure after UV irradiation, particularly in the Amide region (1650 cm^{-1} – 1200 cm^{-1}). Previous studies with Raman spectroscopy have shown changes in the Amide I region (1535-1640 cm^{-1}) and Amide III (1220-1359 cm^{-1}) peaks, as well as the S-H stretch (2475-2676 cm^{-1}) after exposure to UVA and UVB separately (Mwanza, 2015). In contrast to the Raman analysis, these regions appeared to be UV insensitive to UV irradiation when ATR-FTIR analysis was conducted, even after 2000 scans. It was suspected that the water in which the viruses were suspended was interfering with the analysis, as it is known to absorb strongly in this region. However, subsequent analysis with dried virus gave inconclusive results. Minor changes were observed in the fingerprint region where peaks corresponding to -CH side chains were altered. These may be critical in maintaining the structural integrity of the OB.

This study has provided evidence of how UV irradiation affects the OB and virion integrity, which likely leads to loss of virulence of baculovirus biopesticides in the field. The ability to visualise and quantify UV damage could provide a complimentary diagnostic method to the traditional bioassays. The presence of only 11 % UV damaged OBs from the cycle 5 samples, compared with 82 % in the cycle 1 samples, further confirms the successful isolation of UV tolerant CrleGV-SA.

Chapter 5

The effect of selected UV-protectants on CrleGV-SA and UV-tolerant CrleGV-SA in the laboratory

5.1 Introduction

In chapters 2-4, the isolation of UV-tolerant CrleGV-SA was discussed as one way of overcoming the detrimental effect of UV on baculoviruses. In this chapter the use of UV-protectants as an additional method to improve the UV-tolerance of baculoviruses is reported. Additionally, the combination of UV-tolerant CrleGV-SA and the most successful UV-protectant is reported.

Ultraviolet radiation remains one of the major drawbacks to the use of baculovirus biopesticides (Shapiro, 1995). Most viruses lose more than 90 % of their original activity within several days after application in the field, reducing the efficacy of the virus or prolonging the time to death of the target organism (Sood *et al*., 2013; Grzywacz & Moore, 2017). Several materials have been tested in the laboratory and field as potential UV-protectants (Burges & Jones, 1998; Hunter-Fujita *et al.,* 1998; Grzywacz & Moore, 2017). These include inorganic and organic substances. Some of these substances have been shown to act synergistically with the virus. For instance, the optical brightener Tinopal LPW was shown to have a synergistic effect on the Nicaraguan Spodoptera frugiperda nucleopolyhedrovirus isolate (SfMNPV), reducing its LC_{50} by 115-fold in bioassays with the maize pest, *Spodoptera frugiperda* (J. E. Smith) (Lepidoptera: Noctuidae) larvae (Martínez *et al.,* 2000). Previously, 0.1 %

Tinopal LPW had been reported to reduce the LC_{50} values of two isolates of SfMNPV by 164- to 303 000-fold (Hamm & Shapiro, 1992).

Several UV-protectants have showed promise for use with baculoviruses. The UV-protectants tested include adjuvants used in the spray mix, plant extracts, active ingredients of sunscreen formulations, dyes and fluorescent brighteners (Burges & Jones, 1998; Hunter-Fujita *et al.,* 1998; Grzywacz & Moore, 2017). According to Burges and Jones (1998), of all the tested substances, the most promising were lignin, flour carriers, clay molasses coax, Orzan lignosuphate, optical brighteners, insect remains and melanin.

Arthurs *et al.* (2006) tested three adjuvants, NuFilm-17® (Miller Corp. Hanover, USA), Organic Biolink® (Westbridge, Vista, USA) and the apple sunburn protectant, Raynox® (Pace International; USA) with CpGV, with the aim of improving virus uptake by larvae and ultimately improving the persistence of the virus in the field. However, despite the labels on the adjuvants indicating that the adjuvants protected against sunlight degradation, this was not evident at the application rates used in the study. The authors pointed out that the UV protective effect of these adjuvants could become pronounced if the application rates were raised. However, increasing the application rates might not be easily accepted by growers and regulatory bodies and would increase cost.

The aim of this study was to identify potential UV-protectants that could be used with CreGV-SA formulations and evaluate whether there was a difference in the UV protective effect of the protectants when combined with the original CrleGV-SA or when combined with the UV-tolerant CrleGV-SA selected for in Chapter 2. To achieve this, the effectiveness of three potential UV-protectants: lignin sulphate, BREAK-

THRU®OE446 and Uvinul Easy was evaluated at three different concentrations. BREAK-THRU®OE446 is a polyether polysiloxane that is used to lower the surface tension of oil-based pesticides and thereby prevent crystallization of active ingredients and make application of pesticides more effective (Evonik Industries, Technical Information). Uvinul Easy is an active component of sunscreens that is marketed by BASF as an effective UV-protectant (Acker *et al.,* 2014). Lignin and its derivatives have been used in numerous published UV-protection studies to evaluate their potential as effective UV-protectants (Hunter-Fujita *et al,* 1998; Arthurs *et al*., 2006 & 2008).

5.2 Methods and Materials

5.2.1 Preparation of UV-protectants, virus and exposure to UV

The potential UV-protectants lignin sulphate (Sappi, SA), BREAK-THRU®OE446 (OE446) (Evonik Industries, Germany) and Uvinul Easy (BASF, Germany) were prepared in three concentrations. For the lignin sulphate, three concentrations, were prepared by adding 0.05 g, 0.5 g and 5 g to 50 ml double distilled water to give 0.1 %, 1 % and 10 % (w/v) concentrations respectively. For each of OE446 and Uvinul Easy, 0.05 ml protectant was added to 49.95 ml double distilled water, 0.5 ml was added to 49.50 ml double distilled water and 5 ml was added to 45 ml double distilled water to give final concentrations of each protectant of 0.1 %, 1 % and 10 % (v/v) respectively. To 9 ml of UV-protectant, 1 ml of the original CrleGV-SA virus suspension at a concentration of 1 x 10^{11} OBs/ml was added to give final UV-protectant concentrations of 0.09 %, 0.9 % and 9 %. Subsequently, 3 ml was placed in a petri dish and allowed to dry before being exposed to UV in a Q-Sun Xe-3 HC Test Chamber (Q-lab, USA) for 24 h. The 24h irradiation was chosen based on results from Chapter 2 which showed sufficient UV damage at that time point. The parameters used were the same

as those described in Chapter 2, with the temperature set at 30°C, irradiance at 300 Wm^{-2}, relative humidity at 42 % and with a Daylight Q filter fitted to allow for UV conditions in natural sunlight. After UV exposure, the virus was resuspended in 3 ml double distilled water. It was then recounted in a Helber Thoma (Hawksley, UK) counting chamber, using an Olympus BX 51 TF (Olympus Corporation, Japan) microscope under dark field at magnification of X400. After evaluation by bioassays, the experiment was repeated with the UV-tolerant CrleGV-SA virus (referred to as CrleGV-SA C5 in this chapter, denoting that it is derived from the fifth exposure cycle) selected after 72 h UV exposure (see Chapter 2) and the most effective concentration of each UV-protectant.

5.2.2 Effect of Potential UV Protectants on larval survival and feeding habits.

To elucidate whether each UV protectant affected the survival and/or the feeding habits of the FCM larvae, a comparison was carried out with water as the control. FCM diet was prepared and placed in six 25-well bioassay plates for each UV protectant (e.g. 9 % lignin). Aliquots of 50 µl per well of each UV protectant were spread on the surface of the diet, using a micropipette and allowed to dry under a laminar flow hood for 30 min. Each test was carried out in triplicate using 50 larvae per concentration for protectant. A single neonate larva was then picked up from the egg sheet using a small art paint brush and placed on the surface of the diet in each well. Each plate was covered with two layers of paper towel and a lid and incubated in a temperature-controlled room at 28°C for 7 days. At the end of the incubation period, each well was inspected, and larval mortality recorded. The mean percentage mortality was determined and a two tailed *t-test* in Microsoft Excel was used to determine whether there was a significant difference (P=0.05) in the response of the larvae to the UV protectants compared to the water only.

5.2.3 Surface dose bioassays

In order to evaluate the effect of the UV-protectants, surface dose bioassays were conducted after UV irradiation with first instar FCM. The bioassays were performed in 25 well bioassay plates with well dimensions of 20 mm x 20 mm x 17 mm deep. FCM eggs sheets supplied by River Bioscience (Addo, South Africa) were incubated in a temperature-controlled room at 28 °C for 72 h or until they hatched. The neonates were used within two days of hatching. FCM diet was prepared as described in section 2.2.4. Each virus preparation was diluted to 3 x 10^7 OBs/ml and serially diluted 10-fold to give concentrations of 3 x 10^6 OBs/ml, 3 x 10^5 OBs/ml, 3 x 10^4 OBs/ml and 3 x 10^3 OBs/ml. Aliquots of 50 µl per well of a single virus concentration were spread on the surface of the diet, using a micropipette and allowed to dry under a laminar flow hood for 30 min. Each bioassay was carried out in triplicate using 25 larvae per concentration for each replicate.

A single neonate larva was then picked up from the egg sheet using a small art paint brush and placed on the surface of the diet in each well. Each plate was covered with two layers of paper towel and a lid and incubated in a temperature-controlled room at 28°C for 7 days. At the end of the incubation period, each well was inspected, and larval mortality recorded. A larva was recorded as dead if upon being touched by a blade it did not move or it ruptured; and was recorded as alive if it moved when touched by the blade. A control plate with sterile double distilled water instead of UV-exposed virus was prepared. To test the effect of the UV-protectants on the virulence of CrleGV-SA, an unexposed virus-protectant mixture for each protectant concentration was evaluated in surface dose bioassays with FCM first instars and compared with the

unexposed CrleGV-SA. All bioassays were carried out in triplicate. Surface dose bioassays with unexposed CrleGV-SA were also conducted concurrently to provide a comparison.

The mean mortality data obtained were subjected to probit analysis using PROBAN, a statistical software programme used for analysis of bioassay data (Van Ark, 1995). This software takes into consideration the mortality of the treated larvae, and corrects this for mortality of control larvae, based on the Abbot formula (Abbott, 1925), giving a dose response curve from which the LC_{50} and LC_{90} values were determined at each protectant concentration. Regression lines comparing the effect of a particular protectant on larval mortality and hence virus potency across its three concentrations of protectant were determined and the slopes of the lines were compared and significant differences at $P \leq 0.05$ determined. Where lines were found to be parallel, relative potency comparisons were carried out. For each comparison, one sample was chosen as a reference (r) and compared against another sample (t). Where t was less than 1 ($t<1$) the test sample was more potent than the reference sample. Where the value of t equalled 1 ($t=1$) there was no difference in potency between the two samples being compared. A value of t that was greater than 1 ($t>1$), indicated that the test sample was less potent than the reference sample (Finney, 165; Finney 1971; Dinse & Umbach 2011; van Ark 1995; Opoku-Debrah *et al.*, 2016). The Bartlett's test was used to compare the homogeneity of variances in the lines at $P \leq 0.01$.

5.3 Results

The effectiveness of three potential UV-protectants, lignin sulphate, OE446 and Uvinul Easy was evaluated after exposure to UV in a Q-Sun Test Chamber for 24 h using surface dose bioassays. There was no significant difference ($P = 0.05$) in the percentage mortality of the FCM first instars when tested with unexposed UV-

protectants only or water only, thereby suggesting that the protectants alone did not affect larval survival or improve or decrease the feeding habits of the larvae (Table A15. Apendix IV).

5.3.1 The effect of lignin on the LC_{50} of CrleGV-SA after 24 h UV irradiation

Surface dose-response bioassays conducted with CrleGV-SA samples combined with lignin followed by 24 h UV-irradiation, were used to plot regression lines fitted to the corrected data (Fig 5.1). Negative control mortality of all samples ranged from 0 % to 13 %. The regression lines fitted to the corrected data for all replicates were compared and the residual variances of the lines determined by Bartlett's test. The variances were determined to be homogeneous (X^2 = 0.082; DF = 4; P = 0.01) and thus comparisons of slopes and elevations could be carried out. The lines were determined to be parallel by the Chi-square test, and their elevations, were shown to be comparable (X^2 = 5.200; DF= 4; P = 0.05). Using the Bonferroni multiple range test (MRT), it was determined that the elevations of the lines differed significantly from each other ($F_{4, 19}$ = 2.94; P = 0.05). It was determined that all the samples differed significantly from the unexposed CrleGV-SA sample without protectant (Fig 5.1). However relative potency comparisons also showed differences between the three protectant concentrations (0.09 %, 0.9 % and 9 %) used (Table A11, Appendix III).

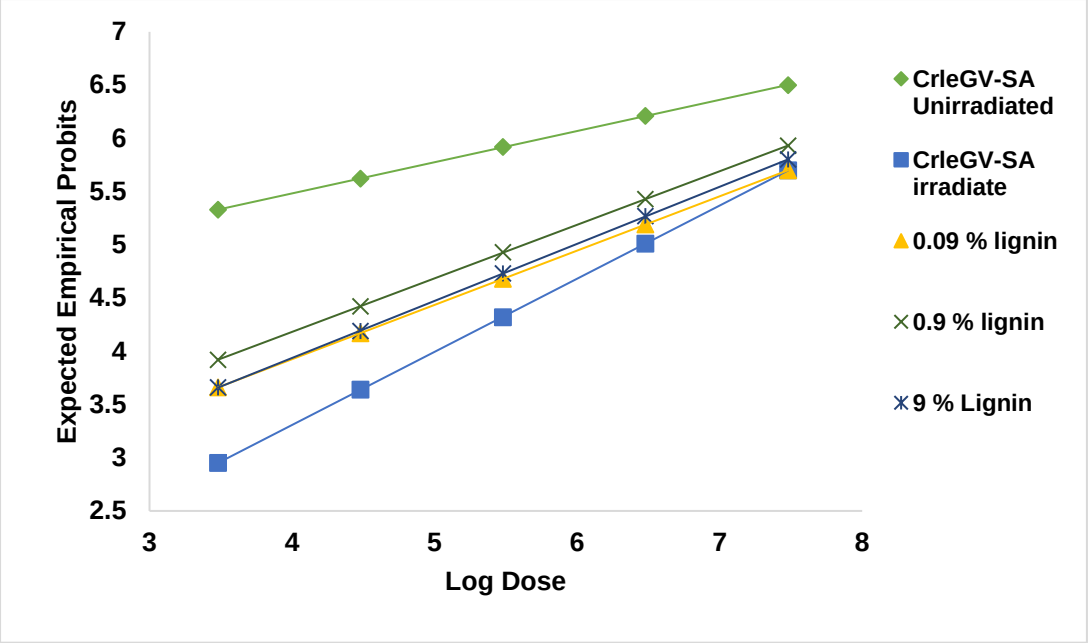

Figure 5.1: Log dose-probit regression lines for CrleGV-SA combined with lignin in bioassays of neonate FCM larvae after UV irradiation for 24 h in the Q-Sun test chamber.

The LC_{50} of the CrleGV-SA exposed to UV without any UV-protectant was determined to be 2.89 x 10^8 OBs/ml in surface dose bioassays (Table 5.1). While lignin offered some protection to the virus, as indicated by the increase in elevation of the expected empirical probit line as the concentration of lignin was increased (Fig 5.1 and Table 5.1), none of the concentrations used in this study could yield an LC_{50} value close to that of the unirradiated CrleGV-SA control (Table 5.1) When CrleGV-SA was combined with 0.09 % lignin the LC_{50} decreased to 1.26 x10^8 OBs/ml. This was not significantly different to the unprotected CrleGV-SA, however relative potency comparison showed that the 0.09 % lignin sample was more potent than the unprotected sample (t=2.416). The virus sample combined with 0.9 % lignin had an LC_{50} of 4.23 x 10^7 OBs/ml after UV irradiation. Relative potency comparison values showed this sample to be more potent than the unprotected CrleGV-SA (t=7.759), the 0.09 % lignin-virus combination (t=3.212) and the 9 % lignin-virus combination

(t=2.383) (Table A11, Appendix III). Thus, for the lignin-virus combination, 0.9 % lignin was the most effective and was selected to be used with the UV-tolerant CrleGV-SA selected in Chapter 2.

Table 5.1: The effect of lignin, OE446 and Uvinul Easy on the LC_{50} of CrleGV-SA after UV-irradiation for 24 h

Time (h)	LC_{50} (OBs/ml)	95 % Fiducial limits		X^2	P
		Lower	Upper		
Unirradiated CrleGV-SA	$2.28x\ 10^4$	3.37×10^{-2}	4.73×10^5	0.613	0.892
Irradiated CrleGV-SA	2.89×10^8	8.44×10^7	1.17×10^9	1.089	0.783
0.09 % Lignin	1.26×10^8	3.87×10^7	5.37×10^8	0.694`	0.874
0.9 % Lignin	4.23×10^7	9.32×10^6	1.70×10^8	0.895	0.828
9 % Lignin	9.55×10^7	2.74×10^7	$3.75x\ 10^8$	0.792	0.852
0.09 % OE446	2.06×10^8	6.32×10^7	9.99×10^8	0.214	0.970
0.9 % OE446	4.23×10^7	3.94×10^7	6.51×10^8	0.423	0.932
9 % OE446	4.81×10^7	9.95×10^6	2.18×10^8	1.285	0.736
0.09 % Uvinul Easy	1.03×10^8	3.18×10^7	3.73×10^8	0.694`	0.874
0.9 % Uvinul Easy	4.89×10^7	1.41×10^7	1.77×10^8	0.335	0.949
9 % Uvinul Easy	2.94×10^7	6.96×10^6	1.17×10^8	1.474	0.692

5.3.2 The effect of BREAK-THRU®OE446 (OE446) on the LC_{50} of CrleGV-SA after 24 h UV irradiation

Surface dose-response bioassays conducted with CrleGV-SA samples combined with OE446 followed by 24 h UV-irradiation, were used to determine a dose response relationship (Fig 5.2). Negative control mortality of all samples ranged from 0 % to 13 %. The regression lines fitted to the corrected data for all replicates were compared

and the residual variances of the lines determined by Bartlett's test. The variances were determined to be homogeneous (X^2 = 0.776; DF = 4; P = 0.01) and thus comparisons of slopes and elevations could be carried out. The lines were determined to be parallel by the Chi-square test, and their elevations, were shown to be comparable (X^2 = 4.950; DF= 4; P = 0.05). The Bonferroni MRT determined that the elevations of the lines differed significantly from each other ($F_{4, 19}$ = 2.94; P = 0.05). It was determined that all the samples differed significantly from the unexposed CrleGV-SA sample without protectant (Fig 5.2). However relative potency comparisons also showed differences among the three OE446 concentrations used (0.09 %, 0.9 % and 9 %) (Table A12, Appendix III).

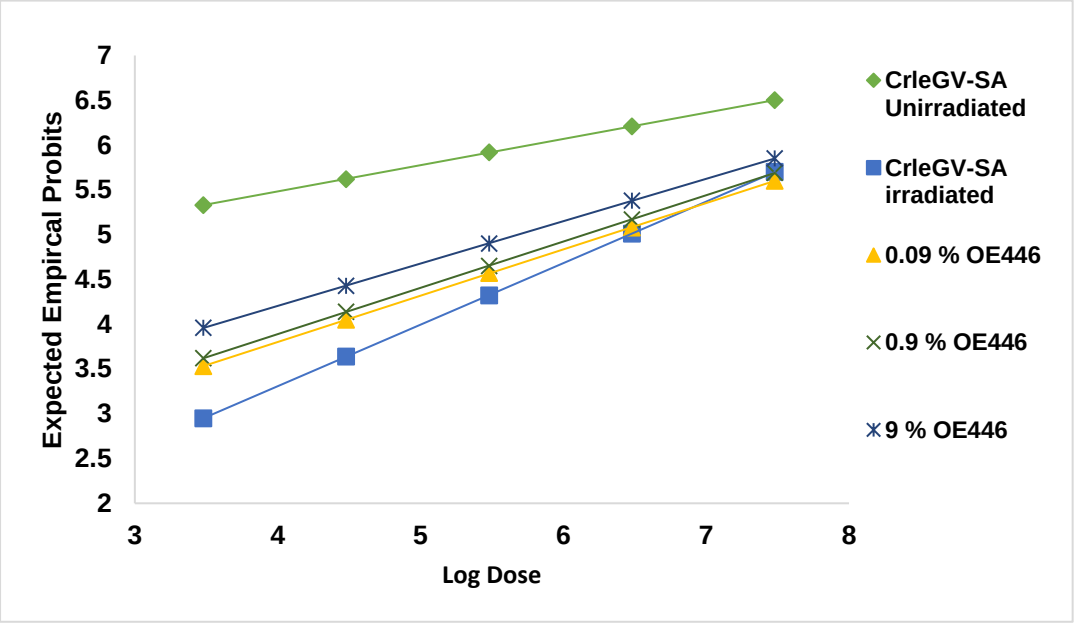

Figure 5.2: log dose-probit regression lines for CrleGV-SA combined with BREAK-THRU®OE446 (OE446) in bioassays of neonate FCM larvae after UV irradiation for 24 h in the Q-Sun test chamber.

Of the three OE446 concentrations used in this study, the 0.9 % gave the lowest LC_{50} value (4.23 x 10^7 OBs/ml) after UV irradiation (Table 5.1). This was determined to be more potent that the 0.09 % OE446-virus combinations (LC_{50}=2.06 x 10^8 OBs/ml, t=1.534) but less potent than the 9 % OE446-virus combination (LC_{50}=4.81 x 10^7 OBs/ml, t=0.320). The 9 % OE446-virus combination was also more potent than the 0.09 % combination (t=4.800) (Table A12, Appendix III). Thus, based on the higher relative potency, the 9 % OE446-virus combination was determined to be the most effective concentration among the three concentrations used and was selected to be used in combination with the UV-tolerant CrleGV-SA

5.3.3 The effect of Uvinul Easy on the LC50 of CrleGV-SA after 24 h UV irradiation

Surface dose-response bioassays conducted with CrleGV-SA samples combined with Uvinul Easy followed by 24 h UV-irradiation, were used to determine a dose response relationship (Fig 5.3). Negative control mortality of all samples ranged from 0 % to 13 %. The regression lines fitted to the corrected data for all replicates were compared and the residual variances of the lines determined by Bartlett's test. The variances were determined to be homogeneous (X^2 = 0.761; DF = 4; P = 0.01) and thus comparisons of slopes and elevations could be carried out. The lines were determined to be parallel by the Chi-square test, and their elevations, were shown to be comparable (X^2 = 5.590; DF= 4; P = 0.05). The Bonferroni MRT determined that the elevations of the lines differed significantly from each other ($F_{4, 19}$ = 2.94; P = 0.05). It was determined that all the samples differed significantly from the unexposed CrleGV-SA sample without protectant (Fig 5.3). However relative potency comparisons also showed differences among the three protectant concentrations used (0.09 %, 0.9 % and 9 %) (Table A13, Appendix III).

While the Uvinul Easy offered some protection to the virus as evidenced by the LC_{50} values, none of the concentrations used in this study yielded an LC_{50} value close to that of the unirradiated CrleGV-SA control (Table 5.1) When CrleGV-SA was combined with 0.09 % Uvinyl Easy and exposed to UV, the LC_{50} obtained was 1.03 $x10^8$ OBs/ml. The 0.9 % sample resulted in an LC_{50} value of 4.89 $x10^7$ OBs/ml while the 9 % sample had an LC_{50} value of 2.94 $x10^7$ OBs/ml. While the three samples did not appear to be significantly different at P=0.05, relative potency values determined that the 9 % sample was more potent than the other two samples (t=3.721 for 0.09 % and t=1.670 for the 0.9 % sample) (Table A13, Appendix III). Thus, the 9 % Uvinul Easy-virus combination was determined to be the most effective of three Uvinul Easy concentrations and was used in combination with the UV-tolerant CrleGV-SA.

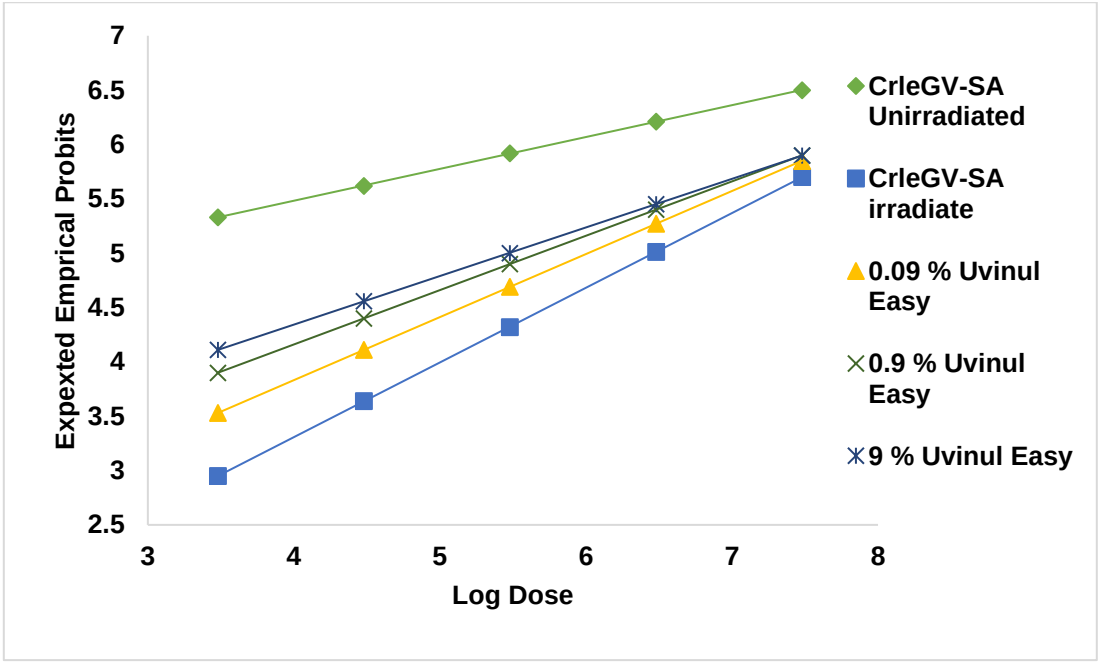

Figure 5.3: log dose-probit regression lines for CrleGV-SA combined with Uvinul Easy in bioassays of neonate FCM larvae after UV irradiation for 24 h in the Q-Sun test chamber.

5.3.4 The effect of selected concentrations of the three potential UV-protectants on the LC50 of UV-tolerant CrleGV-SA after 24 h UV irradiation

The most effective concentrations of each potential UV-protectant described in section 5.2.1 were selected after UV exposure and analysis in bioassays with the original CrleGV-SA used in the Cryptogran formulations. The most effective concentrations were 0.9 % lignin, 9 % OE446 and 9 % Uvinul Easy. These were subsequently combined with the UV-tolerant virus (CrleGV-SA C5) obtained in Chapter 2, exposed to UV for 72 h and surface dose bioassays using first instar FCM conducted (Fig 5.4). Negative control mortality of all samples ranged from 0 % to 4 %.The regression lines fitted to the corrected data for all replicates were compared and the residual variances of the lines determined by Bartlett's test. The variances were determined to be homogeneous (X^2 = 2.134; DF = 4; P = 0.01) and thus comparisons of slopes and elevations could be carried out. The lines were determined to be parallel by the Chi-square test, and their elevations, were shown to be comparable (X^2 = 0.198; DF= 4; P = 0.05). The Bonferroni MRT determined that the elevations of the lines differed significantly from each other ($F_{4, 19}$ = 2.94; P = 0.05). It was determined that all the samples did not differ significantly from the unexposed UV-tolerant CrleGV-SA sample without protectant (Fig 5.4). However relative potency comparisons also showed differences among the three protectant concentrations used (0.09 %, 0.9 % and 9 %) (Table A14, Appendix III).

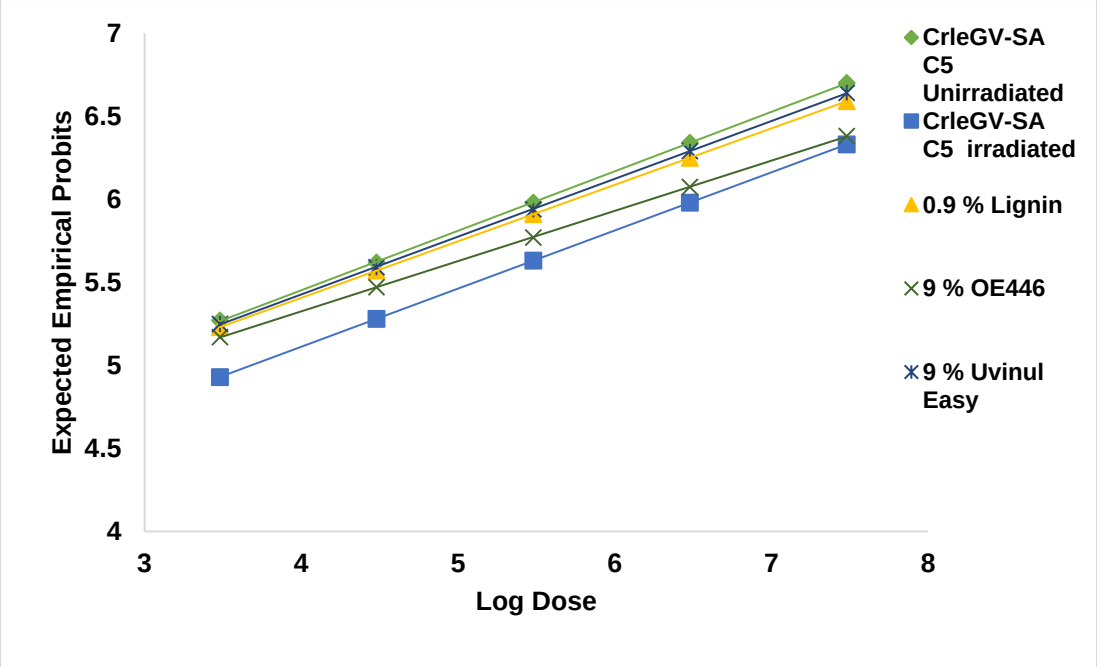

Figure 5.4: log dose-probit regression lines for UV-tolerant CrleGV-SA combined with selected UV-protectants in bioassays using neonate FCM larvae after UV irradiation for 24 h in the Q-Sun test chamber.

The LC_{50} value of the CrleGV-SA C5 increased from 5.50 x 10^4 OBs/ml to 4.68 x 10^5 OBs/ml after UV irradiation. Combination with UV-protectant improved the LC_{50} to 6.45 x 10^5 with 0.9 % lignin, 5.85 x 10^4 with 9 % Uvinul Easy and 8.57 x 10^4 OBs/ml with 9 % OE446 (Table 5.2). When relative potency comparisons were carried out, the 0.9 % lignin-virus combination was more potent that the 9 % OE446 (t=2.320) but less potent than the 9 % Uvinul Easy (t=0.810) (Table A14, Appendix III). The 9 % Uvinul Easy was also more potent than the 9 % OE446 (t=2.864), thus making the 9 % Uvinul Easy the most effective of the three UV-protectants, followed by the 9 % OE446 and then 0.9 % lignin.

Table 5.2: The effect of selected UV-protectants on the LC_{50} of UV-tolerant CrleGV-SA after UV-irradiation for 24 h.

Time (h)	LC_{50} (OBs/ml)	95 % Fiducial limits		X^2	P
		Lower	Upper		
Unirradiated CrleGV-SA C5	5.50×10^4	2.23×10^0	6.08×10^5	0.135	0.982
Irradiated CrleGV-SA C5	4.68×10^5	5.79×10^3	2.89×10^6	1.620	0.659
0.9 % lignin	6.45×10^4	3.21×10^1	7.01×10^5	0.255	0.963
9 % Uvinul Easy	5.85×10^4	3.04×10^1	6.34×10^5	0.214	0.970
9 % OE446	8.57×10^4	1.65×10^1	1.03×10^6	0.148	0.980

5.4 Discussion and Conclusion

In this chapter, the effect of three UV-protectants on the LC_{50} of the original CrleGV-SA and the isolated UV-tolerant CrleGV-SA after UV exposure was evaluated. The most effective concentrations for each UV-protectant were 0.9 % lignin, 9 % OE446 and 9 % Uvinul Easy. When combined with the UV-tolerant CrleGV-SA the UV-protectants offered approximately the same degree of protection as they did with the original CrleGV-SA. When the LC_{50} of the irradiated unprotected and protected viruses were compared, it was found that the 0.9 % lignin improved the LC_{50} of the original virus 6.88-fold, while it improved the LC_{50} of the UV-tolerant virus 7.3-fold. The 9 % OE446 improved the LC_{50} of the original CrleGV-SA 6.01-fold and improved the LC_{50} of the UV-tolerant virus by 5.44-fold. The Uvinul Easy decreased the LC_{50} 9.83 and 8.63 times with the original CrleGV-SA and UV-tolerant CrleGV-SA respectively. Thus, the performance of the UV-protectants was not altered (neither improved nor

reduced) by the UV-tolerant virus. This agrees with the preliminary experiments (data not included) conducted in this study which showed that none of the protectants had an effect on the mortality of the FCM larvae, even at protectant concentrations as high as 9 %.

There is some promise with all three UV-protectants at the selected concentrations, however, this will have to be proven in the field. In the past, potential UV-protectants have produced exciting results in the laboratory, but when tested in the field have not provided significantly different efficacy than spraying without UV protection (Arthurs *et al.,* 2006; Kirkman, 2007). Arthurs *et al.* (2006) reported that in the field, lignin-based formulations were effective only with high CpGV concentrations. In another study with lignin, Kirkman (2007) reported that in laboratory studies, lignin provided protection for CrleGV-SA. However, when the study was conducted in the field, the protective effect of the lignin was found to be comparable to spraying the CrleGV-SA in the evening without any protection (Kirkman, 2007). Additionally, the lignin needed a carrier, which was costly and would not have been commercially viable for farmers or biopesticide manufacturers. In the present study, lignin sulphate was used without a carrier, giving improvement in the virulence of the virus after UV irradiation. However, there is a strong possibility that the lignin could be washed off in the field and hence a carrier or some form of encapsulation especially at the micro-, and nano-level would be a better method to ensure the lignin retains the effectiveness achieved in the laboratory tests. Micro - and nano encapsulation is currently used successfully for drug delivery in humans (Ulanova *et al.,* 2014). For this to work with granulovirus biopesticides, the encapsulation material needs to be readily soluble in the alkaline mid-gut of the insect, otherwise the infectivity of the virus could be adversely affected.

Several encapsulation techniques with baculoviruses have been attempted with mixed results (Pemsela *et al*., 2010; Gómez *et al*., 2013; Gifani *et al.,* 2015). Gómez *et al*. (2013) reported that the microencapsulation of SfMNPV did not result in enhanced viral activity in comparison with the non-encapsulated virus. Despite these setbacks, lignin is one of the most promising UV-protectants, with several patents already filed for lignin sulphate as a UV-protectant (Smith & Herbig 1998; Hobbs *et al.,* 1999). Lignin production in plants is induced by stressors such as ozone, plant pathogens and UV irradiation, and this explains why there is a lot of interest in the protection of baculovirus biopesticides with lignin (Shapiro *et al.,* 2009). While most publications have highlighted the low effectiveness of potential UV-protectants in the field, Wu *et al*. (2015) reported that zinc oxide (ZnO) and titanium oxide (TiO_2) provided protection to CpGV, both in the laboratory and after 7 days irradiation in the field, when applied at a virus concentration of 1 x 10^6 OBs/ml, being more effective with 0.5 % ZnO alone or TiO_2 alone. These promising findings could lead to more effective UV-protectants for use in the field.

BASF states that Uvinul Easy can be used in sunscreen formulations with the concentration ranging from 6-50 % (Acker *et al.,* 2014). Thus, while only up to 9 % Uvinul Easy was tested in this study, there is room to increase the concentration in tests with CrleGV-SA. Although higher concentrations may be more effective, they will be more costly and would also bring into consideration the issue of chemical residue on fruit. Every government or block of countries such as the European Union has its own recommendations on what is the acceptable maximum residue limit (MRL) on fruit and other crops, therefore any commercial biopesticide with a UV-protectant would have to comply with all customer government requirements (Reeves *et al.,* 2019).

Additionally, Burges and Jones (1998) suggest that the use of UV protectants at concentrations 1-10% in low or high-volume tanks is wasteful.

While in this study, 0.9 % lignin, 9 % OE446 and 9 % Uvinul Easy were the most effective protectants, it has been shown that in some instances higher protectant concentrations than those used in the laboratory may be needed to achieve sufficient protection in the field. This is the case with green tea extracts tested by Shapiro *et al.* (2009), which provided excellent protection in the laboratory at 1 % concentration but needed to be at 10 % in the field to achieve similar levels of UV protection of *Spodoptera exigua* multiple nucleopolyhedrovirus (SeMNPV), which is pathogenic to the beet armyworm, *Spodoptera exigua* (Hübner). Similarly, Sajap *et al*. (2009), found that the adjuvant Tinopal conferred significant UV protection to Spodoptera litura multinucleocapsid nucleopolyhedrovirus (SpltMNPV) in the laboratory but this was not translated to similar levels in the field as there was no clear difference with the unprotected SpltMNPV. Thus, it is possible that in this study, higher concentrations of the protectants may be needed to achieve the same level of UV protection to CrleGV-SA in the field.

Some UV-protectants have a negative influence on the effectiveness of the virus at the protectant concentration required for protection. Wu *et al.,* (2015) noted that as the concentrations of both ZnO and TiO_2 increased, the activity of CpGV decreased. They attributed this to the photocatalytic activities of both compounds. In the present study however, none of the UV-protectants significantly affected the activity of the virus, even at high concentrations.

In conclusion, three potential UV-protectants, were tested at various concentrations in this study, to determine their ability to protect CrleGV-SA OBs from the harmful effects

of UV irradiation in the laboratory. With the tightening restrictions on the use of chemical pesticides it is important that alternatives such as baculovirus biopesticides are as effective as possible in the field. Addition of economically and scientifically viable UV-protectants would help to achieve this. The 0.9 % lignin, 9 % OE446 and 9 % Uvinul Easy concentrations gave the most promising results for both the wild type CrleGV-SA and the UV-tolerant CrleGV-SA. It is recommended that they be further tested to evaluate their effectiveness under field conditions as well as when combined together.

Chapter 6

General Discussion

6.1 Introduction

The aim of this study was to select for a UV-tolerant CrleGV-SA virus with potential to be used as a biopesticide with longer persistence in the field. To achieve this, CrleGV-SA was repeatedly exposed to UV irradiation, resulting in the selection of UV-tolerant CrleGV-SA with a lower LC_{50} value after UV exposure (Chapter 2). The genomes of the virus exposed once to UV (cycle 1) and virus exposed five times with repassage (cycle 5) were sequenced and analysed. Various SNPs were detected in both sequences (Chapter 3). These SNPs may be related to the development of the UV-tolerance recorded in the cycle 5 sample. The morphological effects of UV damage on the CrleGV-SA as analysed by TEM were reported (Chapter 4). Additionally, the differences in the morphology of samples from exposure cycle 1 and cycle 5 were highlighted. Finally, the effect of selected UV protectants on CrleGV-SA and the UV tolerant CrleGV-SA in the laboratory was described (Chapter 5).

6.2 The selection of UV-tolerant CrleGV-SA

The use of baculovirus biopesticides has grown over time, particularly because of the need to find an alternative to chemical biopesticides, which come with negative side effects to the environment and non-target organisms (Hu, 2006; Kost *et al.,* 2005; Aktar *et al.,* 2009; Lapointe *et al.,* 2012; Moscardi, 1999; Moscardi *et al.,* 2011; Pidre *et al.,* 2013). However, rapid degradation of the virus due to exposure to the UV A and

B component of sunlight means that persistence of baculovirus biopesticides in the field is of limited duration (Shapiro *et al.,* 1983; Black *et al.,* 1997; McGuire *et al.,* 2000). Researchers have investigated various ways to improve the UV-tolerance of baculoviruses. These include testing UV-protectants to add to the baculovirus formulations, looking for baculovirus isolates with better UV-tolerance levels, as well as genetic engineering of baculoviruses to help them overcome, or reverse, the effects of UV irradiation (Shapiro & Robertson, 1990; Asano, 2005; Shapiro *et al*., 2009;). Another option that has been explored to overcome the effect of UV irradiation is the use of a naturally occurring, or laboratory generated, UV-tolerant baculovirus, produced by selecting through a series of UV exposure and re-exposure experiments (Brassel & Benz, 1979; Jeyarani *et al.,* 2013). The principle is that in each UV exposure cycle, surviving viruses that have acquired UV tolerant properties through mutation, or have inherent UV tolerant properties, are selected and introduced into the next exposure cycle, until the UV-tolerant strain becomes the dominant strain in a given virus population (Brassel and Benz, 1979; Jeyarani *et al*., 2013). It is important to emphasize that this is not necessarily selection of a more virulent strain within the existing population, but rather of a UV-tolerant strain, hence the stable LC_{50} values recorded in this study for the unexposed control strain. If the LC_{50} of the unexposed control virus had been shown to fluctuate, that could have suggested the presence of a more virulent strain. However, van der Merwe *et al.* (2017) demonstrated that the CrleGV-SA genome has remained stable in the past 15 years, and therefore the differences in UV-tolerance demonstrated in the present study have been generated by the repeated UV exposure and re-exposure of the virus.

This is not a foreign concept, as isolates of the same virus species with different UV-tolerance levels have already been discovered. Akhanaev *et al.* (2017), compared the

UV-tolerance of two strains of Lymantria dispar multiple nucleopolyhedrovirus (LdMNPV) by measuring the relative rate of inactivation and virus half-life. The isolates, LdMNPV-27/0 and LdMNPV-45/0 were isolated from Western Siberia and North America respectively. After exposure to sunlight, it was observed that the North American strain, LdMNPV-45/0, previously shown to be more virulent towards *L. dispar* larvae, was more sensitive to UV and lost its potency faster than the Asian strain, LdMNPV-27/0. A significant delay was observed in LdMNPV-45/0 induced pathogenesis after 15 min sunlight exposure, while the LdMNPV-27/0 strain showed the same delay after 2 h exposure to sunlight. These differences in UV-tolerance may relate to the environment or to a genetic difference in certain ORFs of the genome. In the LdMNPV case, differences in the genomes were observed, including the deletion of the *vef-1* gene in the Asian strain and a severe frameshift in *vef-2*, which resulted in an early stop codon that might have resulted in the loss of protein function. Thus, the authors concluded that in regions of high UV loading, the effectiveness against *L. dispar* larvae of the highly potent LdMNPV-45/0 could be significantly reduced. In South Africa, new genetically distinct isolates of CrleGV-SA were identified from geographically distinct insect populations, with some degree of phenotypic variation. (Opoku-Debrah *et al.,* 2013). While the UV-tolerance of these new isolates has not yet been determined, it was demonstrated that the virulence of the CrleGV-SA isolates differed significantly between different FCM hosts (Opoku-Debrah *et al.,* 2016). Therefore, their UV-tolerance might also differ.

A limited number of studies have described the successful selection and isolation of UV-tolerant baculoviruses, however of those that have done so, none have described the possible molecular causes for the selected UV-tolerance (Brassel & Benz, 1979; Shapiro & Bell, 1984; Jeyarani *et al*., 2013). A consequence of this selection method

is that the resultant UV tolerant strain has virulence that is comparable to the original strain, whereas previously it has been demonstrated that the developed UV tolerant strain had lower virulence compared to the original strain (Witt & Hink, 1979). In the present study the successful isolation of a UV tolerant CrleGV-SA strain as evidenced by the data from bioassays was described.

6.3 The Sequencing of CrleGV-SA C1 and CrleGV-SA C5

To understand the mechanism of UV-tolerance in the isolated UV tolerant strain, the sequences of the virus samples from cycle 1 and cycle 5 were analysed. The 72 h sample was selected based on the bioassays results obtained in Chapter 2. Additionally, while there was little difference in bioassays results with the 24 h sample, it was also important to establish whether tolerance could be achieved even after prolonged exposure to UV. It has been shown previously that UV tolerance can be improved by expression of a DNA repair enzyme (Petrik *et al*., 2003). The UV-tolerance of AcMNPV budded virus improved by more than 3-fold when an algal virus pyrimidine-dimer specific glycosylase was expressed in AcMNPV (Petrik *et al.,* 2003). However, the occluded virus was not more tolerant to UV when fed to *S. frugiperda* or *Trichoplusia ni* first instars. It has also been reported that group II NPVs have conserved DNA photolyase genes, which have been identified in NPVs isolated from the insects *Chrysodeixis chalcites* and *Trichoplusia ni* (Van Oers *et al.,* 2004; Xu *et al*., 2008b; Van Oers *et al.,* 2008). The Chrysodeixis chalcites nucleopolyhedrovirus photolyase gene was found to be active and its function was confirmed by expression in photolyase deficient *Escherichia coli* cells, which conferred photo-reactivating ability (Van Oers *et al*., 2004; Van Oers *et al*., 2008).

While previous studies have focused solely on bioassay data, the present study is the first published study to investigate the molecular basis of the selected UV-tolerance. In this study several SNPs were found in the genomes of the viruses from UV exposure cycle 1 and cycle 5. The SNPs were largely substitutions and did not consist of other variations, such as deletions or insertions. These SNPs occurred in regions of known proteins, as well as hypothetical protein regions. Some of the SNPs that were detected were found in genes that regulate or are involved in the infection cycle, such as the *pif-2* and the metalloproteinase genes. This could explain the reduction in LC_{50} of virus selected after the fifth cycle of UV exposure. Another SNP was found in the granulin gene that encodes the major protein forming the OB. This could improve the stability of the protein, or potentially confer UV protective capacity to the OB by influencing the crystalline structure of the OB. The SNPs detected in cycle 1 and retained in cycle 5 are thought to be responsible for UV tolerance, whilst the SNPs detected only in cycle 5 most likely further enhance the UV tolerance and may be associated with virulence, as evidenced by the bioassay data in which the LC_{50} is reduced in cycle 5 isolates.

6.4 The effect of UV on the morphological structure by TEM

It is known that UV damages the DNA of living organisms, including baculoviruses, by inducing the formation of pyrimidine dimers, promoting deletions and strand breakage, as a result of the formation of radicals (Ignoffo *et al*. 1989; Ravanat *et al.*, 2001; Rohrmann, 2013). This study has demonstrated for the first time, that in addition to damage at the molecular level, UV leads to morphological damage to the virus and surrounding OB that can be detected by transmission electron microscopy (TEM). This is particularly important in demonstrating that the OB, despite protecting the virion from

various other harsh environmental stresses, is unable to provide effective protection against UV irradiation.

The detected damage to the virion in cycle 1 samples, corroborates the data from bioassays of the same samples, where the virulence was seen to decrease after UV irradiation. The observed SNP in the granulin gene could be critical in strengthening the crystalline faceting or altering another aspect of the OB structure, thereby making it less susceptible to UV degradation, as observed in the cycle 5 UV-exposed CrleGV-SA, where the majority of OBs retained their crystalline faceting and bioassay data showed an increase in virulence compared to the cycle 1 samples. It is known that granulin is the major OB protein and that it confers the environmental protective ability to the OB (Rohrmann, 1986; Jehle & Backhaus, 1994). It is quite interesting that SNPs did not map to structrural genes encoding the nucleocapsid envelope given the extensive damage observed under TEM. This might because these SNPS may have been present in the 18 % of intact virions observed but were masked by sequencing of the dominant population of the damaged virus. In addition, the size of the OB could influence the level of UV-protection that the OB provides to the virion. In this study cycle 5 OBs were found to be significantly larger than the cycle 1 OBs. It has been suggested that the larger the OB, the more granulin is present and hence the better the UV-protection provided (Nakai *et al*., 2015). Nakai *et al.* (2015) deduced that the cuboidal shape of the granulin OB of a new isolate of AdorGV-M provided better UV protection because it had a larger volume and therefore had more granulin than the typical ovo-cylindrical granulovirus OB shape of the English isolate AdorGV-E. In this study the shape of the CrleGV-SA remained unchanged.

TEM analysis also provided evidence that UV damage to the virus is possibly a stepwise process, which raises the possibility of reversing the effect of UV-induced

DNA damage by the introduction of DNA photolyases for example. Certain organisms that possess DNA photolyases can reverse DNA damage caused by UV-exposure (Eker *et al.,* 1990; Carell *et al.,* 2001). An option would be to incorporate a DNA photolyase in the baculovirus genome, which would enable the virus to reverse the effects of UV-induced DNA damage in the field and remain viable for longer periods. Baculovirus DNA photolyases, such as those discovered by Van Oers *et al.* (2004; 2008), could be studied further to determine the conditions that would activate them in the field.

The TEM observations made after UV irradiation gave rise to two hypotheses regarding the mechanism of UV damage. The first being that UV damages the virion and its DNA first, then the nuclear envelope membrane raptures, followed by the granulin crystalline lattice, disintegrating outwards, leaving an enlarged space around the nucleocapsid. The second hypothesis is that UV damages the structure of the granulin OB first, and subsequently the virion and DNA material. This could form part of a follow up study to this project, to investigate the mechanism of UV damage to the OB and virion.

6.5 UV protectants

Most of the research conducted on improving the UV-tolerance of baculoviruses has focused on finding natural and artificial UV protectants (sunscreens) that can be applied around the virus, or sprayed with the virus (Burges & Jones, 1998; Hunter-Fujita *et al.,* 1998). While some have shown promise in the laboratory, use in the field did not result in significant differences in persistence to warranty commercial use.

In this study, the three UV protectants used, all provided a limited level of UV protection. When the best three protectants were each individually combined with the

UV tolerant CrleGV-SA, there was no significant difference in the response to UV exposure, compared to the response of wild CrleGV-SA in combination with these protectants. However, several factors need to be considered when using UV-protectants. Kirkman (2007) reported that the lignin sulphate carrier used in his studies with CrleGV-SA was expensive, needed to be used at high concentrations to be effective in the field, and that when CrleGV-SA was sprayed in the field at night, there was no subsequent significant difference in the efficacy of the virus with or without the lignin sulphate. Grzywacz & Moore (2017), also argue that applying baculoviruses at a higher concentration could increase the persistence of the virus in the field. Most of the potential UV protectants, need to be applied in large volumes when scaled up to the field application stage, which also makes the use of UV protectants expensive and more difficult to apply, further adding to the reluctance of manufacturers to develop the products for commercial purposes. Encapsulation of the OB has been suggested as an alternative form of protection. However, for this to be successful, the encapsulated virus needs to be liberated from the encapsulating material within the insect gut, to enable infection of the insect gut epithelial cells. Thus, while the UV protectants tested in this study were shown to provide a level of protection, this needs to be scaled up and evaluated in the field to determine if it is worthwhile pursuing commercial production with the protectants.

6.6 Conclusions and Future Work

The main aim of this study was to select and isolate UV-tolerant CrleGV-SA and investigate the possible mechanism of this tolerance by sequencing and analysing the genomes of the UV tolerant samples. UV-tolerant CrleGV-SA was successfully isolated, as evidenced by the improved LC_{50} values obtained for the 24 h and 72 h

samples and TEM data obtained for the 72 h samples, after UV exposure cycle 5. This is the first report where a UV-tolerant CrleGV strain has been produced. Seven SNPs were detected in the genome sequences from virus samples after exposure to UV in cycle 1 and and 14 SNPs were detected in cycle 5. The SNPs detected in cycle 5 included 7 that were detected in cycle 1 and an additional 7 detected only in cycle 5. These were suspected to be responsible for the UV-tolerance. However, further work needs to be carried out to identify the roles of the mutated known genes and to establish whether the SNPs in hypothetical proteins have functional roles in conferring UV-tolerance. Data obtained from TEM imaging showed structural damage to the virion and OB after UV exposure. This is the first such instance that damage to the OB has been visualised by TEM imaging. Additionally, TEM provided a contrast between samples exposed to UV at cycle 1, where the crystalline OB had become amorphous and the virion disintegrated, and the cycle 5 exposed samples in which most of the OBs (82 %) were intact with visible crystalline faceting. It was also shown that cycle 5 exposed CrleGV-SA OBs (mean length=347.29 ± 4.62) were significantly larger than cycle 1 OBs (mean length=301.30 ± 6.03). Finally, the tested UV protectants were shown to provide limited protection to both the original CrleGV-SA and the selected UV-tolerant CrleGV-SA at a comparable level, thus adding limited value to the selected UV-tolerant isolate.

Going forward, it is necessary for the UV-tolerant virus to be bulked up in fifth instars, the homogeneity of its population confirmed and for its efficacy to be tested in the field. It would be interesting to make a comparative bioassay among the UV-tolerant CrleGV-SA isolates (3 h, 24 h and 72 h). This could be performed with field dosage using first, second and third instar larvae. The stability of the mutations detected also

needs to be confirmed. Lastly, the most promising UV-protectants from this study, need to be tested in the field as well.

In conclusion, this study has provided a platform to investigate and further develop a UV-tolerant CrleGV-SA that has improved efficacy (as measured by persistence) in the field and will provide a more effective biopesticide to combat FCM in South African fruit orchards.

References

Abbott, W.S., 1925. A method of computing the effectiveness of an insecticide. Journal of Economic Entomology, 18: 265-267.

Acker, S., Hloucha, M., Osterwalder, U., 2014. The easy way to make a sunscreen. SOFW-Journal, 140 (7): 24-30.

Aizawa, K., 1953. On the inactivation of the silkworm jaundice virus. Japanese Journal of Applied Zoology, 4: 181-190.

Akermann, H.W., Smirnoff W.A., 1983. A morphological investigation of 23 baculoviruses. Journal of Invertebrate Pathology, 41:269–280.

Akhanaev, Y.B., Belousova, I.A., Ershov, N.I., Nakai, M., Martemyanov, V.V., Glupov, V.V., 2017. Comparison of tolerance to sunlight between spatially distant and genetically different strains of Lymantria dispar nucleopolyhedrovirus. PLoS One, 12(12): e0189992.

Aktar, W., Sengupta, D., Chowdhury, A., 2009. Impact of pesticides use in agriculture: their benefits and hazards Interdisciplinary Toxicology, 2(1): 1–12.

Alemanno, L., T. Ramos, T., Gargadenec, A., Andary, C., Ferriere, N., 2003. Localization and identification of phenolic compounds in *Theobroma cacao* L. somatic embryogenesis. Annals of Botany, 92: 613-623.

Alletti, G. G., Sauer, A. J., Weihrauch, B., Fritsch, E., Undorf-Spahn, K., Wennmann, J. T., Jehle, J. A., 2017. Using next generation sequencing to identify and quantify the genetic composition of resistance-breaking commercial isolates of Cydia pomonella granulovirus. Viruses, 9(9): 250-266.

Al-Zaidi, A. A., Elhag, E.A., Al-Otaibi, S. H., Baig, M.B., 2011. Negative effects of pesticides on the environment and the farmers' awareness in Saudi Arabia: A case study. The Journal of Animal & Plant Sciences, 21(3): 605-611.

Anduleit, K., Sutton, G., Diprose, J. M., Mertens, P. P. C., Grimes, J. M., Stuart, D. I., 2005. Crystal lattice as biological phenotype for insect viruses. Protein Science, 14(10): 2741-2743.

Angelini, A., Amargier, A., Vandamme, P., Dutoit, J. L., 1965. Une virose a granules chez Ie lèpidoptére *Argyroploce leucotreta.* Coton et Fibres Tropicales, 20: 277-282.

Arrizubieta, M., Simón, O., Williams, T., Caballero, P., 2015. A novel binary mixture of Helicoverpa armigera single nucleopolyhedrovirus genotypic variants has improved insecticidal characteristics for control of cotton bollworms. Applied & Environmental Microbiology, 81 (12): 3984-3993.

Arnott, H.J., Smith, K.M., 1968. An ultrastructural study of the development of a granulosis virus in the cells of the moth *Plodia interpunctella* (Hbn.). Journal of Ultrastructure Research, 21: 251-268.

Arthurs, S. P., Lacey, L. A., Behle, R. W., 2006. Evaluation of spray-dried lignin-based formulations and adjuvants as solar protectants for the granulovirus of the codling moth, *Cydia pomonella* (L). Journal of Invertebrate Pathology, 93: 88-95.

Arthurs, S. P., Lacey, L. A., Behle, R. W., 2008. Evaluation of lignins and particle films as solar protectants for the granulovirus of the codling moth, *Cydia pomonella*. Biocontrol Science and Technology, 18: 829-839.

Arthurs S., Dara, S. K., 2018. Microbial biopesticides for invertebrate pests and their markets in the United States. Journal of Invertebrate Pathology, 165: 13-21.

Asano, S., 2005. Ultraviolet protection of a granulovirus product using iron oxide. Applied Entomology and Zoology, 40: 359-364.

Asser-Kaiser, S., Fritsch, E., Undorf-Spahn, K., Kienzle, J., Eberle, K. E., Gund, N. A., Reineke, A., Zebitz, C. P. W., Heckel, D.G., Huber, J., Jehle, J. A., 2007. Rapid emergence of baculovirus resistance in codling moth due to dominant, sex-linked inheritance. Science, 318: 1916 –1917.

Asser-Kaiser, S., Heckel, D. G., Jehle, J. A., 2010a. Sex linkage of CpGV resistance in a heterogeneous field strain of the codling moth *Cydia pomonella* (L.). Journal of Invertebrate Pathology, 103: 59-64.

Asser-Kaiser, S., Radtke, P., El-Salamouny, S., Winstanley, D., Jehle, J. A., 2010b. Baculovirus resistance in codling moth (*Cydia pomonella* L.) caused by early block of virus replication. Virology, 410: 360-367.

Au, S., Cohen, S., Panté, N., 2010. Microinjection of *Xenopus laevis* oocytes as a system for studying nuclear transport of viruses. Methods, 51: 114-120.

Au, S., Pante, N., 2012. Nuclear transport of baculovirus: revealing the nuclear pore complex passage. Journal of Structural Biology, 177(1): 90–98.

Bajwa, W. I., Kogan, M., 2002. Compendium of IPM Definitions (CID)- What is IPM and how is it defined in the Worldwide Literature? IPPC Publication No. 998, Integrated Plant Protection Center (IPPC), Oregon State University, Corvallis, OR 97331, USA.

Baker, M.J., Trevisan,J., Bassan, P., Bhargava, R., Butler, H.J., Dorling, K.M., Fielden, P.R., Forgaty, S.W., Fullwood, N.J., Heys, K.A., Hughes, C., Lasch, P., Martin-Hirsch, P.L., Obinaju, B., Sockalingum, G.D., Sule-suso, J., Strong, R.J.,

Wood, B.R., Gardner, P., Martin, F.L., 2014. Using Fourier transform IR spectroscopy to analyse biological materials. Nature Protocols 9: 1771-1791.

Barker, R.E., 1968. The availability of solar radiation below 290 mn and its importance in photomodification of polymers. Photochemistry and Photobiology, 7: 275-295.

Bayramoglu, Z., Gencer, D., Muratoglu, H., Efe, D., Nalcacioglu, R., Demirbag Z., Demir, I., 2018. Characterization of a nucleopolyhedrovirus variant of the gypsy moth, Lymantriadispar (Lepidoptera: Lymantriidae) in Turkey, International Journal of Pest Management, 64(2): 119-127.

Beas-Catena, A., Sanchez-Miron, A., Garcia-Camacho, F., Contreras-Gomez, A., Molina-Grima, E., 2014. Baculovirus biopesticides: an overview. Journal of Animal and Plant Sciences, 24(2): 362-373.

Behle, R., Birthisel, T., 2014. Formulation of entomopathogens as bioinsecticides. In: Morales-Ramos, J. A., Guadalupe Rojas, M., Shapro-Ilan, D. L., (Eds.), Mass Production of Beneficial organisms. Elsevier, Amsterdam, pp. 483-517.

Behle, R. W., Tamez-Guerra, P., Mcguire, M. R., 2003. Field activity and storage stability of Anagrapha falcifera nucleopolyhedrovirus (AfMNPV) in spray-dried lignin-based formulations. Journal of Economic Entomology, 96: 1066-1075.

Bergold, G.H., 1947. Die isolierung des polyeder-virus and die natur der polyeder. Zeitschrift für Naturforschung B, 2: 122-143.

Berling, M., Blachere-Lopez, C., Soubabere, O., Lery, X., Bonhomme, A., Sauphanor, B., Lopez-Ferber, M., 2009. Cydia pomonella granulovirus genotypes overcome virus resistance in the codling moth and improve virus efficiency by selection against resistant hosts. Applied Environmental Microbiology, 75: 925–930.

Bideshi, D. K., Bigot, Y., Federici, B. A., 2000 Molecular characterization and phylogenetic analysis of the Harrisina brillians granulovirus granulin gene. Archives of Virology, 145: 1933-1945.

Black, B. C., Brennan, L. A., Dierks, P. M., Gard, I. E., 1997. Commercialisation of baculovirus insecticides. In: The Baculoviruses. L.K Miller (Ed.) Plenum Press, New York, USA, pp. 341-387.

Blissard G. W., Rohrmann G. F., 1989. Location, sequence, transcriptional mapping, and temporal expression of the gp64 envelope glycoprotein gene of the Orgyia pseudotsugata multicapsid nuclear polyhedrosis virus. Virology, 170: 537–555.

Blissard G. W., 1996. Baculovirus–insect cell interactions. Cytotechnology, 20: 73 – 93.

Bloomquist, J. R., 1996. Ion Channels as Targets for Insecticides. Annual Review of Entomology 41(1): 163-190.

Brassel, J., Benz, G., 1979. Selection of a strain of the granulosis virus of the codling moth with improved resistance against artificial ultraviolet radiation and sunlight. Journal of Invertebrate Pathology, 33: 358-363.

Bulach, D. M., Kumar, C. A., Zaia, A., Liang, B., Tribe, D. E., 1999. Group II nucleopolyhedrovirus subgroups revealed by phylogenetic analysis of polyhedrin and DNA polymerase gene sequences. Journal of Invertebrate Pathology, 73: 59-73.

Burgess, S., 1977. Molecular weights of lepidopteran baculovirus DNAs: Derivation by electron microscopy. Journal of General Virology, 37: 501-510.

Burges, H.D., Jones, K.A., 1998. Formulation of Bacteria, Viruses and Protozoa to Control Insects. In: Burges H.D. (Ed.) Formulation of Microbial Biopesticides. Springer, Dordrecht, pp. 33-127.

Carell, T., Burgdorf, L.T., Kundu, L. M., Cichon, M., 2001. The mechanism of action of DNA photolyases, Current Opinion in Chemical Biology, 5: 491–498.

Carpentier, D. C., Griffiths, C. M., King, L. A., 2008. The baculovirus P10 protein of Autographa californica nucleopolyhedrovirus forms two distinct cytoskeletal-like structures and associates with polyhedral occlusion bodies during infection. Virology, 371(2): 278-91.

Casida, J. E., Quistad G. B., 1998. Golden age of insecticide research: past, present, or future? Annual Review of Entomology, 43(1): 1-16.

Catling, H. D., 1969. Citrus pest control: recommendations for Swaziland. Bulletin of the Swaziland Ministry of Agriculture, 26: 1-13.

Catling, H. D., Aschenborn, H., 1974. Population studies of the false codling moth, *Cryptophlebia leucotreta* (Meyrick), on citrus in the Transvaal. Phytophylactica, 6: 31–38.

Chandler, D., Bailey, A. S., Tatchell, G. M., Davidson, G., Greaves, J., Grant, W. P., 2011. The development, regulation and use of biopesticides for integrated pest management. Philosophical Transactions of the Royal Society B: Biological Sciences, 366 (1573): 1987-1998.

Chen, X. W., Hu, Z. H., Jehle, J. A., Zhang, Y. Q., Vlak, J. M., 1997. Analysis of the ecdysteroid UDP-glucotransferase gene of Heliothis armigera single nucleocapsid baculovirus. Virus Genes, 15: 219-225.

Chen, X., Ijkel, W. F. J., Dominy, C., Zanotto, P., Hashimoto, Y., Faktor, O., Hayakawa, T., Wang, C.-H., Prekumar, A., Mathavan, S., Krell, P. J., Hu, Z., Vlak, J. M., 1999. Identification, sequence analysis and phylogeny of the *lef-2* gene of Helicoverpa armigera single-nucleocapsid baculovirus. Virus Research, 65: 21-32.

Clarke, J.F.G., 1958. Catalogue of the type specimens of Microlepidoptera in the British Museum (Natural History) described by Edward Meyrick. Vol.III. London, British Museum (Natural History).

Clarke, E. E., Tristem, M., Cory, J. S., O'Reilly, D. R., 1996. Characterization of the ecdysteroid UDP-glucosyltransferase gene from Mamestra brassicae nucleopolyhedrosis virus. Journal of General Virology, 77: 2865-2871.

Claus, J. D., Gioria, V. V., Micheloud, G. A., Visnovsky, G., 2012. Production of insecticidal baculoviruses in insect cell cultures: potential and limitations. In: Soloneski, S., Larramendy, M., (Eds.), Insecticides-basic and other applications. INTECH, Rijeka, pp. 127-152.

Couilloud, R., 1994. *Cryptophlebia leucotreta* (Meyrick) (Lepidoptera: Tortricidae). In: Matthews, G. A., Tunstall, J. P., (Eds.), Insect Pests of Cotton. CAB International, Wallingford, pp. 207-213.

Coulibaly, F., Chiu, E., Gutmann, S., Rajendran, C., Haebel, P. W., Ikeda, K., Metcalf, P., 2009. The atomic structure of baculovirus polyhedra reveals the independent emergence of infectious crystals in DNA and RNA viruses. Proceedings of the National Academy of Sciences, 106 (52): 22205–22210.

CPC (Crop Protection Compendium). 2007. CAB International, Wallingford, UK. http://www. cabicompendium.org/cpc/home.asp

Cutchis, P., 1982. A formula for comparing annual damaging ultra-violet (DUV) radiation doses at tropical and mid-latitude sites. In: Calkins, J., (Ed.), The Role of Solar Ultra-Violet Radiation in Marine Ecosystems. NATO Conference Series, volume 7. Springer, Boston, MA, pp. 213-228.

Daiber, C., 1980. A study of the biology of the false codling moth [*Cryptophlebia*

leucotreta (Meyr.)]: The adult and generations during the year. Phytophylactica, 12: 187-193.

David, W.A.L., Gardiner, B. O. C., 1966. Persistence of a granulosis virus of *Pieris brassicae* on cabbage leaves. Journal of Invertebrate Pathology, 8: 180-183.

David, W. A., 1969. The effect of ultraviolet radiation of known wavelengths on a granulosis virus of Pieris brassicae. Journal of Invertebrate Pathology, 14: 336-42.

Detvisitsakun C., Cain E.L., Passarelli A.L., 2007. The Autographa californica M nucleopolyhedrovirus fibroblast growth factor accelerates host mortality. Virology, 365(1): 70-78.

Dhladhla, B. I. R., 2012. Enumeration of insect viruses using microscopic and molecular analyses; South African isolate of Cryptophlebia leucotreta granulovirus as a case study. Masters' thesis: Nelson Mandela Metropolitan University.

Dhladhla, B. I. R., Mwanza, P., Lee, M. E., Moore, S. D, Dealtry, G. B., 2018. Comparison of microscopic and molecular enumeration methods for insect viruses: Cryptophlebia leucotreta granulovirus as a case study. Journal of Virological Methods 256: 107-110.

Dinse, G. E., Umbach, D. M., 2011. Characterizing non-constant relative potency. Regulatory toxicology and pharmacology, 60(3): 342-353.

Eberle, K. E., Asser-Kaiser, S., Sayed, S. M., Nguyen, H. T., Jehle, J. A., 2008. Overcoming the resistance of codling moth against conventional Cydia pomonella granulovirus (CpGV-M) by a new isolate CpGV-I12. Journal of Invertebrate Pathology, 98: 293-298.

Eker, A. P., Kooiman, P., Hessels, J. K., Yasui, A., 1990. DNA photoreactivating enzyme from the cyanobacterium *Anacystis nidulans.* Journal of Biological Chemistry, 265: 8009–8015.

El-Helaly, A., 2013. Additives for a baculovirus against ultraviolet effect. Applied Science Report, 4: 1987-191.

El-Salamouny, S., Ranwala, D., Shapiro, M., Shepard, B. M., Farrar, R. R., 2009. Tea, coffee, and cocoa as ultraviolet radiation protectants for the beet armyworm nucleopolyhedrovirus. Journal of Economic Entomology, 102: 1767-1773.

El Salamouny, S., Shapiro, M., Ling, K. S., Shepard B. M., 2009. Black Tea and Lignin as Ultraviolet Protectants for the Beet Armyworm Nucleopolyhedrovirus. Journal of Entomological Science, 44: 50-68.

Engelhard, E.K., Kam-Morgan, L. N., Washburn, J. O., Volkman, L. E., 1994. The insect tracheal system: a conduit for the systemic spread of Autographa californica M nuclear polyhedrosis virus. Proceedings of the National Academy of Sciences, USA, 91: 3224–3227.

Erlandson, M., 2008. Insect pest control by viruses. Encyclopaedia of Virology, 3: 125-133.

Erichsen, C., Schoeman, A.S., 1992. Economic losses due to insect pests on avocado fruit in Nelspruit/Hazyview region of South Africa during 1991. South African Avocado Growers' Association Yearbook, 15: 49-54.

Erichsen, C., Schoeman, A.S., 1994. Moth pests of avocados. South African Avocado Growers' Association Yearbook, 17: 109-112.

Evans, H.F., Shapiro, M., 1997. Viruses. In: Lacey, L.A., (Ed.), Manual of Techniques in Insect Pathology. Academic Press, San Diego, pp. 17–53.

Fabian, H., Mäntele, W., 2002. Infrared Spectroscopy of Proteins. In: Chalmer, J. M., Griffiths, P. R., (Eds.), Handbook of vibrational spectroscopy. John Wiley & Sons Chichester, UK, pp. 3399-3425.

Fang, M., Nie, Y., Wang, Q., Deng, F., Wang, R., Wang, H., Wang, H., Vlak, J. M., Chen, X., Hu, Z., 2006. Open reading frame 132 of Helicoverpa armigera nucleopolyhedrovirus encodes a functional per os infectivity factor (PIF-2). Journal of General Virology, 87(9): 2563-2569.

Farrar, R. R., Shapiro, M., Javaid, I., 2003. Photostabilized titanium dioxide and a fluorescent brightener as adjuvants for a nucleopolyhedrovirus. BioControl 48: 543-560.

Finney, D. J., 1965. The meaning of bioassay. Biometrics, 21: 785-798.

Finney, D. J., 1971. Probit analysis, 3rd Edition. Cambridge University Press, London.

Fitches, E. C., Bell, H. A., Powell, M. E., Back, E., Sargiotti, C., Weaver, R. J., Gatehouse, J. A., 2009. Insecticidal activity of scorpion toxin (ButaIT) and snowdrop lectin (GNA) containing fusion proteins towards pest species of different orders. Pest Management Science, 66(1): 74-83.

Food Quality Protection Act., 1998. Food Quality Protection Act of 1996, P.L. 104-170, Title II, Section 303, Enacted August 3, 1996. Codified in: Title 7, U.S. Code, Section 136r-1. Integrated Pest Management.

Fritsch, E., 1989. Das granulosevirus des falschen apfelwicklers, Cryptophlebia leucotreta Meyrick. PhD. Thesis. TU Darmstadt, Germany.

Fritsch, E. K., Undorf-Spahn, J., Kienzle, C. P., Zebitz, W., Huber, J., 2005. Apfelwickler granulovirus: erste hinweise auf unterschiede in der empfindlichkeit lokaler apfelwickler populationen. Nachrichtenblatt des Deutschen Pflanzenschutzdienstes, 57: 29-34.

Fuller, C., 1901. The Natal codling moth, Carpocapsa sp., First report of government entomologist 1899 - 1900. Natal Department of Agriculture Report, 48-51.

Gati, C., Oberthuer, D., Yefanov, O., Bunker R. D., Stellato, F., Chiu, E., Yeh, S., Aquila, A., Basu, S., Bean, R., Beyerlein, K. R., Botha, S., Boutet, S., DePonte D. P., Doak, R.B., Fromme, R., Galli, L., Grotjohann, I., James, D.R., Kupitz, C., Lomb, L., Messerschmidt, M., Nass, K., Rendek, K., Shoeman, R. L., Wang, D., Weierstall, U., White, T.A., Williams, G. J., Zatsepin, N. A., Fromme, P., Spence, J. C. H., Goldie, K. N., Jehle, J. A., Metcalf, P., Barty, A., Chapman, H. N., 2017. Atomic structure of granulin determined from native nanocrystalline granulovirus using an X-ray free-electron laser. Proceedings of the National Academy of Sciences, USA, 114: 2247–2252.

Gebhardt, M. M., Eberle, K. E., Radtke, P., Jehle, J. A., 2014. Baculovirus resistance in codling moth is virus isolate-dependent and the consequence of a mutation in viral gene pe38. Proceedings of the National Academy of Sciences, USA, 111: 15711-15716.

Gifani, A., Marzban, R., Safekordi, A., Ardjmand, M., Dezianian, A., 2015. Ultraviolet protection of nucleopolyhedrovirus through microencapsulation with different polymers. Biocontrol Science and Technology, 25 (7): 814–827.

Girard, P. M., Francesconi, S., Pozzebon. M., Graindorge, D., Rochette, P., Drouin, R., Sage, E., 2011. UVA-induced damage to DNA and proteins: direct versus indirect photochemical processes. Journal of Physics Conference Series, 261:012002.

Glassford, S.E., Byrne, B., Kazarian, S.G., 2013. Recent applications of ATR FTIR spectroscopy and imaging to proteins. Biochimica et Biophysica Acta, 1834: 2849-2858.

Goble, T., 2007. The genetic characterization and biological activity of the South African Cryptophlebia leucotreta granulovirus (CrleGV-SA) in two biopesticides, Cryptogran and Cryptex. Honours Dissertation, Rhodes University.

Gómez, J., Guevara, J., Cuartas, P., Espinel, C., Villamizar, L., 2013. Microencapsulated Spodoptera frugiperda nucleopolyhedrovirus: insecticidal activity and effect on arthropod populations in maize. Biocontrol Science Technology, 23: 829-846.

Gomi, S., Zhou, C. E., Yih, W., Majima, K., Maeda, S., 1997. Deletion analysis of four of eighteen late gene expression factor gene homologues of the baculovirus, BmNPV. Virology, 30: 35-47.

Graillot, B., Blachère-Lòpez, C., Besse, S., Siegwart, M., Lòpez-Ferber, M., 2017. Host range extension of Cydia pomonella granulovirus: adaptation to Oriental Fruit Moth, *Grapholita molesta*. BioControl, 62:19-27.

Granados, R. R., Lawler, K. A., 1981. *In vivo* pathway of Autographa californica baculovirus invasion and infection. Virology, 108: 297-308.

Grasela, J. J., McIntosh, A. H., Shelby, K. S., Long, S., 2008. Isolation and characterization of a baculovirus associated withthe insect parasitoid wasp, *Cotesia marginiventris*, or its host, *Trichoplusia ni.* Journal of Insect Science, 8:42, www.insectscience.org accessed on 15 January 2019.

Griego, V. M., Martignoni, M. E., Claycomb, A. E., 1985. Inactivation of nuclear polyhedrosis virus (Baculovirus subgroup A) by monochromatic UV radiation. Applied Environmental Microbiology, 49 (3): 709-10.

Grove, T., de Beer, M. S., Joubert, P. H., 2010. Developing a systems approach for *Thaumatotibia leucotreta* (Lepidoptera: Tortricidae) on “Hass” Avocado in South Africa. Journal of Economic Entomology, 103: 1112-1128.

Grzywacz, D., 2017. Basic and Applied Research: Baculoviruses. In: Lacey, L.A., (Ed.) Microbial control of insect and mite pests: from theory to practice. Academic Press, London, pp. 27-46.

Grzywacz, D., Moore, S.D., 2017. Production, formulation, and bioassay of baculoviruses for Pest Control. In: L.A. Lacey (Ed.) Microbial control of insect and mite pests: from theory to practice. Academic Press, London, pp. 109-124.

Guarino, L. A., Gonzalez, M. A., Summers, M. D., 1986. Complete sequence and enhancer function of the homologous DNA regions of Autographa californica nuclear polyhedrosis virus. Journal of Virology, 60: 224–229.

Guarino, L. A., Dong, W., Xu, B., Broussard, D. R., Davis, R.W., Jarvis, D. L., 1992. The baculovirus phosphoprotein pp31 is associated with the virogenic stroma. Journal of Virology, 66: 7113-7120.

Haase, S., Alicia Sciocco-Cap, A., Romanowski, V., 2015. Baculovirus insecticides in Latin America: Historical overview, current status and future perspectives. Viruses, 7: 2230-2267.

Hajek, A., 2004. Natural enemies: An introduction to biological control. Cambridge University Press, Cambridge, UK.

Hall, N., 2007. Advanced sequencing technologies and their wider impact in microbiology. Journal of Experimental Biology, 210: 1518-1525.

Hamm, J. J., Shapiro, M., 1992. Infectivity of fall armyworm (Lepidoptera: Noctuidae) nuclear polyhedrosis virus enhanced by a fluorescent brightener. Journal of Economic Entomology, 85: 2149-2152.

Hansen, L., De Beer, T., Pierre, K., Pastoret, S., Bonnegarde-Bernard, A., Daoussi, R., Vervaet, C., Remon, J.P., 2015. FTIR spectroscopy for the detection and evaluation of live attenuated viruses in freeze dried vaccine formulations. Biotechnology Progress, 31(4): 1107-1118.

Harrison, R. L., Hoover, K., 2012 Baculoviruses and Other Occluded Insect Viruses. In: Vega, F. E., Kaya, H. K., (Eds.). Insect Pathology, 2nd Edition. Boston: Academic Press, Boston, USA, pp. 73-131.

Hatting, J. L., Moore, S. D., Malan, A. P., 2018. Microbial control of phytophagous invertebrate pests in South Africa: Current status and future prospects Journal of Invertebrate Pathology, 165: 54-66.

Hepburn, G.A., 1947. Insect pests of citrus in the eastern districts of the Cape Province: I- False codling moth. Citrus Grower, 162: 9 - 11.

Hering, J. A., Innocent, P. R., Haris, P.I., 2004. Towards developing a protein infrared spectra databank (PISD) for proteomics research. Proteomics, 4: 2310-2319.

Herniou, E. A., Luque, T., Chen, X., Vlak, J. M., Winstanley, D., Cory, J. S., O'reilly, D. R., 2001. Use of whole genome sequence data to infer baculovirus phylogeny Journal of Virology, 75(17): 8117-8126.

Herniou, E. A., Arif, B. M., Bonning, B. C., Theilmann, D. A., Blissard, G. W., Becnel, J. J., Jehle, J. A., Harrison, H., 2011. Baculoviridae. In: King, A. M. Q., Adams, M. J., Carstens, E. B., Lefkowitz, E.J., (Eds.), Virus Taxonomy. Elsevier, Oxford, pp. 163-174.

Hobbs, D. G., Campbell, B., Lister, W. D., 1999. Ultraviolet radiation lignin protected pesticidal compositions. U.S. Patent No. 5,994,266.

Honiball, S. J., 2004. Opnames van gasheerplante vir valskodlingmot (*Cryptophlebia leucotreta*) in die Ctrusdal-omgewing. CRI Group Annual Research Report, pp 140-142.

Howard, C. W., 1909. Orange codling moth (Enarmonia batrachopa). Transvaal Department of Agriculture Report 1907 – 1908, pp. 189.

Hu, Y. C., 2006. Baculovirus vectors for gene therapy. Advances in Virus Research, 68: 287‑320.

Hughes, K. M., Addison, R. B., 1970. Two nuclear polyhedrosis viruses of the Douglas-fir tussock moth. Journal of Invertebrate Pathology 16:196–204.

Hunter-Fujita, F. R., Entwistle, P. F., Evans, H. F., Crook, N. E., 1998. In: Insect viruses and pest management. Wiley, Chichester: England.

Hyten, D. L., Qijian Song, Q., Fickus, E. D., Quigley, C. V., Lim, J., Choi, I., Hwang, E., Pastor-Corrales, M., Cregan, P. B., 2010. High-throughput SNP discovery and assay development in common bean. BMC Genomics, 11: 475-483.

Ignoffo, C. M., 1973. Development of a viral insecticide: Concept to commercialization. Experimental Parasitology, 33: 380-406.

Ignoffo, C. M., Hostetter, D.L., Sikorowski, P. P., Sutter, G., Brooks, W. M., 1977. Inactivation of representative species of entomopathogenic viruses, a bacterium, fungus, and protozoan by an ultraviolet light source. Environmental Entomology, 6 (3): 411-415.

Ignoffo, C. M., Garcia, C., 1978. UV photo inactivation of cells and spores Bacillus thuringiensis and effects of peroxidase on inactivation. Environmental Entomology, 7: 270-272.

Ignoffo, C. M., Rice, W. C. Mcintosh, A. H., 1989. Inactivation of nonoccluded and occluded baculoviruses and baculovirus-DNA exposed to simulated sunlight. Environmental Entomology, 18(1): 177-183.

Ignoffo, C. M., Garcia, C., 1994. Antioxidant and oxidative enzyme effects on the inactivation of inclusion bodies of the Heliothis baculovirus by simulated sunlight-UV. Biological control, 23: 1025-1029

Ijkel, W. F., Westenberg, M., Goldbach, R. W., Blissard, G. W., Vlak, J. M., Zuidema, D., 2000. A novel baculovirus envelope fusion protein with a proprotein convertase cleavage site. Virology, 275: 30-41.

Inceoglu, A. B., Kamita, S. G., Hinton, A. C., Huang, Q., Severson, T. F., Kang, K., Hammock, B. D., 2001. Recombinant baculoviruses for insect control. Pest Management Science, 57: 981-9817.

Inceoglu, A. B., Kamita, S. G., Hammock, B. D., 2006. Genetically modified baculoviruses: historical overview and future outlook. In: Bonning, B.C., (Ed.), Advances in Virus Research: Insect Viruses: Biotechnological Applications, vol. 68, Academic Press, San Diego, USA, pp. 109-126.

Jack, R.W., 1916a. The citrus codling moth (*Argyroploce leucotreta*). Rhodesian Citrus Pests. Bulletin of the Department of Agriculture of Southern Rhodesia, 228: 26-27.

Jack, R.W., 1916b. Rhodesian citrus pests. Rhodesian Agricultural Journal, 13:69-83.

Jacques, R. P., 1977. Stability of entomopathogenic viruses. Miscellaneous Publications of the Entomological. Society of America, 10: 99-116.

Jacques, R. P., 1985. Stability of entomopathogenic viruses in the environment. In: Maramorosch, K., Sherman, K.E., (Ed.), Viral insecticides for biological control. Academic Press, New York, pp. 285-360.

Jehle, J. A., Baekhaus, H., Fritsch, E., Huber, J., 1992. Physical map of the Cryptophlebia leucotreta granulosis virus genome and its relationship to the genome of Cydia pomoneila granulosis virus. Journal of General Virology, 73: 1621-1626.

Jehle, J. A., Baekhaus, H., 1994**.** The granulin gene region of Cryptophlebia leucotreta granulosis virus: sequence analysis and phylogenetic considerations. Journal of General Virology, 75: 3667-3671.

Jehle, J. A., Lange, M., Wang, H., Hu, Z., Wang, H., Hauschild, R., 2006a. Molecular identification and phylogenetic analysis of baculoviruses from Lepidoptera. Virology, 346: 180-193.

Jehle, J.A., Blissard, G.W., Bonning, B.C., Cory, J.S., Herniou, E.A., Rohrmann, G.F., Theilmann, D.A., Thiem, S.M.M., Vlak, J.M., 2006b. On the classification and nomenclature of baculoviruses: A proposal for revision. Archives of Virology, 151(7): 1257-1266.

Jehle, J. A., Schulze-Bopp, S., Undorf-Spahn, K., Fritsch, E., 2017. Evidence for a second type of resistance against Cydia pomonella granulovirus in field populations of codling moths. Applied Environmental Microbiology, 83: e02330-16.

Jeyarani, S., Sathiah, N., Karuppuchamy, P., 2013. An in vitro method for increasing UV-tolerance in a strain of Helicoverpa armigera (Lepidoptera: Noctuidae) nucleopolyhedrovirus. Biocontrol Science and Technology, 23: 305-316.

Jones, K. A., 1988. The use of insect viruses for pest control in developing countries. Aspects of Applied Biology 17:425-433.

Jones, K. A., Moawad, G., Mckinley, D. J., Grzywacz, D., 1993. The effect of natural sunlight on Spodoptera-littoralis nuclear polyhedrosis-virus. Biocontrol Science and Technology, 3: 189-197.

Jones, K. A., 2000. Bioassays of entomopathogenic viruses. In: Navon, A., Ascher, K. R. S., (Eds.), Bioassay of entomopathogenic microbes and nematodes. CAB Publishing, Wallingford, pp. 95–140.

Kang, W., Tristem, M., Maeda, S., Crook, N. E., O'Reilly, D. R., 1998. Identification and characterization of the Cydia pomonella granulovirus *cathepsin* and *chitinase* genes. Journal of General Virology, 79: 2283-2292.

Kataoka, C., Kaname, Y., Taguwa, S., Abe, T., Fukuhara, T., Tani, H., Matsuura, Y., 2012. Baculovirus GP64-Mediated Entry into Mammalian Cells. Journal of Virology, 86(5): 2610-2620.

Katsuma, S., Horie, S., Daimon, T., Iwanaga, M., Shimada, T., 2006. In vivo and in vitro analyses of a Bombyx mori nucleopolyhedrovirus mutant lacking functional vfgf. Virology, 355(1): 62-70.

Katsuma, S., Horie, S., Shimada, T., 2008. The fibroblast growth factor homolog of Bombyx mori nucleopolyhedrovirus enhances systemic virus propagation in *B. mori* larvae. Virus Research, 137: 80-85.

Kazarian, S., Chan, K.L., 2013. ATR-FTIR spectroscopic imaging: Recent advances and applications to biological systems. Analyst, 138: 1940-1951.

Keddie, B. A., Aponte, G. W., Volkman, L. E., 1989. The pathway of infection of Autographa californica nuclear polyhedrosis virus in an insect host. Science, 243: 1728–1730.

Kessler, P., Zingg, D., 2008. New baculovirus products offer solutions for the biological control of *Cydia pomonella* and *Cryptophlebia leucotreta.* In: Pest management: perennial crops, 23rd International Congress of Entomology. Durban, South Africa. 6 - 12 July, 2008.

Killick, H.J., Warden, S.J., 1991. Ultraviolet penetration of pine trees and insect virus survival. Entomophaga, 36: 87-94.

Kirkman, W., 2007. Understanding and improving the residual efficacy of the Cryptophlebia leucotreta granulovirus (CRYPTOGRAN). Masters Thesis, Rhodes University, Grahamstown, South Africa.

Kirkman, W., Moore, S.D., 2007. A study of alternative hosts for the false codling moth, *Thaumatotibia leucotreta* in the Eastern Cape. SA Fruit Journal, 6(2): 33-38.

Knox C. M., Moore S. D., Luke, G. A., Hill M. P., 2015. Baculovirus-based strategies for the management of insect pests: a focus on development and application in South Africa. Biocontrol Science and Technology, 25(1): 1-20.

Komai, F., 1999. A taxonomic review of the genus Grapholita and allied genera (Lepidoptera, Tortricidae) in the Palaerctic region. Entomologica Scandinavica, 55: 1-219.

Koshiro, Y., Jackson, M. C., Katahira, R., Wang, M. L., Nagai, C., Ashihara, H., 2007. Biosynthesis of chlorogenic acids in growing and ripening fruits of Coffea arabica and Coffea canephora plants. Zeitschrift fur Naturforschung. C, Journal of biosciences 62(9-10): 731-742.

Kost, T. A., Condreay, J. P., Jarvis, D. L., 2005. Baculovirus as versatile vectors for protein expression in insect and mammalian cells. Nature Biotechnology, 23: 567-575.

Lacey, L. A., Frutos, R., Kaya, H. K., Vail, P., 2001. Insect pathogens as biological control agents: do they have a future? Biological Control, 21: 230–248.

Lacey, L. A., Grzywacz, D., Shapiro-Ilan, D. I., Frutos, R., Brownbridge, M., Goettel, M. S., 2015. Insect pathogens as biological control agents: Back to the future. Journal of Invertebrate Pathology, 132: 1–41.

Lange, M., Jehle, J. A., 2003. The Genome of the Cryptophlebia leucotreta granulovirus. Virology, 317: 220-236.

Lapointe, R., Thumbi, D., Lucarotti, C. J., 2012. Recent advances in our knowledge of baculovirus molecular biology and its relevance for the registration of baculovirus-based products for insect pest population control, integrated pest management and pest control - current and future tactics. S. Soloneski, S., (Ed.). ISBN: 978-953-51-0050-8, InTech. Retrieved from *http://www.intechopen.com/books/integrated-pest-*

management-and-pest-control-current-and-futuretactics/recentadvances-in-our-knowledge-of-baculovirus-molecular-biology-and-its-relevance-for-theregistra.

Leahy, J., Mendelsohn, M., Kough, J., Jones, R., Berckes, N., 2014. Biopesticide oversight and registration at the US Environmental Protection Agency. In Gross, A.D., Coats, J.R., Duke, S.O., Seiber, J.N., (Eds.), Biopesticides: State of the Art and Future Opportunities. pp.3–18.

Lee, K. W., Kim, Y. J., Lee, H. J., Lee, C. Y., 2003. Cocoa has more phenolic phytochemicals and a higher antioxidant capacity than teas and red wine. Journal of Agricultural and Food Chemistry, 51(25): 7292-7295.

Lima, C. A., Goulart, V. P., Côrrea, L., Pereira, T. M., Zezell, D. M., 2015. ATR-FTIR Spectroscopy for the Assessment of Biochemical Changes in Skin Due to Cutaneous Squamous Cell Carcinoma. International Journal of Molecular Sciences, 16: 6621-6630.

Liu, S., Vijayendran, D., Bonning, B.C. 2011. Next generation sequencing technologies for insect virus discovery. Viruses, 3: 1849-1869.

Long G., Pan, X., Kormelink, R., Vlak, J.M., 2006. Functional entry of baculovirus into insect and mammalian cells is dependent on clathrin-mediated endocytosis. Journal of Virology, 80(17): 8830–3.

Lua, L.H., Reid, S., 2003. Growth, viral production and metabolism of a Helicoverpa zea cell line in serum-free culture. Cytotechnology, 42: 109-120.

Lynn, D.E., 2007. Available Lepidopteran Insect Cell Lines. In: Murhammer, D.W., (Ed.), Baculovirus and Cell Expresion Protocols: 2nd Edition. Humana Press: Totowa, USA, pp. 117-137.

Maeda, S., 1989. Increased insecticidal effect by a recombinant baculovirus carrying a synthetic diuretic hormone gene. Biochemical and Biophysical Research Communications, 165: 1177-1183.

Maeda, S, Volrath, S. L., Hanzlik, T. N., Harper, S. A., Maddox, D. W., Hammock, B. D., Fowler, E., 1991. Insecticidal effects of an insect-specific neurotoxin expressed by a recombinant baculovirus. Virology, 184: 777-80.

Mardis, E. R., 2007. The impact of next-generation sequencing technology on genetics. Trends in Genetics, 24(3): 133-141.

Marsberg, T., Jukes, M. D., Krejmer-Rabalski, M., Rabalski, L., Knox C. M., Moore S. D., Hill M. P., Szewczyk B., 2018. Morphological, genetic and biological characterisation of a novel alphabaculovirus isolated from *Cryptophlebia peltastica* (Lepidoptera: Tortricidae). Journal of Invertebrate Pathology, 157: 90-99.

Martínez, A. M., Goulson, D., Chapman, J. W., Caballero, P., Cave, R. D., Williams, T., 2000. Is it feasible to use optical brightener technology with a baculovirus bioinsecticide for resource-poor maize farmers in Mesoamerica? Biological Control, 17: 174-181.

Matilainen, H., Rinne, J., Gilbert, L., Marjomäki, V., Reunanen, H., Oker-Blom, C., 2005. Baculovirus Entry into Human Hepatoma Cells. Journal of Virology, 79(24): 15452-15459.

McGuire, M.R., Shasha, B.S., Lewis, L.C., & Nelsen, T.C., 1994. Residual activity of granular starch-encapsulated *Bacillus thuringiensis*. Journal of Economic Entomology, 87(3): 631-637.

McGuire, M. R., Behle, R. W., Goebel, H. N., Fry, T. C., (2000). Calibration of a sunlight simulator for determining solar stability of *Bacillus thuringiensis* and

Anagrapha flacifera nuclear polyhedrovirus. Environmental Entomology, 29: 1070-1074.

Means, J. C., Passarelli A. L., 2010. Viral fibroblast growth factor, matrix metalloproteases, and caspases are associated with enhancing systemic infection by baculoviruses. Proceedings of the National Academy of Sciences, 107(21): 9825-9830.

Meyrick, E., 1912. Descriptions of South African Micro-Lepidoptera. Annals of the Transvaal Museum, pp. 63-83.

Micheloud, G. A., Gioria, V. V., Pérez, G., Claus, J.D., 2009. Production of occlusion bodies of Anticarsia gemmatalis multiple nucleopolyhedrovirus in serum-free suspension cultures of the saUFL-AG-286 cell line: influence of infection conditions and statistical optimization. Journal of Virological Methods, 162: 258-266.

Mikhailov, V.S., Mikhailova, A. L., Iwanaga, M., Gomi, S., Maeda, S., 1998. Bombyx mori nucleopolyhedrovirus encodes a DNA-binding protein capable of destabilizing duplex DNA. Journal of Virology, 72: 3107-3116.

Mikhailov, V., Okano, K., Rohrmann, G. F., 2003. Baculovirus alkaline nuclease possesses a 5'->3' exonuclease activity and associates with the DNA-Binding Protein LEF-3. Journal of Virology, 77(4): 2436-2444.

Mikhailov, V. S., Vanarsdall, A. L., Rohrmann, G. F., 2007. Isolation and characterization of the DNA-binding protein (DBP) of the Autographa californica multiple nucleopolyhedrovirus. Virology, 370: 415-429.

Minnes, R., Nissinmann, M., Maizels, Y., Gerlitz, G., Katzir, A., Raichlin, Y., 2017. Using Attenuated Total Reflection–Fourier Transform Infra-Red (ATR-FTIR) spectroscopy to distinguish between melanoma cells with a different metastatic potential. Scientific Reports, 7: 4381-4387.

Mitchnick, M. A., Fairhurst, D., Pinnell, S. R., 1999. Microfine zinc oxide (Zcote) as a photostable UVA/UVB sunblock agent. Journal of the American Academy of Dermatology, 40: 85-90.

Monsma, S. A., Oomens, A. G., Blissard, G. W., 1996. The GP64 envelope fusion protein is an essential baculovirus protein required for cell-to-cell transmission of infection. Journal of Virology, 70: 4607-4616.

Moore, S., 2002. The development and evaluation of Cryptophlebia leucotreta granulovirus (CrleGV) as a biological control agent for the management of false codling moth, Cryptophlebia leucotreta, on citrus. PhD thesis, Rhodes University.

Moore, S. D., Kirkman, W., Stephen, P., 2004. Cryptogran, a virus for the biological control of false codling moth. South African Fruit Journal, 3: 35-39.

Moore, S. D., Hendry, D., Richards, G. I., 2011. Virulence of a South African isolate of the Cryptophlebia leucotreta granulovirus to *Thaumatotibia leucotreta* neonate larvae. BioControl, 56: 341-352.

Moore, S.D., Hattingh, V., 2012. A review of current pre-harvest control options for false codling moth in citrus in southern Africa. South African Fruit Journal, 11: 82-85.

Moore, S. D., Richards, G. I., Chambers, C., Hendry, D., 2014. An improved larval diet for commercial mass rearing of the false codling moth, Thaumatotibia leucotreta (Meyrick) (Lepidoptera: Tortricidae). African Entomology, 22: 216-219.

Moore, S. D., Kirkman, W., Richards, G. I., Stephen, P., 2015a. The Cryptophlebia leucotreta granulovirus – 10 years of commercial field use. Viruses, 7: 1284-1312.

Moore, S. D., Kirkman, W., Hattingh, V., 2015b. The host status of lemons for the false codling moth, Thaumatotibia leucotreta (Meyrick) (Lepidoptera: Tortricidae) with particular reference to export protocols. African Entomology, 23(2): 519-525.

Moore, S. D., Kirkman, W., Albertyn, S., Hattingh, V., 2016. Comparing the use of laboratory reared and field collected *Thaumatotibia leucotreta* (Lepidoptera: Tortricidae) larvae for demonstrating efficacy of post-harvest cold treatments in citrus fruit. Journal of Economic Entomology, 109(4): 1571-1577.

Moore, S. D., Kirkman, W., Stephen, P., Albertyn, S., Love, C. N., Grout, T.G., Hattingh, V., 2017. Development of an improved postharvest cold treatment for *Thaumatotibia leucotreta* (Meyrick) (Lepidoptera: Tortricidae). Postharvest Biology and Technology, 125: 188-195.

Morris, O. N., 1971. The effect of sunlight, ultraviolet and gamma radiations, and temperature on the infectivity of a nuclear polyhedrosis virus. Journal of Invertebrate Pathology, 18: 292-294.

Moscardi, F., 1999. Assessment of the application of baculoviruses for control of Lepidoptera. Annual Review of Entomology, 44: 257‑289.

Moscardi, F., Lobo de Souza, M., Batista de Castro, M.E., Moscardi M. L., Szewczyk B., 2011. Baculovirus pesticides: present state and future perspectives. In: Ahmad, I., Ahmad, F., Pichtel, J., (Eds.)., Microbes and microbial technology. Springer, New York, USA, pp. 415-445.

Movasaghi, Z., Rehman, S., Rehman, I., 2008. Fourier Transform Infrared (FTIR) Spectroscopy of Biological Tissues. Applied Spectroscopy Reviews, 43(2): 134-179.

Mück, O., 1985. Biologie, verhalten und wirtschaftliche bedeutung von parasiten schädlicher lepidopteren auf den kapverden; Bauer: Exeter, NH, USA.

Murphy, F. A., Fauquet, C. M., Bishop, D. H. L., Ghabrial, S. A., Jarvis, A. W., Martelli, G. P., Mayo, M. A., Summers, M. D., (Eds), 1995. Virus Taxonomy – The Classification and Nomenclature of viruses: Sixth Report of the International Committee on Taxonomy of Viruses. Springer, New York, USA.

Mwanza, P., 2015. Determination of the effects of sunlight and uv irradiation on the structure, viability and reapplication frequency of the biopesticide Cryptophlebia leucotreta granulovirus in the protection against false codling moth infestation of citrus crops. Masters Thesis, Nelson Mandela Metropolitan University, Port Elizabeth, South Africa.

Nakai, M., Harrison, R. L., Uchida, H., Ukuda, R., Hikihara, S., Ishii, K., Kunimi, Y., 2015. Isolation of an Adoxophyes orana granulovirus (AdorGV) occlusion body morphology mutant: biological activity, genome sequence and relationship to other isolates of AdorGV. Journal of General Virology, 96: 904-914.

National Department of Agriculture (NDA)., 2019. Banned and Restricted substances in the Republic of South Africa. www.nda.agric.za/doaDev/sideMenu/ActNo36_1947/bannedAndRestricted.htm

Newton, P. J., Anderson, T., 1985. Crop loss due to false codling moth, *Cryptophlebia leucotreta* (Meyr.) (Lepidoptera: Tortricidae), and other factors on different navel orange selections at Citrusdale. Information Bulletin, Citrus and Subtropical Fruit Research Institute, 159: 22-24.

Newton P. J., 1988. Inversely density-dependent egg parasitism in patchy distribution of the citrus pest *Cryptophlebia leucoptreta* (Lepidoptera: Tortricidae), and its agricultural efficiency. Applied Ecology, 25: 145-162.

Newton, P.J., 1989. The influence of citrus fruit condition on egg laying by the false codling moth, *Cryptophlebia leucotreta*. Entomologia Experimentalis *et* Applicata, 52: 113–117.

Newton, P.J., 1998. False codling moth, *Cryptophlebia leucotreta* (Meyrick). In: Bedford, E. C. G., Van den Berg, M. A., De Villiers, E. A., Citrus Pests in the Republic

of South Africa. 2nd edition (revised). Institute for Tropical and Subtropical Crops: Nelspruit, South Africa, 192–200.

Nguyen, Q., Qi, Y. M., Wu, Y., Chan, L. C. L., Nielsen, L. K., Reid, S., 2011. *In-vitro* production of Helicoverpa baculovirus biopesticides—automated selection of insect cell clones for manufacturing and systems biology studies. Journal of Virological Methods, 175: 197-2005.

Patmanidi, A. L., Possee, R. D., King, L. A., 2003. Formation of P10 tubular structures during AcMNPV infection depends on the integrity of host-cell microtubules. Virology, 317(2): 308–20.

Pearson, M. N., Groten, C., Rohrmann, G. F., 2000. Identification of the Lymantria dispar nucleopolyhedrovirus envelope fusion protein provides evidence for a phylogenetic division of the Baculoviridae. Journal of Virology, 74: 6126-6131.

Pearson, M. N., Russell, R., Rohrmann, G. F., 2001. Characterization of a baculovirus encoded protein that is associated with infected-cell membranes and budded virions. Virology, 291: 22-31.

Pearson, M. N., Rohrmann, G. F., 2002. Transfer, incorporation, and substitution of envelope fusion proteins among members of the Baculoviridae, Orthomyxoviridae, and Metaviridae (insect retrovirus) families. Journal of Virology, 76: 5301–5304.

Pedrini, M. R., Reid, S., Nielsen, L. K., Chan, L.C., 2011. Kinetic characterization of the group II Helicoverpa armigera nucleopolyhedrovirus propagated in suspension cell cultures: Implications for development of a biopesticides production process. Biotechnology Progress, 27: 614-624.

Pellegrini, N., Serafini, M., Colombi, B., Del Rio, D., Salvatore, S., Bianchi, M., Brighenti, F., 2003. Total antioxidant capacity of plant foods, beverages and oils

consumed in Italy assessed by three different in vitro assays. Journal of Nutrition, 133: 2812-2819.

Pemsela, M., Schwab, S., Scheurer, S., Freitag, D., Schatz, R., Schlucker, E., 2010. Advanced PGSS process for the encapsulation of the biopesticide Cydia pomonella granulovirus. The Journal of Supercritical Fluids, 53: 174-178.

Peng, K., Wu, M., Deng, F., Song, J., Dong, C., Wang, H., Hu, Z., 2010. Identification of protein protein interactions of the occlusion-derived virus-associated proteins of Helicoverpa armigera nucleopolyhedrovirus. Journal of General Virology, 91: 659-670.

Petrik, D. T., Iseli, A., Montelone, B. A., Van Etten, J. L., Clema, R. J., 2003. Improving baculovirus resistance to UV inactivation: increased virulence resulting from expression of a DNA repair enzyme. Journal of Invertebrate Pathology, 82: 50-56.

Pidre, M. L., Ferrelli, M. L., Haase, S., Romanowski, V., 2013. Baculovirus display: A novel tool for vaccination. In: Romanowski, V., (Ed.), Current issues in molecular virology - viral genetics and biotechnological applications. ISBN: 978-953-51-1207-5, InTech. Retrieved from *http://www.intechopen.com/books/current-issues-in-molecular-virologyviral-genetics-and-biotechnological-applications/baculovirus display-a-novel-tool-forvaccination.*

Pinnell, S. R., Fairhurst, D., Gillies, R., Mitchnick, M. A., Kollias, N., 2000. Microfine zinc oxide is a superior sunscreen ingredient to microfine titanium dioxide. Dermatologic Surgery, 26: 309-14.

Ohkawa, T., Volkman, L. E., Welch, M. D., 2010. Actin-based motility drives baculovirus transit to the nucleus and cell surface. Journal of Cell Biology, 190(2): 187-95.

Opoku-Debrah, J. K, Hill, M. P., Knox, C., Moore, S. D., 2013. Overcrowding of false codling moth, Thaumatotibia leucotreta leads to the isolation of five new Cryptophlebia

leucotreta granulovirus (CrleGV-SA) isolates. Journal of Invertebrate Pathology, 112: 219–228.

Opoku-Debrah, J. K, Hill, M. P., Knox, C., Moore, S. D., 2016. Heterogeneity in virulence relationships between Cryptophlebia leucotreta granulovirus isolates and geographically distinct host populations: lessons from codling moth resistance to CpGV-M. BioControl, 61: 449-459.

O'Reilly, D. R., Miller, L. K., 1991. Improvement of a baculovirus pesticide by deletion of the egt gene. Biotechnology, 9: 1086-1089.

Orr, D., 2009. Biological control and Integrated Pest Management. In: R. Peshin, R., Dhawan, A.K., (Eds.), Integrated Pest Management: Innovation-Development Process. Springer, Dorderecht, Netherlands, pp. 207-239.

Radtke, J., Linseisen, J., Wolfram, G., 1998. Phenolic acid intake of adults in a Bavarian subgroup of the national food consumption survey. Zeitschrift für. Ernährungswissenschaft, 37: 190 -197.

Ravanat, J. L., Douki, T., Cadet, J., 2001. Direct and indirect effects of UV radiation on DNA and its components. Journal of Photochemistry and Photobiology B, 63(1-3): 88-102.

Reardon, R. C., Podgwaite, J., Zerillo, R., 2009. Gypchek-Bioinsecticide for the Gypsy Moth. FHTET 2009-01 Fort Collins: U.S. Department of Agriculture, Forest Health Technology Enterprise Team.

Reeves, W. R., McGuire, M. K., Stokes, M., Vicini, J. L., 2019. Assessing the safety of pesticides in food: How current regulations protect human health. Advances in Nutrition, 10: 80-88.

Reid, S., Chan, L., Van Oers, M., 2014. Production of entomopathogenic viruses. In: Morales-Ramos, J. A., Guadalupe Rojas, M., Shapiro-Ilan, D. I., (Eds.), Mass Production of Beneficial Organisms. Elsevier, London, pp. 437–482.

Ridley, A.J., Whiteside, J. R., Mcmillan, T. J., Allinson, S. L., 2009. Cellular and sub-cellular responses to UVA in relation to carcinogenesis. International Journal of Radiation Biology, 85(3): 177–195.

Robberecht, R., 1989. Environmental photobiology. In: Smith, K. C., (Ed), The Science of photobiology. Plenum Press, New York, USA, pp. 135-154

Rohrmann, G. F., 1986. Polyhedrin structure. Journal of General Virology, 67: 1499-1513.

Rohrmann, G. F., 1992. Baculovirus structural proteins. Journal of General Virology, 73: 749–761.

Rohrmann, G. F., 2013. Baculovirus Molecular Biology [Internet]. 3rd edition. Bethesda (MD): National Center for Biotechnology Information, USA. Retrieved from: https://www.ncbi.nlm.nih.gov/books/NBK138298/.

Russell, R. L. Q., Rohrmann, G. F., 1990. A baculovirus polyhedron envelope protein: Immunogold localization in infected cells and mature polyhedra. Virology, 174: 177-184.

Sajap, A. S., Bakir, M. A., Kadir, H. A., Samad, N. A., 2009. Efficacy of selected adjuvants for protecting Spodoptera litura nucleopolyhedrovirus from sunlight inactivation. Journal of Asia-Pacific Entomology, 12: 85-88.

Sambandan, D. R., Ratner, D., 2011. Sunscreens: An overview and update. Journal of the American Academy of Dermatology, 64(4): 748-758.

Sauphanor, B., Berling, M., Toubon, J. F., Reyes, M., Delnatte, J., Allemoz, P., 2006. Carpocapse des pommes. Cas de résistance au virus de la granulose envergers biologique. Phytoma, 590: 24-27.

Sauer, A. J., Fritsch, E., Undorf-Spahn, K., Nguyen, P., Marec, F., Heckel, D. G., Jehle, J. A., 2017a. Novel resistance to Cydia pomonella granulovirus (CpGV) in

codling moth shows autosomal and dominant inheritance and confers cross-resistance to different CpGV genome groups. PLoSONE, 12(6): e0179157.

Sauer, A. J., Schulze-Bopp, S., Fritsch, E., Undorf-Spahn, K., Jehle, J. A., 2017b. A Third Type of Resistance to Cydia pomonella Granulovirus in Codling Moths Shows a Mixed Z-Linked and Autosomal Inheritance Pattern. Applied and Environmental Microbiology, 83(17): e01036-17.

Scalbert, A., Williamson, G., 2000. Dietary intake and bioavailability of polyphenols. Journal of Nutrition, 130: 2073-2085.

Schucter, S. C., 2008. Next-generation sequencing transforms today's biology. Nature Methods, 5: 16-18.

Schwartz, A., 1981. 'n Bydrae tot die biologie en beheer van die valskodlingmot Cryptophlebia leucotreta (Meyr.) (Lepidoptera: Eucosmidae) op nawels. PhD thesis, University of Stellenbosch.

Shapiro, M., 1986. *In vivo* production of baculoviruses. In: Granados, R. R., Federici, B.A., (Eds), The Biology of Baculoviruses Volume III: Practical Application for Insect Control. CRC Press, Inc., Boca Raton, pp. 32-61.

Shapiro, M., 1992. Use of optical brighteners as radiation protectants for the gypsy moth (Lepidoptera: Lymantriidae) nuclear polyhedrosis virus. Journal of Economic Entomology, 85: 1682-1686.

Shapiro, M., 1995. Radiation protection and activity enhancement of viruses. In: Hall, F.R., Barray, J.W. (Eds.), Biorational Pest Control Agents: Formulation and Delivery. American Chemical Society, Washington, DC, USA, pp. 153–164.

Shapiro, M., Agin, P. P., Bell, R. A., 1983. Ultraviolet protectants of the gypsy moth (Lepidoptera: Lymantriidae) nucleopolyhedrosis virus. Environmental Entomology, 12: 982‑985.

Shapiro, M., Bell, R. A., 1984. Selection of a UV-tolerant strain of gypsy moth, Lymantria dispar (L.) (Lepidoptera: Lymantriidae), nucleopolyhedrosis virus. Environmental Entomology, 13: 1522-1526.

Shapiro, M., Robertson, J. L, 1990. Laboratory evaluation of dyes as ultraviolet screens for the gypsy moth (Lepidoptera: Lymantriidae) nuclear polyhedrosis virus. Journal of Economic Entomology, 83: 168-172.

Shapiro, M., Robertson, J. L., 1992. Enhancement of gypsy moth (Lepidoptera: Lymantriidae) baculovirus by optical brighteners. Journal of Economic Entomology, 85: 1120-1124.

Shapiro, M., Domek, J., 2002. Relative effects of ultraviolet and visible light on the activities of corn earworm and beet armyworm (Lepidoptera: Noctuidae) nucleopolyhedroviruses. Journal of Economic Entomology, 95(2): 261-268.

Shapiro, M., Farrar, R. R., Domek, J., Javais, I., 2002. Effects of virus concentration and ultraviolet irradiation on the activity of corn earworm and beet army worm (Lepidoptera: Noctuidae) nucleopolyhedroviruses. Journal of Economic Entomology, 95 (2): 243-249.

Shapiro, M., El Salamouny, S., Shepard, B. M., 2008. Green tea extracts as ultraviolet protectants for the beet armyworm, Spodoptera exigua, nucleopolyhedrovirus. Biocontrol Science and Technology, 18: 599-611.

Shapiro, M., El Salamouny, S., Shepard, B. M., 2009. Plant Extracts as Ultraviolet Radiation Protectants for the Beet Armyworm (Lepidoptera: Noctuidae) Nucleopolyhedrovirus: Screening of Extracts. Journal of Agricultural and Urban Entomology, 26: 47-61.

Shokralla, S., Spall, J. L., Gibson, J. F., Hajibabaei, M., 2012. Next-generation sequencing technologies for environmental DNA research. Molecular Ecology, 21: 1794-1805.

Singh, S., Moore, S. D., Spillings, B. Hendry, D., 2003. South African Isolate of Cryptophlebia leucotreta granulovirus. Journal of Invertebrate Pathology, 83: 249-252.

Smith, K. L., Herbig, S. H., 1998. Labile insecticide compositions. U.S. Patent No. 5,750,126.

Sood, P., Mehta, P. K., Prabhakar, C. S., 2013. Effect of UV protectants on the efficacy of Pieris brassicae granulovirus. Biological Agriculture & Horticulture, 29: 69-81.

Stevenson, H. P, Lin, G., Barnes, C. O., Sutkeviciute, I., Krzysiak, T., Weiss, S.C., Reynolds, S., Wu,Y., Nagarajan, V., Makhov, A. M., Lawrence, R., Lamm, E., Clark, L., Gardella, T. J., Hogue, B. G., Ogata, C. M., Ahn, J., Gronenborn, A. M., Conway, J. F., Vilardaga, J., Coheng, A. E., Caleroa, G., 2016. Transmission electron microscopy for the evaluation and optimization of crystal growth. Acta Crystallographica D, 72: 603-615.

Stibick, J. N. L., Bloem, S., Carpenter, J. E., Ellis, S., Gilligan, T., Usnick, S. J., Vennette, R. C., 2007. New Pest Response Guidelines: false codling moth, Thaumatotibia leucotreta. (www.aphis.gov/import_export/plants/manuals/emergency/downloads/nprg_fasle_codling_moth.pdf).

Stofberg, F.J., 1939. Bionomical notes on the false codling moth. Proceedings of the Entomology Conference, pp. 50-53.

Stofberg, F.J., 1954. False codling moth of citrus. Farming in South Africa, pp. 273-276.

Sukuta, S. Bruch, R., 1999. Factor analysis of cancer Fourier transform infrared evanescent wave fiberoptical (FTIR-FEW) spectra. Lasers in Surgery and Medicine, 24: 382–388.

Szewczyk, B., Hoyos-Carvajal, L., Paluszek, M., Skrzecz, I., Lobo De Souza, M., 2006. Baculoviruses - re-emerging biopesticides. Biotechnology Advances, 24: 143-160.

Tani H., Nishijima, M., Ushijima, H., Miyamura, T., Matsuura, Y., 2001 Characterization of cell-surface determinants important for baculovirus infection. Virology, 279(1): 343–53.

Timans, U., 1982. Zur Wirkungvon UV-Strahlen auf des Kernpolyedevirus des Schwammspinners, Lymantria dispar L. (Lep., Lymantriidae). Zeitschrift für Angewandte Etomologie, 94: 382-401.

Toprak, U., Harris, S., Baldwin, D., Theilmann, D., Gillott, C., Hegedus, D. D., Erlandson, M. A., 2012. Role of enhancin in Mamestra configurata nucleopolyhedrovirus virulence: selective degradation of host peritrophic matrix proteins. Journal of General Virology, 93(4): 744-753.

Tyrrell, R. M., Ley, R. D., Webb, R. B., 1974. Induction of single-double breaks (alkali-labile bonds) in bacterial and phage DNA by near-UV (365 nm) radiation. Photochemistry and Photobiology, 20: 395-398.

Ulanova, L. S., Isapour, G., Maleki, A., Fanaian, S., Zhu, K., Hoenen, A., X., Evensen, Ø., Griffiths, G., Nyström, B., 2014. Development of methods for encapsulation of viruses into polymeric nano- and microparticles for aquaculture vaccines. Journal of Applied Polymer Science, 131(17): 40714-40716.

U.S. Department of Agriculture (USDA), Animal Plant Health Inspection Service, Plant Protection and Quarantine, Emergency and Domestic Programs., 2010.

New Pest Response Guidelines: False Codling Moth Thaumatotibia leucotreta. Riverdale, Maryland [http://www.aphis.usda.gov/import_export/plants/ manuals/online_manuals.shtml].

Van Ark, H., 1995. Introduction to the analysis of quantal response. Agricultural Research Council Agrimetrics Institute, Pretoria, pp. 1-78.

van der Merwe, M., Jukes, M., Rabalski, L., Knox, C., Opoku-Debrah, J., Moore, S. D., Krejmer-Rabalska, M., Szewczyk, B., Hill, M., 2017. Genome analysis and genetic stability of the Cryptophlebia leucotreta granulovirus (CrleGV-SA) after 15 years of commercial use as a biopesticide. International Journal of Molecular Sciences, 18: 2327.

van Oers, M. M., Herniou, E. A., Usmany, M., Messelink, G. J., Vlak, J. M., 2004. Identification and characterization of a DNA photolyase-containing baculovirus from *Chrysodeixis chalcites*. Virology. 330: 460-470.

van Oers, M. M., Lampena, M. H., Bajek, M. I., Vlak, J. M., Eker, A. P. M., 2009. Active DNA photolyase encoded by a baculovirus from the insect *Chrysodeixis chalcites.* DNA Repair, 7: 1309-1318.

Venette, R. C., Davis, E. E., Da Costa, M., Heisler, H., Larson, M., 2003. Mini risk assessment. False codling moth, *Thaumatotibia* (= Cryptophlebia) *leucotreta* (Meyrick) (Lepidoptera: Tortricidae). Department of Entomology, University of Minnesota, Minneapolis, USA.

Wang, P., Granados, R. R., 1997. An intestinal mucin is the target substrate for a baculovirus enhancin. Proceedings of the National Academy of Sciences, USA, 94(13): 6977-6982.

Washburn, J. O., Kirkpatrick, B. A., Haas-Stapleton, E., Volkman, L. E., 1998. Evidence that the stilbene-derived optical brightener M2R enhances Autographa

californica M nucleopolyhedrovirus infection of *Trichoplusia ni* and *Heliothis virescens* by preventing sloughing of infected midgut epithelial cells. Biological Control, 11: 58-69

Watanabe, S., 1951. Studies on the grasserie virus of the silkworm, Bombyx mori: Physical and chemical effects upon the virus. Japan Journal of Experimental Medicine, 21: 299-313.

Wennmann, J. T., Radtke, P., Eberle, K. E., Gueli Alletti, G., Jehle, J.A., 2017. Deciphering Single Nucleotide Polymorphisms and Evolutionary Trends in Isolates of the Cydia pomonella granulovirus. Viruses, 9 (8): 227-239.

Whitt, M. A., Manning, J. S., 1988. A phospholylated 34-kDa protein and a subpopulation of polyhedrin are thiol linked to the carbohydrate layer surrounding a baculovirus occlusion body. Virology, 163: 33-42.

Williams, G.V., Rohel, D. Z., Kuzio, J., Faulkner, P., 1989. A cytopathological investigation of Autographa californica nuclear polyhedrosis virus p10 gene function using insertion/deletion mutants. Journal of General Virology, 70: 187-202.

Wilson, K., Walker, J., 2010. Principles and techniques of biochemistry and molecular biology, 7th ed. Cambridge University Press, New York, USA, pp. 522-526.

Witt, D. J., Stairs, G. R., 1975. The effects of ultraviolet irradiation on a Baculovirus infecting *Galleria mellonella*. Journal of Invertebrate Pathology, 26: 321-327.

Witt, D. J., Hink, W. F., 1979. Selection of autographa califomica nuclear polyhedrosis virus for resistance to inactivation by near ultraviolet, far ultraviolet, and thermal radiation. Journal of Invertebrate Pathology, 33: 222-232.

Wolff, J. L., Moraes, R. H. P., Kitajima, P., de Souza Leal, E., Zanotto, P. M. A., 2002. Identification and characterization of a baculovirus from *Lonomia obliqua* (Lepidoptera: Saturniidae). Journal of Invertebrate Pathology, 79: 137-145.

Wu, Z. W., Fan, J. B., Yu, H., Wang, D., Zhang, Y. L., 2015., Ultraviolet protection of the Cydia pomonella granulovirus using zinc oxide and titanium dioxide. Biocontrol Science and Technology, 25: 97-107.

Xu, H., Yang, Z., Zhao, J., Tian, C., Ge, J., Tang, X., Bao, Y., Zhang, C., 2008a. Bombyx mori nucleopolyhedrovirus ORF56 encodes an occlusion-derived virus protein and is not essential for budded virus production. Journal of General Virology, 89: 1212–1219.

Xu, F., Vlak, J.M., van Oers, M.M., 2008b. Conservation of DNA photolyase genes in group II nucleopolyhedroviruses infecting plusiine insects, Virus Research, 136: 58-64.

Yamagishi, J., Burnett, E. D., Harwood, S. H., Blissard, G. W., 2007. The AcMNPV pp31 gene is not essential for productive AcMNPV replication or late gene transcription but appears to increase levels of most viral transcripts. Virology, 365(1): 34–47.

Young, S. Y., Yearian, W. C., 1974. Persisstence of heliothis NPV on foliage of cotton, soybean and tomato, Environmental Entomology, 3: 253-255.

Zhou, W., Greer, H. F., 2016. What can electron microscopy tell us beyond crystal structures? European Journal of Inorganic Chemistry, 7: 941-950.

Zuidema, D., Klinge-Roode, E. C, Van Lent, J. W. M., Vlak, J. M., 1989. Construction and analysis of an Autographa californica nuclear polyhedrosis virus mutant lacking the polyhedral envelope. Virology, 73: 98-108.

Appendix I

Relative potency comparisons between the different time points in each exposure cycle

Table A1. Relative potency comparisons (LC_{50}) between CrleGV-SA samples in UV exposure cycle 1 in surface dose–response bioassays against neonate FCM larvae.

Reference	Test	Potency
Unexposed Control	Unexposed CrleGV-SA control	1.000
	1 h	0.971
	3 h	7.432
	8 h	289.981
	24 h	ND
	72 h	ND
1 h	1 h	1.000
	Unexposed CrleGV-SA control	1.030
	3 h	7.655
	8 h	298.698
	24 h	ND
	72 h	ND
3 h	3 h	1.000
	Unexposed CrleGV-SA control	0.135
	1 h	0.131
	8 h	39.019
	24 h	321.356
	72 h	ND
8 h	8 h	1.000
	Unexposed CrleGV-SA control	0.003
	1 h	0.003
	3 h	0.026
	24 h	8.236
	72 h	45.463
24 h	24 h	1.000
	Unexposed CrleGV-SA control	0.000
	1 h	0.000
	3 h	0.003
	8 h	0.121
	72 h	5.520
72 h	72 h	1.000
	Unexposed CrleGV-SA control	0.000
	1 h	0.000
	3 h	0.001
	8 h	0.022
	24 h	0.181

*ND-Not determined, value too large to be displayed by software

Table A2. Relative potency comparisons (LC_{50}) between CrleGV-SA samples in UV exposure cycle 2 in surface dose–response bioassays against neonate FCM larvae.

Reference	Test	Potency
Unexposed CrleGV-SA control	Unexposed CrleGV-SA control	1.000
	1 h	4.881
	3 h	61.503
	8 h	338.985
	24 h	ND
	72 h	ND
1 h	1 h	1.000
	Unexposed CrleGV-SA control	0.205
	3 h	12.600
	8 h	69.450
	24 h	332.188
	72 h	ND
3 h	3 h	1.000
	Unexposed CrleGV-SA control	0.016
	1 h	0.079
	8 h	5.512
	24 h	26.363
	72 h	282.763
8 h	8 h	1.000
	Unexposed CrleGV-SA control	0.003
	1 h	0.014
	3 h	0.181
	24 h	4.783
	72 h	51.302
24 h	24 h	1.000
	Unexposed CrleGV-SA control	0.001
	1 h	0.003
	3 h	0.038
	8 h	0.209
	72 h	10.726
72 h	72 h	1.000
	Unexposed CrleGV-SA control	0.000
	1 h	0.000
	3 h	0.004
	8 h	0.019
	24 h	0.093

*ND-Not determined, value too large to be displayed by software

Table A3. Relative potency comparisons (LC_{50}) between CrleGV-SA samples in UV exposure cycle 3 in surface dose–response bioassays against neonate FCM larvae.

Reference	Test	Potency
Unexposed CrleGV-SA control	Unexposed CrleGV-SA control	1.000
	1 h	12.696
	3 h	54.295
	8 h	184.522
	24 h	334.631
	72 h	438.726
1 h	1 h	1.000
	Unexposed CrleGV-SA control	0.079
	3 h	4.277
	8 h	14.534
	24 h	26.358
	72 h	34.557
3 h	3 h	1.000
	Unexposed CrleGV-SA control	0.018
	1 h	0.234
	8 h	3.399
	24 h	6.163
	72 h	8.080
8 h	8 h	1.000
	Unexposed CrleGV-SA control	0.005
	1 h	0.069
	3 h	0.294
	24 h	1.814
	72 h	2.378
24 h	24 h	1.000
	Unexposed CrleGV-SA control	0.003
	1 h	0.038
	3 h	0.162
	8 h	0.551
	72 h	1.311
72 h	72 h	1.000
	Unexposed CrleGV-SA control	0.002
	1 h	0.029
	3 h	0.124
	8 h	0.421
	24 h	0.763

*ND-Not determined, value too large to be displayed by software

Table A4. Relative potency comparisons (LC_{50}) between CrleGV-SA samples in UV exposure cycle 4 in surface dose–response bioassays against neonate FCM larvae.

Reference	Test	Potency
Unexposed CrleGV-SA Control	Unexposed CrleGV-SA control	1.000
	1 h	16.788
	3 h	18.223
	8 h	120.505
	24 h	4.366
	72 h	28.778
1 h	1 h	1.000
	Unexposed CrleGV-SA control	0.060
	3 h	1.086
	8 h	7.178
	24 h	0.260
	72 h	1.714
3 h	3 h	1.000
	Unexposed CrleGV-SA control	0.055
	1 h	0.921
	8 h	6.613
	24 h	0.240
	72 h	1.579
8 h	8 h	1.000
	Unexposed CrleGV-SA control	0.008
	1 h	0.139
	3 h	0.151
	24 h	0.036
	72 h	0.239
24 h	24 h	1.000
	Unexposed CrleGV-SA control	0.229
	1 h	3.845
	3 h	4.174
	8 h	27.603
	72 h	6.592
72 h	72 h	1.000
	Unexposed CrleGV-SA control	0.035
	1 h	0.583
	3 h	0.633
	8 h	4.187
	24 h	0.152

*ND-Not determined, value too large to be displayed by software

Table A5. Relative potency comparisons (LC_{50}) between CrleGV-SA samples in UV exposure cycle 5 in surface dose–response bioassays against neonate FCM larvae.

Reference	Test	Potency
Unexposed CrleGV-SA control	Unexposed CrleGV-SA control	1.000
	1 h	1.693
	3 h	4.323
	8 h	173.583
	24 h	11.333
	72 h	21.953
1 h	1 h	1.000
	Unexposed CrleGV-SA control	0.591
	3 h	2.554
	8 h	102.539
	24 h	6.695
	72 h	12.968
3 h	3 h	1.000
	Unexposed CrleGV-SA control	0.231
	1 h	0.392
	8 h	40.153
	24 h	2.621
	72 h	5.078
8 h	8 h	1.000
	Unexposed CrleGV-SA control	0.006
	1 h	0.010
	3 h	0.025
	24 h	0.065
	72 h	0.126
24 h	24 h	1.000
	Unexposed CrleGV-SA control	0.088
	1 h	0.149
	3 h	0.381
	8 h	15.317
	72 h	1.937
72 h	72 h	1.000
	Unexposed CrleGV-SA control	0.046
	1 h	0.077
	3 h	0.197
	8 h	7.907
	24 h	0.516

*ND-Not determined, value too large to be displayed by software

Appendix II

Relative potency comparisons between the same time point across the five UV exposure cycles.

Table A6. Relative potency comparisons (LC_{50}) between CrleGV-SA samples at 1 h exposure time across the five UV exposure cycles in surface dose–response bioassays against neonate FCM larvae.

Reference	Test	Potency
Unexposed Control	Unexposed CrleGV-SA control	1.00
	Cycle 1	5.050
	Cycle 2	39.624
	Cycle 3	33.327
	Cycle 4	148.952
	Cycle 5	13.548
Cycle 1	Cycle 1	1.000
	Unexposed CrleGV-SA control	0.198
	Cycle 2	7.846
	Cycle 3	6.599
	Cycle 4	29.494
	Cycle 5	2.683
Cycle 2	Cycle 2	1.000
	Unexposed CrleGV-SA control	0.025
	Cycle 1	0.127
	Cycle 3	0.841
	Cycle 4	3.759
	Cycle 5	0.342
Cycle 3	Cycle 3	1.000
	Unexposed CrleGV-SA control	0.030
	Cycle 1	0.152
	Cycle 2	1.189
	Cycle 4	4.469
	Cycle 5	0.407
Cycle 4	Cycle 4	1.000
	Unexposed CrleGV-SA control	0.007
	Cycle 1	0.034
	Cycle 2	0.266
	Cycle 3	0.224
	Cycle 5	0.091
Cycle 5	Cycle 5	1.000
	Unexposed CrleGV-SA control	0.074
	Cycle 1	0.373
	Cycle 2	2.925
	Cycle 3	2.460
	Cycle 4	10.995

*ND-Not determined, values too large to be displayed by software.

Table A7. Relative potency comparisons (LC_{50}) between CrleGV-SA samples at 3 h exposure time across the five UV exposure cycles in surface dose–response bioassays against neonate FCM larvae.

Reference	Test	Potency
Unexposed Control	Unexposed CrleGV-SA control	1.000
	Cycle 1	11.656
	Cycle 2	143.343
	Cycle 3	25.706
	Cycle 4	27.333
	Cycle 5	6.246
Cycle 1	Cycle 1	1.000
	Unexposed CrleGV-SA control	0.086
	Cycle 2	12.298
	Cycle 3	2.205
	Cycle 4	2.345
	Cycle 5	0.536
Cycle 2	Cycle 2	1.000
	Unexposed CrleGV-SA control	0.007
	Cycle 1	0.081
	Cycle 3	0.179
	Cycle 4	0.191
	Cycle 5	0.044
Cycle 3	Cycle 3	1.000
	Unexposed CrleGV-SA control	0.039
	Cycle 1	0.453
	Cycle 2	5.576
	Cycle 4	1.063
	Cycle 5	0.243
Cycle 4	Cycle 4	1.000
	Unexposed CrleGV-SA control	0.037
	Cycle 1	0.426
	Cycle 2	5.244
	Cycle 3	0.940
	Cycle 5	0.229
Cycle 5	Cycle 5	1.000
	Unexposed CrleGV-SA control	0.160
	Cycle 1	1.866
	Cycle 2	22.949
	Cycle 3	4.115
	Cycle 4	4.376

*ND-Not determined, values too large to be displayed by software.

Table A8. Relative potency comparisons (LC_{50}) between CrleGV-SA samples at 8 h exposure time across the five UV exposure cycles in surface dose–response bioassays against neonate FCM larvae.

Reference	Test	Potency
Unexposed Control	Unexposed CrleGV-SA control	1.000
	Cycle 1	ND
	Cycle 2	ND
	Cycle 3	193.375
	Cycle 4	460.965
	Cycle 5	424.480
Cycle 1	Cycle 1	1.000
	Unexposed CrleGV-SA control	0.001
	Cycle 2	1.213
	Cycle 3	0.134
	Cycle 4	0.318
	Cycle 5	0.293
Cycle 2	Cycle 2	1.000
	Unexposed CrleGV-SA control	0.010
	Cycle 1	0.825
	Cycle 3	0.110
	Cycle 4	0.263
	Cycle 5	0.242
Cycle 3	Cycle 3	1.000
	Unexposed CrleGV-SA control	0.005
	Cycle 1	7.485
	Cycle 2	9.075
	Cycle 4	2.384
	Cycle 5	2.195
Cycle 4	Cycle 4	1.000
	Unexposed CrleGV-SA control	0.002
	Cycle 1	3.140
	Cycle 2	3.807
	Cycle 3	0.420
	Cycle 5	0.921
Cycle 5	Cycle 5	1.000
	Unexposed CrleGV-SA control	0.002
	Cycle 1	3.410
	Cycle 2	4.134
	Cycle 3	0.456
	Cycle 4	1.086

*ND-Not determined, values too large to be displayed by software.

Table A9. Relative potency comparisons (LC_{50}) between CrleGV-SA samples at 24 h exposure time across the five UV exposure cycles in surface dose–response bioassays against neonate FCM larvae.

Reference	Test	Potency
Unexposed Control	Unexposed CrleGV-SA control	1.000
	Cycle 1	ND
	Cycle 2	ND
	Cycle 3	275.108
	Cycle 4	19.826
	Cycle 5	45.051
Cycle 1	Cycle 1	1.000
	Unexposed CrleGV-SA control	0.000
	Cycle 2	0.699
	Cycle 3	0.027
	Cycle 4	0.002
	Cycle 5	0.004
Cycle 2	Cycle 2	1.000
	Unexposed CrleGV-SA control	0.000
	Cycle 1	1.430
	Cycle 3	0.039
	Cycle 4	0.003
	Cycle 5	0.006
Cycle 3	Cycle 3	1.000
	Unexposed CrleGV-SA control	0.004
	Cycle 1	36.551
	Cycle 2	25.551
	Cycle 4	0.072
	Cycle 5	0.164
Cycle 4	Cycle 4	1.000
	Unexposed CrleGV-SA control	0.050
	Cycle 1	507.163
	Cycle 2	354.536
	Cycle 3	13.876
	Cycle 5	2.272
Cycle 5	Cycle 5	1.000
	Unexposed CrleGV-SA control	0.022
	Cycle 1	223.196
	Cycle 2	156.027
	Cycle 3	6.107
	Cycle 4	0.440

*ND-Not determined, values too large to be displayed by software.

Table A10. Relative potency comparisons (LC_{50}) between CrleGV-SA samples at 72 h exposure time across the five UV exposure cycles in surface dose–response bioassays against neonate FCM larvae.

Reference	Test	Potency
Unexposed Control	Unexposed CrleGV-SA control	1.000
	Cycle 1	ND
	Cycle 2	ND
	Cycle 3	544.834
	Cycle 4	111.767
	Cycle 5	91.083
Cycle 1	Cycle 1	1.000
	Unexposed CrleGV-SA control	0.000
	Cycle 2	1.262
	Cycle 3	0.004
	Cycle 4	0.001
	Cycle 5	0.001
Cycle 2	Cycle 2	1.000
	Unexposed CrleGV-SA control	0.000
	Cycle 1	0.792
	Cycle 3	0.003
	Cycle 4	0.001
	Cycle 5	0.001
Cycle 3	Cycle 3	1.000
	Unexposed CrleGV-SA control	0.002
	Cycle 1	239.781
	Cycle 2	302.722
	Cycle 4	0.205
	Cycle 5	0.167
Cycle 4	Cycle 4	1.000
	Unexposed CrleGV-SA control	0.009
	Cycle 1	ND
	Cycle 2	ND
	Cycle 3	4.575
	Cycle 5	0.815
Cycle 5	Cycle 5	1.000
	Unexposed CrleGV-SA control	0.011
	Cycle 1	ND
	Cycle 2	ND
	Cycle 3	5.982
	Cycle 4	1.227

*ND-Not determined, values too large to be displayed by software.

Appendix III

Relative potency comparisons between the concentrations of each UV protectant

Table A11. Relative potency comparisons (LC_{50}) between UV exposed CrleGV-SA-lignin samples in surface dose–response bioassays against neonate FCM larvae.

Reference	Test	Potency
Unexposed Control	Unexposed CrleGV-SA control	1.000
	24 h UV exposed CrleGV-SA control	ND
	0.09 % lignin	535.181
	0.9 % lignin	166.634
	9 % lignin	397.066
24 h UV exposed control	24 h UV exposed CrleGV-SA control	1.000
	Unexposed CrleGV-SA control	0.001
	0.09 % lignin	0.414
	0.9 % lignin	0.129
	9% lignin	0.307
0.09 % lignin	0.09 % lignin	1.000
	Unexposed CrleGV-SA control	0.002
	24 h UV exposed CrleGV-SA control	2.416
	0.9 % lignin	0.311
	9 % lignin	0.742
0.9 % lignin	0. 9% lignin	1.000
	Unexposed CrleGV-SA control	0.006
	24 h UV exposed CrleGV-SA control	7.759
	0.09 % lignin	3.212
	9 % lignin	2.383
9 % lignin	9 % lignin	1.000
	Unexposed CrleGV-SA control	0.003
	24 h UV exposed CrleGV-SA control	3.256
	0.09 % lignin	1.348
	0.9 % lignin	0.420

*ND-Not determined, value too large (>1000) to be displayed by software

Table A12. Relative potency comparisons (LC_{50}) between UV exposed CrleGV-SA-OE446 samples in surface dose–response bioassays against neonate FCM larvae.

Reference	Test	Potency
Unexposed Control	Unexposed CrleGV-SA control	1.000
	24 h UV exposed CrleGV-SA control	ND
	0.09 % OE446	ND
	0.9 % OE446	655.458
	9 % OE446	209.542
24 h UV exposed control	24 h UV exposed CrleGV-SA control	1.000
	Unexposed control	0.001
	0.09 % OE446	0.707
	0.9 % OE446	0.461
	9% OE446	0.147
0.09 % OE446	0.09 % OE446	1.000
	Unexposed CrleGV-SA control	0.001
	24 h UV exposed CrleGV-SA control	1.414
	0.9 % OE446	0.652
	9 % OE446	0.208
0.9 % OE446	0. 9% OE446	1.000
	Unexposed CrleGV-SA control	0.002
	24 h UV exposed CrleGV-SA control	2.169
	0.09 % OE446	1.534
	9 % OE446	0.320
9 % OE446	9 % OE446	1.000
	Unexposed CrleGV-SA control	0.005
	24 h UV exposed CrleGV-SA control	6.786
	0.09 % OE446	4.800
	0.9 % OE446	3.128

*ND-Not determined, value too large (>1000) to be displayed by software

Table A13. Relative potency comparisons (LC_{50}) between UV exposed CrleGV-SA-Uvinul Easy samples in surface dose–response bioassays against neonate FCM larvae.

Reference	Test	Potency
Unexposed Control	Unexposed CrleGV-SA control	1.000
	24 h UV exposed CrleGV-SA control	ND
	0.09 % Uvinul Easy	475.363
	0.9 % Uvinul Easy	213.363
	9 % Uvinul Easy	127.752
24 h UV exposed control	24 h UV exposed CrleGV-SA control	1.000
	Unexposed CrleGV-SA control	0.001
	0.09 % Uvinul Easy	0.339
	0.9 % Uvinul Easy	0.152
	9% Uvinul Easy	0.091
0.09 % Uvinul Easy	0.09 % Uvinul Easy	1.000
	Unexposed CrleGV-SA control	0.002
	24 h UV exposed CrleGV-SA control	2.953
	0.9 % Uvinul Easy	0.449
	9 % Uvinul Easy	0.269
0.9 % Uvinul Easy	0. 9% Uvinul Easy	1.000
	Unexposed CrleGV-SA control	0.005
	24 h UV exposed CrleGV-SA control	6.582
	0.09 % Uvinul Easy	2.229
	9 % Uvinul Easy	0.599
9 % Uvinul Easy	9 % Uvinul Easy	1.000
	Unexposed CrleGV-SA control	0.008
	24 h UV CrleGV-SA exposed control	10.989
	0.09 % Uvinul Easy	3.721
	0.9 % Uvinul Easy	1.620

*ND-Not determined, value too large (>1000) to be displayed by software

Table A14. Relative potency comparisons (LC_{50}) of selected UV exposed CrleGV-SA (C5)-UV protectant samples in surface dose–response bioassays against neonate FCM larvae.

Reference	Test	Potency
Unexposed C5 Control	Unexposed C5 control	1.000
	24 h UV exposed C5 control	10.646
	0. 9 % lignin	1.584
	9 % Uvinul Easy	1.283
	9 % OE446	3.674
24 h UV exposed C5 control	24 h UV exposed C5 control	1.000
	Unexposed C5 control	0.094
	0. 9 % lignin	0.149
	9 % Uvinul Easy	0.121
	9 % OE446	0.345
0. 9 % lignin	0. 9 % lignin	1.000
	Unexposed C5 control	0.631
	24 h UV exposed C5 control	6.723
	9 % Uvinul Easy	0.810
	9 % OE446	2.320
9 % Uvinul Easy	9 % Uvinul Easy	1.000
	Unexposed C5 control	0.780
	24 h UV exposed C5 control	8.298
	0. 9 % lignin	1.234
	9 % OE446	2.864
9 % OE446	9 % OE446	1.000
	Unexposed C5 control	0.272
	24 h UV exposed C5 control	2.897
	0. 9 % lignin	0.431
	9 % Uvinul Easy	0.349

*ND-Not determined, value too large (>1000) to be displayed by software

Appendix IV

Table A15. Comparison of the effect of each UV protectant on larval mortality

UV protectant	Replicate 1	Replicate 2	Replicate 3	Mean	*P (T<=t)
	% Mortality	% Mortality	% Mortality	% Mortality	
Water	6	10	12	11	
9% lignin	10	14	8	11	1
0.9 % lignin	4	12	16	14	0.3118
0.09 % lignin	18	6	10	8	0.3118
9 % OE 446	20	14	8	11	1
0.9 % OE446	16	6	8	7	0.1055
0.09 % OE446	4	10	18	14	0.543
9% Uvinul Easy	8	16	4	10	0.885
0.9 % Uvinul Easy	22	10	12	11	1
0.09 % Uvinul Easy	12	8	6	7	0,105

*two-tailed *t-test* at P=0.05